Studies on Pervaporation for Aroma Compound Recovery from Aqueous Solutions

By

Muhammad Mujiburohman

A thesis
presented to the University of Waterloo
in fulfillment of
thesis requirement for the degree of
Doctor of Philosophy
in
Chemical Engineering

Waterloo, Ontario, Canada, 2008

I hereby declare that I am the sole author of this thesis. This is a true copy of the thesis, including any required final revisions, as accepted by my examiners.

I understand that my thesis may be made electronically available to the public.

Muhammad Mujiburohman

Abstract

This study was concerned with the recovery of aroma compounds from aqueous solutions by pervaporation using poly(ether-block-amide) (PEBA) membranes. Three model aroma compounds (i.e., propyl propionate, C_6-aldehyde and benzaldehyde) were used in the study to represent ester, aldehyde and aromatic aroma compounds, respectively. The effects of process conditions (i.e., feed concentration and operating temperature) on the pervaporation performance (in terms of permeation flux and selectivity) for aroma-water separations were investigated. It was found that both the aroma permeation flux and the selectivity were affected significantly by the feed aroma concentration. The aroma permeability was in the order of propyl propionate > C_6-aldehyde > benzaldehyde, and the membrane selectivity for aroma/water separation followed the order of C_6-aldehyde > propyl propionate > benzaldehyde. In general, the aroma flux was found to be proportional to the aroma compound concentration in the solution. In the concentration range (390-3,200 ppm) tested, the effect of temperature on the permeation flux followed an Arrhenius type of relation.

The solubility and diffusivity of the aroma compounds in PEBA membrane, which determine their permeabilities through the membrane, were determined from the pervaporation and sorption/desorption data. It was shown that the solubility of the aroma compounds in the PEBA membrane generally followed the Henry's law where the sorption uptake was proportional to the feed aroma concentration. Among the three aroma compounds studied, benzaldehyde was found to have the highest solubility selectivity in the PEBA membrane, followed by C_6-aldehyde and propyl propionate. The solubilities of pure propyl propionate and water in PEBA membrane were also estimated; the solubility of pure propyl propionate was around 130 times higher than that of pure water. This confirmed that PEBA was an excellent organophilic membrane. The diffusivity of the aroma compounds through PEBA membrane was affected by the feed aroma concentration. From steady state pervaporation and equilibrium sorption data, the diffusivity was calculated on the basis of solution-diffusion model, and the diffusivity was shown to be linearly dependent on the feed aroma concentration. On the other hand, from the sorption kinetics data obtained from the time-

dependent sorption experiments, the diffusivity was shown to be affected by the feed aroma concentration exponentially. The main reason may be that the simple form of the solution-diffusion model is unable to precisely describe the mass transport through the membrane during pervaporation.

As an alternative to pervaporation where the liquid feed is in contact with the membrane and the mass transport involves permeation and evaporation (thus the word "pervaporation"), evaporation-permeation (or evapermeation, where the feed liquid is not in direct contact with the membrane and the mass transfer involves evaporation and then permeation) was also studied for aroma compound separation from water. It was shown that evapermeation was no better than pervaporation in terms of permeation flux and selectivity. This again demonstrated that the state of the membrane and the location for liquid-vapor phase change were important to the mass transport through the membrane.

For aroma recovery from dilute aqueous solutions, batch pervaporation is often preferred. Batch pervaporation coupled with permeate decantation and water phase recycle was studied parametrically. It was demonstrated that compared to the conventional pervaporation, the aroma recovery can be enhanced by recycling the water phase from the permeate decanter to the feed for further recovery. In addition, unlike the conventional batch operation where the product concentration starts to decrease beyond certain time, the modified batch pervaporation allows a longer period of operation without compromising the product purity.

Acknowledgements

All praise is just for Allah the Almighty, who is the only source of knowledge.

At this moment, I would like to express my sincere and great appreciation to my supervisor Prof. Xianshe Feng. His supervision indeed helped me to overcome arising problems throughout this research. His excellent writing experiences became an invaluable inspiration for me.

I would also convey much gratitude to Prof. Ali Elkamel for the discussion in some matters. I would greatly appreciate to all the Committee Members, Prof. B. Kruczek, Prof. X. Li, Prof. E. Croiset and Prof. C. Moresoli, for their valuable comments. Their suggestions became an important part for the completion of this work.

The research support from the Natural Sciences and Engineering Research Council (NSERC) of Canada is acknowledged. Great thanks and appreciation are also addressed to my sponsorship together with all my respected colleagues, in the Technological and Professional Skills Development Sector (TPSD) Project and in the Muhammadiyah University of Surakarta, Indonesia.

Assistance from my colleagues in the Membrane Group and from the technicians as well as the administration staff in the Chemical Engineering Department of University of Waterloo is gratefully acknowledged. Without their help, this work may not finish in proper time, thanks guys…

At last, I don't forget to give a high honor to my dearly loved wife and sons, Dik Upik–Ryan-Haris (my second baby). Their patience and encouragements are the source of my spirit. I dedicate this work to you all as well as my beloved parents (Djuwaini Bachri–Maryatun Ibrahim). Supports from my parents in law and relatives are thankfully acknowledged.

Table of Contents

List of Tables

List of Figures

Nomenclature

a_i	Activity of permeant *i*
A_m	Effective area of membrane
A_d, B_d	Diffusivity parameters related to the shape and size of permeant
c', c''	Concentration of permeant in the permeate stream; inside the membrane
c, C_i	Concentration of permeant in the bulk feed; of permeant *i* inside the membrane
$C_{F,i}$,$C_{F,j}$	Concentration of permeant *i* in the bulk feed; of permeant *j*
$C_{sF,i}$, $C_{sP,i}$	Concentration of permeant *i* on the membrane surface of feed side; on the membrane surface of permeate side
D, D_i	Diffusivity through the membrane; diffusivity of permeant *i*
D_0	Diffusivity at infinite dilution
D_T	Thermodynamic diffusivity
E	Activation energy describing the permeant-polymer physisorption bond
E_P	Activation energy for permeation
E_{rr}	Experimental error
E_T	Polarity of permeant or membrane
f	Fractional free volume
F_0, F	Mass in the feed tank at initial; at any time
F_V	Mass flow rate of feed stream
G	Mass collected in the organic phase
J, J_i	Total permeation flux; partial flux of permeant *i*
J_0	Pre-exponential factor in the permeation flux versus temperature
J_S	Permeation flux at steady state
k_l	Mass transfer coefficient in the boundary layer
l_m	Thickness of membrane
L	Time-lag in unsteady state permeation
$M_{org,recovered}$	Mass of aroma compound recovered
M_t, M_∞	Amount of permeant sorbed onto the membrane at any time; at equilibrium
P_F, P_M, P_P	Pressure at the feed side; inside the membrane; at the permeate side
P_0	Saturated pressure of mixture inside the membrane
P_m	Permeability across the membrane
P_V	Mass flow rate of permeate stream leaving the membrane chamber
Q	Amount of permeant collected in the permeate stream
R	Gas constant
R_t	Mass flow rate of retentate stream
S_i	Solubility coefficient of permeant *i*
t	Operating time
T	Operating temperature
u	Molar average velocity for mass transport
v_i, v_j, v_m	Molar volume of permeant *i*; of permeant *j*; of membrane
W	Mass (or mass flow rate) of water phase (or water phase stream)
W_0, W_t, W_∞	Mass of sample (membrane) at initial; at any time; at equilibrium

x	Distance across the membrane
$x_{F,i}$	Mass fraction of permeant i in the feed solution
x_F, x_G	Mass fraction of aroma compound in the feed stream; in the organic phase
x_P, x_R, x_W	Mass fraction of aroma compound in the permeate stream; in the retentate stream; in the water phase
$X_{m,i}$	Mass fraction of permeant i sorbed onto membrane on the basis of dry membrane
X_{pp}	Mass fraction of permeant propyl propionate in the feed solution
X_s, X_f	Mol fraction of the more permeable component on the membrane surface; in the bulk feed
y_i	Mol fraction of component I
Y, $\bar{Y}$	Measured points; the average value of measurements

Greek symbols

α	Separation factor (selectivity)
α_D	Diffusivity selectivity
α_S	Solubility selectivity
β	Enrichment factor
γ_i	Activity coefficient of permeant i
δ	Solubility parameter of compound
δ_m, δ_i, δ_j	Solubility parameter of membrane, of permeant i; of permeant j
δ_p, δ_d, δ_h	Polarity due to polar forces; due to dispersion forces; due to hydrogen bonds
κ	Proportional (empirical) constant in diffusivity dependency of permeant concentration
λ	Jump length in the polymeric matrix
μ_i, μ_i^0	Chemical potential of permeant i; of pure i at a reference pressure of P_i^0
ρ	Density of compound
ρ_m	Density of dry membrane
σ_{ij}	Interfacial tension between permeant i and j
σ_{im}, σ_{jm}	Interfacial tension between permeant i and membrane m; between permeant j and membrane m
$1/\tau_0$	Vibration frequency of the bond in polymeric membrane
τ	Time needed to attain a sorbed mass of permeant at amount of a half of mass of permeant sorbed at equilibrium
τ_P	Dwell time determined by the strength of permeant-polymer interactions
χ_{im}	Interaction parameter between permeant i and membrane
ΔG_{imj}	Total Gibbs free energy of the mixing of permeants i, j immersed in membrane m
Δ_{Pm}	Solubility parameter difference between permeant and membrane
Φ_c	Degree of crystallinity of polymeric membrane
ω_0, ω	Weighing factors attached on an empirical correlation to predict the preferential sorption based on the solubility parameters

CHAPTER 1
Overview of the Research

1.1 Introduction

Nowadays, aroma compounds are being widely utilized in food, pharmaceutical and cosmetic products. These compounds are usually used as additives for flavoring in food and medical products (medicines), and fragrance in cosmetic (particularly perfume) products due to their pleasant taste or odor. Aroma compounds consist of several functional organic groups including ester, aldehyde, aromatic, ether, amine, ketone, etc. They can be synthesized chemically from aromatic group and its derivatives or through esterification reactions. There are now several hundreds of companies around the world in the aroma compound business either with chemical synthesis or natural source recovery.

In addition to chemical synthesis, aroma compounds with a wide range of varieties can be recovered from various natural sources (including fruits, vegetables and plants) which are enormous and renewable, thereby making them a low cost raw material for aroma compounds. The market price of naturally occurring aroma products is often much higher than the synthetic ones. Obviously, from an economical point of view, the recovery of aroma compounds from natural sources is a viable route.

Natural aroma compounds usually exist at very low concentrations, typically at part per million (ppm) levels (Borjesson *et al.*, 1996). To recover the aroma compounds at a purity of interest for practical applications, a suitable separation process must be applied. Currently, conventional techniques including solvent extraction, flash distillation and adsorption are being used in industry (Lipnizki *et al.*, 2002). These techniques, unfortunately, suffer from such problems as product contamination and degradation as well as high energy consumption (Schafer *et al.*, 1999; Karlsson and Tragardh, 1997). In extraction, a specific solvent is utilized to attract the component that needs to be isolated, and subsequent separation is required to take apart the desired component from the solvent. If the latter separation is not

properly done, the final product will be contaminated by the solvent, which may generate a large extent of toxicity. Distillation is not only costly due to its high energy consumption but also unsuitable for heat sensitive products. At a high operating temperature, the natural properties of aroma will be destroyed (degradation) and oxidation may also occur, converting the aroma into other compounds. These challenges inspire and encourage the development of a safer and more economical separation technique.

Pervaporation (permeation-vaporization), a membrane separation process, is considered as one of the potential alternatives to overcome the aforementioned challenges. Its inherent advantages are: no entrainer addition and thus no contamination, low energy consumption, high selectivity, environmental friendliness, easy operation, space savings and easy installation (Lipnizki *et al.*, 2002; Asada, 1991). Pervaporation has been successfully developed for the dehydration of alcohols (especially ethanol and isopropanol) and has now become well established in industries. Another developing application was for removal of volatile organic compounds from contaminated water in wastewater treatment. These two different applications (one to remove water and the other to remove organics) imply that by using appropriate selective membranes (either hydrophilic or hydrophobic), pervaporation can be used to separate various mixtures, including recovery of aroma compounds from aqueous solutions. In the latter case, a very low concentration of aroma compounds in aqueous solutions will need to be removed to attain a high concentration of aroma compounds in the permeate. For this purpose, a hydrophobic (or organophilic) membrane, through which aroma compounds permeate preferentially over water, is required.

In fact, the separation of aroma compounds from aqueous solutions using membranes has been investigated intensively. Baudot and Marin (1997) has compiled the results of pervaporation on more than 50 aroma compounds with different functional organic groups (lactones, esters, alcohols, aldehydes, sulphur compounds, ketones, pyrazines and hydrocarbons) using poly(ether-block-amide) (PEBA), poly(dimethylsiloxane) (PDMS) and other membranes. The selectivity of pervaporation was shown to be much higher than what would be obtained by distillation based on liquid-vapor equilibrium. Although PEBA and PDMS were found to have different pervaporation performance in terms of permeation flux

and selectivity, depending on types of aroma compounds and process conditions, they both showed reasonable organic flux (up to 28.2 g/m^2.h) and good selectivity (up to 3,150). Other membranes, such as poly(vinylidene fluoride-*co*-hexafluoropropene) (Tian *et al.*, 2005) and silicalite-filled silicone (Baudot *et al.*, 1999) membranes have also been tested and showed good performance (2,000 g/m^2.h of organic flux and 180 of selectivity). Pilot-scale tests have been conducted by the Membrane Technology and Research Inc. in California and the Agrotechnology and Food Innovations in the Netherlands. Unfortunately, the recovery of aroma compounds from aqueous solutions has so far not been commercialized on industrial scales. One of the reasons, and possibly the key reason, is economics of process scale up; pervaporation is competitive on a relatively small scale, but less efficient for processing very large capacities as compared to conventional technologies (Baker, 2004).

1.2 Problem Statement

Besides economical reasons, there are several critical factors, some of which are related one another, that must be taken into account in order for the pervaporation process to succeed (Feng, 1994). The correlation among these factors is illustrated in Figure 1.1.

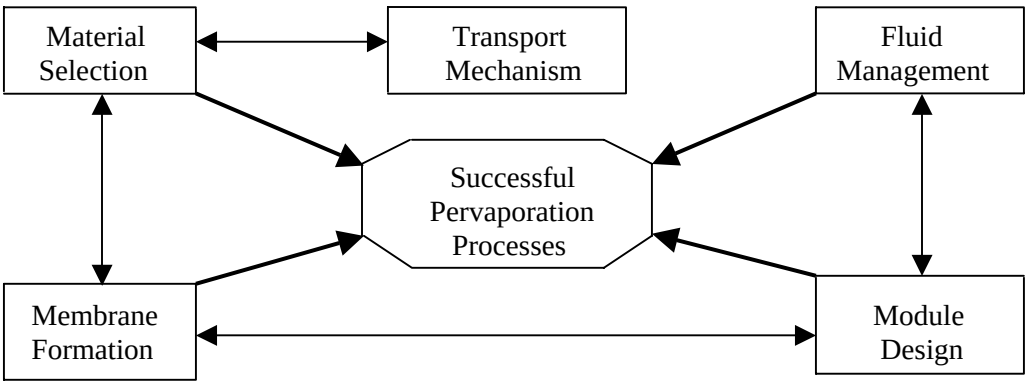

Figure 1.1 The critical factors controlling the successful pervaporation process.

A successful pervaporation process can be measured in terms of permeation flux (productivity), selectivity, reliability and stability. All the factors above should be addressed in order for the process to be used commercially.

Considering that the recovery of aroma compounds from aqueous solutions by pervaporation is very promising, this thesis draws attention to such recovery process as its general topic. Most studies on the pervaporation have focused on improving the pervaporation performance based on membrane material and process condition modifications. In addition to addressing these aspects, the thesis work will attempt to examine some new ideas dealing with process design. The thesis consists of both experimental and modeling (parametric) studies as illustrated in Figure 1.2.

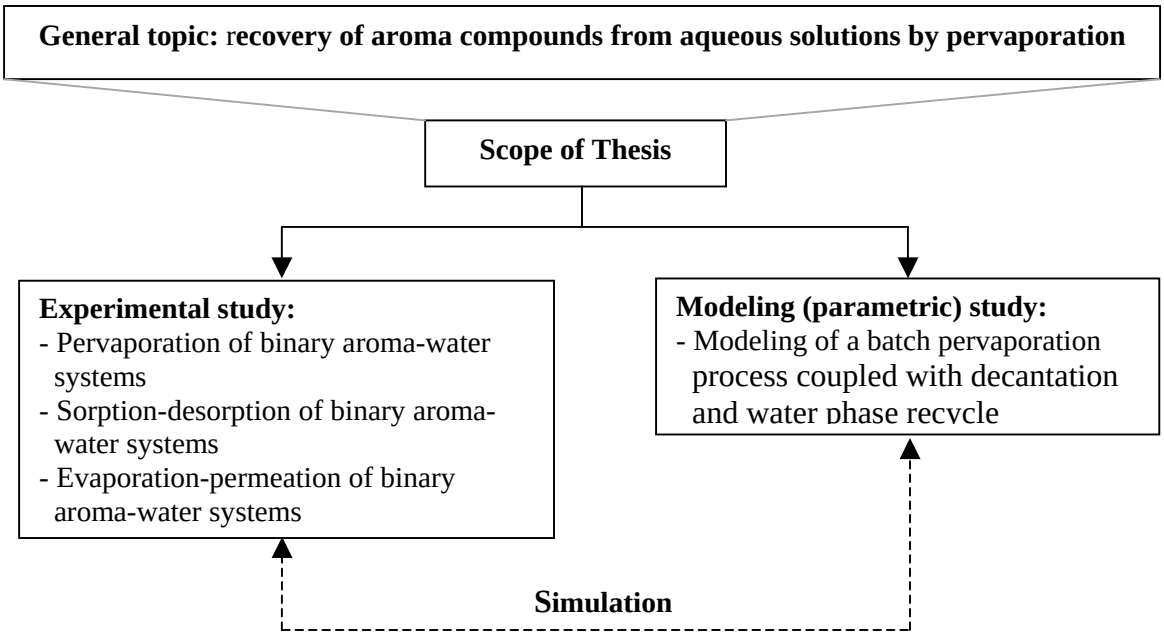

Figure 1.2 Schematic of the scope of thesis.

In the experimental study, a series of experimental runs of pervaporation and sorption-desorption for three model binary aroma-water systems using PEBA membranes will be carried out. As well, evaporation-permeation (or evapermeation), as a possible alternative mode of operation to pervaporation, will also be tested on one of the three representative systems. In the modeling part, on the other hand, an issue pertaining process design in pervaporation is highlighted. The experimental data obtained from the experimental work are used to simulate the parametric model studied.

1.3 Research Objectives

The objectives of this study are described below,

- To investigate the effect of process conditions (i.e., feed concentration and operating temperature) on the pervaporation performance for the separation of three representative binary aroma-water solutions using PEBA membranes.
- To investigate the transport properties (i.e., diffusivity and solubility) of the binary aroma-water solutions in the PEBA membranes.
- To investigate the performance of evapermeation for aroma-water mixtures through PEBA membranes as a potential alternative to pervaporation for aroma separation.
- To provide a mathematical model for a batch pervaporation process with two recycle streams for enhanced recovery of low solubility aroma compounds from aqueous solutions.

In the experimental work, three aroma compounds representing different categories were chosen, i.e., propyl propionate (ester), C_6-aldehyde (aldehyde) and benzaldehyde (aromatic). These model aroma compounds were selected because of their similarities in the number of carbons and type of element constituent (CHO) and their presence in natural sources. The use of PEBA membrane (grade 2533) was based on its well-known organophilic properties and good mechanical stability. The pervaporation experiments were performed at various feed concentrations and operating temperatures because they were important variables bearing much more significant effects on pervaporation performance than others (e.g., feed flow rate, feed pressure). As a comparison to pervaporation, the performance of evapermeation for aroma separation was also tested on one of the three systems (i.e., propyl propionate-water).

Since permeation involves sorption and diffusion, the solubility and diffusivity for the three binary systems were determined from permeation and sorption-desorption experiments. As a comparison, the time-dependent sorption was used to determine the diffusivity. In this case, sorption experiments at various times were conducted. Note that propyl propionate-water system was studied more systematically than the other two aroma compounds because this particular compound had not been investigated previously in the literature. Though the other two aroma systems have been studied by other researchers, but different membranes, mainly PDMS membranes, are used (Lamer *et al.*, 1996; Souchon *et al.*, 1997; Bengtson *et al.*, 1989; Zhang and Matsuura, 1991). PEBA with high polyether content is expected to be more permselective than PDMS membranes for aroma compound separation.

The modeling study deals with process design modifications in the aroma compound recovery processes. It was reported that using organophilic membranes, pervaporation was able to concentrate the aroma compounds with a high separation factor (Baudot and Marin, 1997). In case of recovery of low solubility aroma compounds in water, the concentration of permeate attained by pervaporation can be much higher than the solubility limit. As a consequence, a phase separation takes place in the permeate stream, resulting in two phases: an organic phase and a water phase. The organic phase will contain essentially pure aroma compound, and the water phase still contains a certain amount of aroma compound. Thus, not all aroma compounds in the permeate stream can be recovered. Studies on modifications of the process design are very limited. As mentioned above, most studies focus on improving the pervaporation performance of the membrane based on modifications in the membrane material or operating conditions. In order to enhance the recovery of aroma compound where a phase separation takes place in the permeate collector, the utilization of stream recycle to further recover the aroma compound from the water phase is important. This thesis thus attempts to provide a mathematical model to describe a batch process with stream recycle. A batch process is considered here because pervaporation is very competitive for processing small capacities. From the model, the extent of improvement in the recovery of aroma compounds due to the inclusion of the water phase recycle, as compared to the conventional pervaporation process, is demonstrated. In addition, the model will allow for determining the process parameters at any instant, including the permeation rate, the compositions in the feed

tank, permeate stream and retentate stream, the quantity of product in the permeate collector and the quantity of the aqueous phase.

1.4 Structure of the Thesis

The various chapters in the thesis are arranged based on the research objectives that will be achieved in this work. The introduction, given in Chapter 1, describes the rationale for the research topic, identification of problems, and objectives of the research. The theoretical background related to general pervaporation processes (including definition of pervaporation, pervaporation performance, transport mechanism, transport properties, process variables, selection of membrane material, and process design), and a literature review on particular to pervaporation for aroma compound recovery are given in Chapter 2.

Chapters 3 to 5 present the experimental studies conducted in this work. Chapter 3 deals with pervaporation for separation of three binary aroma-water mixtures using PEBA membranes. The pervaporation performance (i.e., permeation flux and selectivity) as a function of process variables (i.e., feed concentration and operating temperature) is studied in this chapter. Chapter 4 highlights the transport property aspects (i.e., solubility and diffusivity) for the permeation of three aroma-water systems through the PEBA membrane, which were determined from sorption and desorption experiments. The dependency of solubility and diffusivity on aroma concentration is discussed in this chapter. As an alternative operating mode to pervaporation, for the separation using non-porous membranes, evapermeation, was also tested for aroma compound recovery, and this is presented in Chapter 5. In this chapter, a comparison of the performance between evapermeation and pervaporation is also made, which shows that the two modes of operation using the same membrane will yield different separation performance.

Chapter 6 presents a model on batch pervaporation for aroma recovery where the permeate is phase separated. The extent in the improvement of aroma compound recovery by recycling the water phase in the permeate decanter is demonstrated. Finally, Chapters 7 and 8 contain the conclusions drawn from the study and the recommendations for future research.

CHAPTER 2
Background and Literature Review

2.1 Introduction

Many reports in the area of pervaporation have been published in the form of short communications, research articles, books and patents. This chapter will review the theoretical aspects as well as other relevant works.

2.2 Pervaporation

Pervaporation (which refers to permeation and vaporization) is used to separate liquid mixtures by applying a non-porous permselective membrane. This technique, originally called liquid permeation, has subsequently been termed as pervaporation in order to emphasize the fact that the permeant undergoes a phase change from liquid to vapor during its transport through the membrane (Neel, 1991). The feed in liquid state is in contact with one side of the membrane, and the permeate in vapor state is obtained from the other side. The non-permeated components in the retentate are usually recycled into the feed stream for further recovery. A simple scheme of pervaporation process is given in Figure 2.1.

The term of pervaporation was first introduced by Kober (1917) when he attempted to concentrate organics from aqueous solutions using cellulose nitrate. However, investigations concerning the selective transport of hydrocarbon-alcohol mixtures through a thin rubber sheet were actually done by Kahlenberg in 1906. Most of the subsequent efforts focused on the enhancement of membrane performance particularly for ultra-filtration and reverse osmosis on laboratory scales. Such studies continued until the 1960s when Loeb and Sourirajan (1963) developed a new technique for membrane preparation, i.e., the phase inversion technique, to synthesize an asymmetric cellulose acetate membrane for reverse osmosis applications. Using this technique, a membrane with an ultra thin dense layer supported on a thicker porous support could be made and thus defect-free membranes with

much higher permeation flux (10 times) were obtained. This has encouraged pervaporation for potential uses on industrial scales, and extensive work has been done along this line.

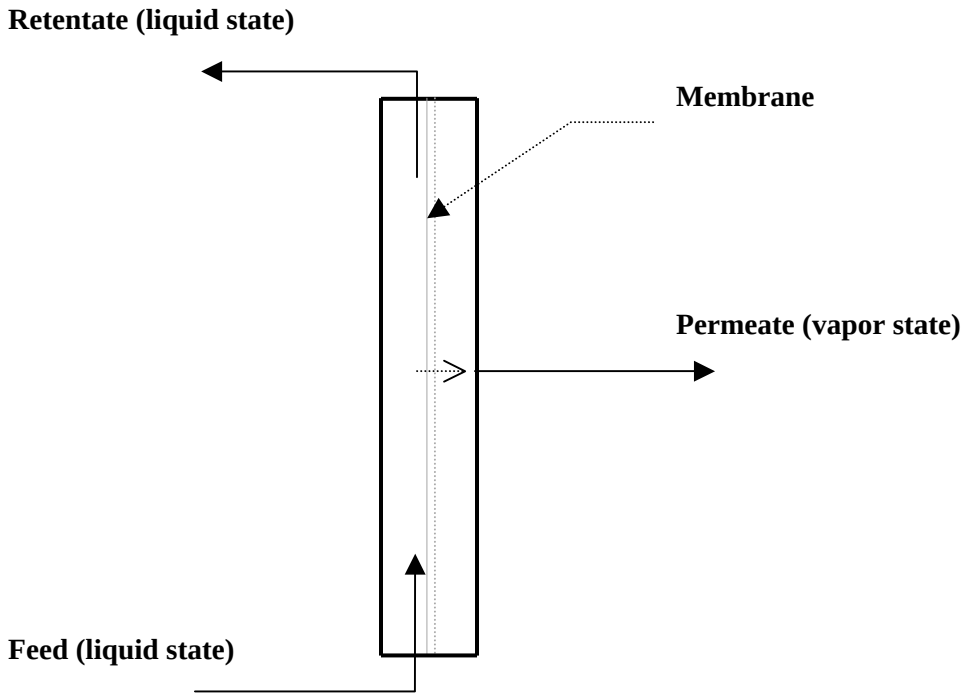

Figure 2.1 Schematic pervaporation process.

Binning *et al.* (1961) studied pervaporation extensively for separation of hydrocarbon mixtures using non-porous polyethylene films. One of the valuable contributions they made is to modify polymeric membranes by irradiation cross-linking. By this way, the membrane becomes more stable at high temperatures (up to 150^{o}C) at which the permeation flux could be high enough for industrial applications. During the same period, systematic and intensive studies on pervaporation and vapor permeation were also conducted by Fries and Neel (1965)

and Aptel *et al.* (1972; 1974a; 1974b). They contributed to the development of qualitative prediction of preferential permeation based on the membrane-permeant affinity.

In 1982, pervaporation eventually came into commercial application after a successful pilot plant run in Sao Paolo, Brazil by Gesellschaft fur Trenntechnik (GFT) for dehydration of ethanol-water mixtures produced from fermentation of biomass. A few years later, more than 20 plants with various capacities (2,000 to 15,000 L/day) were built in Europe and the United States (Tusel and Ballweg, 1983). Other companies, LURGI G.m.b.h. and MITSUI Engineering and Shipbuilding Co. also came into pervaporation business under GFT license. In 1988, the first large scale pervaporation plant was established in Bethenville (France) under GFT–Carbone Lorraine with a capacity of 150,000 L/day of dry ethanol. Around one decade later (1996), pervaporation for removal of volatile organic compounds from contaminated water was developed by Membrane Technology and Research.

Pervaporation research has been extended from dehydration of organics to the removal of organics from aqueous solutions as well as organic-organic separations. In particular, the recovery of aroma compounds from dilute aqueous solutions is one of the potential applications for organic removal from aqueous solutions. The word “aroma” derives from Greek, which means fragrance. Aroma compounds include a wide variety of substances that have pleasant smell (Kirk and Othmer, 1963). These compounds may consist of several functional organic groups including lactone, ether, ester, aldehyde, ketone, alcohol and aromatic, and are available in many natural sources. In order to assess the intensity of aroma released by different aroma compounds, the aroma threshold value (ATV), which is defined as the lowest concentration in a water solution at which the aroma compound is perceptible, is often used (Simpson, 1979). The ATV depends on the types of aroma compounds, but typically in ppm (part per million) levels.

Aroma compound-water separation by pervaporation has been studied intensively. Most studies focus on determining the pervaporation performance of various aroma-water systems based on membrane material and process conditions. The modifications of membrane materials and membrane preparations include polymer synthesis (blending,

copolymerization, etc.) and cross-linking to control the hydrophobicity and the degree of swelling. Feed composition and operating temperature were found to be the most important process variables; some investigations also studied the effect of other process conditions such as membrane thickness and permeate pressure. By 1997, over 50 aroma compounds from different functional organic groups have been investigated for pervaporation recovery using different polymeric membranes, as listed in Table 2.1. The separation factor (α) given in the table shows the selectivity of the membrane in separating the aroma compound from aqueous solution, and is defined as the comparison of aroma compound and water concentrations between in the permeate stream and in the feed stream.

Table 2.1 Investigations on pervaporation separation of aroma compounds from aqueous solutions conducted up to 1997 (Baudot and Marin, 1997).

Aroma compound	Formula	Flavor	Membrane (thickness)	Process conditions ([feed], T_F, P_P)	Organic flux ($g/m^2.h$)	Separation factor (α)
Lactones:						
- γ-Butirolactone	$C_4H_6O_2$	Sweet, caramel	PEBA GKSS (50 μm)	900 ppm		2.2
- δ-Decalactone	$C_{10}H_{18}O_2$	Coconut, peach	PDMS BRAUN	100 mg/L, 55°C	0.021	1.3
			PDMS GFT	100 mg/L, 25°C, 50 Pa	0.02	3
			PDMS GFT	100 mg/L, 45°C, 50 Pa	0.25	10
- γ-Decalactone	$C_{10}H_{18}O_2$	Peach	PEBA GKSS	60-100 ppm, 40°C	0.5-1.6	
			PEBA GKSS (30 μm)	50 ppm		151
			PEBA GKSS (100 μm)	100 ppm, 30°C		278-390
			PEBA GKSS (100 μm)	100 ppm, 40°C		395-526
			PDMS BRAUN	100 mg/L, 30-60°C	0.22-0.8	11-23
			PDMS GFT	85-550 ppm, 25°C, 60 Pa	0.26-0.8	30-41
			PDMS GFT	100-550 ppm, 25°C, 50 Pa	0.2-1.8	30-42
			PDMS GFT	100 mg/L, 45°C, 50 Pa	0.8	30
			PDMS GFTz	100 ppm, 25°C, 35-60 Pa	0.24	46
			PDMS 1060	500 ppm, 30°C, 250-2,000 Pa	1-0.09	14-1.9
			PDMS DC (130 μm)	100 ppm, 25°C, 35-60 Pa	0.24	187
- γ-Octalactone	$C_8H_{14}O_2$	Coconut, creamy	PDMS BRAUN	100 mg/L, 35-60°C	0.1-0.3	40-91
			PDMS GFT	100 mg/L, 25°C, 50 Pa	0.075	9
			PDMS GFT	100 mg/L, 45°C, 50 Pa	0.35	14
- 6-Pentyl α-pyrone	$C_{10}H_{14}O_2$	Coconut	PEBA GKSS	< 1,000 ppm, 25°C		10-20
			PEBA GKSS (30 μm)	1,000 ppm, 68°C, < 500 Pa	4.3	8.9
			PEBA GKSS (50 μm)	360 ppm, 68°C, < 500 Pa	1.4	15.4
			PEBA GKSS (150 μm)	200 ppm, 68°C, < 500 Pa	0.6	31

Table 2.1 Continued

Aroma compound	Formula	Flavor	Membrane (thickness)	Process conditions ([feed], T_F, P_P)	Organic flux ($g/m^2.h$)	Separation factor (α)
Esters:						
- Butyl acetate	$C_6H_{12}O_2$		PDMS GFT	11.2 ppm, 5°C, 500-600 Pa		112
			PDMS GFT	12 ppm, 5°C, 600 Pa		91-133
- Butyl butyrate	$C_8H_{16}O_2$	Fruity	PDMS GFT	2.2 ppm, 5°C, 500-600 Pa		125
- Ethyl acetate	$C_4H_8O_2$	Ethereal	PDMS GFT	90-4,800 ppm, 25°C, 60 Pa	1.1-58	142-143
			PDMS GFT	500 ppm, 33°C, 200-2,000 Pa, 0-10 % ethanol		312-151
			PDMS GFT	500 ppm, 36°C, 0-10 % ethanol	8.5-11	348-235
			PDMS GFT	500 ppm, 40°C, 200-2,000 Pa, 0-10 % ethanol		243-177
			PDMS GFT	500 ppm, 32-45°C, 700 Pa	2-4	
			PDMS GFT	500 ppm, 32-45°C, 700 Pa, 10 % ethanol	2.1	
			PDMS GFT	500 ppm, 32°C, 2,700 Pa		88
			PDMS GFT	500 ppm, 32°C, 2,700 Pa, 10 % ethanol		56
			PDMS 1060	44 ppm, 6-35°C, 100 Pa, 9.6 % ethanol	0.9-1.1	192-163
			PDMS GFTz	100 ppm, 25°C, 35-60 Pa	1.31	261
			PDMS GFTz	100 ppm, 30°C, 300-2,000 Pa, Re = 100	0.77-0.31	194-148
			PDMS GFTz	100 ppm, 30°C, 300-2,000 Pa, Re = 600	1.38-1.11	131-114
			PDMS DC (130 μm)	100 ppm, 25°C, 35-60 Pa	1	382
			PDMS DC (130 μm)	100 ppm, 25°C, 50 Pa, $Re = 10^5$	0.52	472
			PDMS DC (130 μm)	100 ppm, 25°C, 50 Pa, multi-component mixtures	0.50-0.59	

Table 2.1 Continued

Aroma compound	Formula	Flavor	Membrane (thickness)	Process conditions ([feed], T_F, P_P)	Organic flux ($g/m^2.h$)	Separation factor (α)
- Ethyl butyrate	$C_6H_{12}O_2$	Pineapple	PDMS GFT	100 ppm, 5°C, 500-600 Pa	3-5	114
			PDMS GFT	500 ppm, 32-45°C, 700 Pa, 10 % ethanol	3-3.5	
			PDMS GFT	500 ppm, 31°C, 2,700 Pa		151
			PDMS GFT	500 ppm, 31°C, 2,700 Pa, 10 % ethanol		56
			PDMS GFT	500 ppm, 36°C, 0-10 % ethanol	22-28.2	1,215-694
			PDMS GFT	100 ppm, 30°C, 5 Pa	3.2	253
			PDMS GFT	100 ppm, 25°C, 35-60 Pa	2.53	299
			PDMS GFTz	100 ppm, 25°C, 35-60 Pa	2.62	735
			PDMS GFTz	100 ppm, 30°C, 300-2,000 Pa, Re = 100	1.50-0.52	375-253
			PDMS GFTz	100 ppm, 30°C, 300-2,000 Pa, Re = 600	4.73-3.64	465-382
			PDMS DC (130 μm)	100 ppm, 25°C, 35-60 Pa	2.2	1,635
			PDMS DC (130 μm)	100 ppm, 25°C, 50 Pa, Re = 10^5	2.61	2,413
			PDMS DC (130 μm)	100 ppm, 25°C,50 Pa, multi-component mixtures	2.6-3.4	
- Ethyl hexanoate	$C_8H_{16}O_2$	Fruity	PDMS GFT	100 ppm, 25°C, 35-60 Pa	3.83	417
			PDMS GFT	100 ppm, 30°C, 5 Pa	4	271
			PDMS GFTz	100 ppm, 25°C, 35-60 Pa	3.44	1,068
			PDMS GFTz	100 ppm, 30°C, 300-2,000 Pa, Re = 100	1.21-0.70	310-344
			PDMS GFTz	100 ppm, 30°C, 300-2000 Pa, Re = 600	6.38-4.16	636-440
			PDMS DC (130 μm)	100 ppm, 25°C, 35-60 Pa	3.05	2,320
			PDMS DC (130 μm)	106 ppm, 25°C, 50 Pa	8.13	4,729
			PDMS DC (130 μm)	100 ppm, 25°C, 50 Pa, multi-component mixtures	8.13-6.18	
- Ethyl isobutyrate	$C_6H_{12}O_2$	Citrus	PDMS GFT	100 ppm, 25°C, 35-60 Pa	2.72	293
			PDMS GFTz	100 ppm, 25°C, 35-60 Pa	1.65	549
			PDMS DC (130 μm)	100 ppm, 25°C, 35-60 Pa	2.11	1,641

Table 2.1 Continued

Aroma compound	Formula	Flavor	Membrane (thickness)	Process conditions ([feed], T_F, P_P)	Organic flux ($g/m^2.h$)	Separation factor (α)
- Ethyl isobutyrate	$C_6H_{12}O_2$	Citrus	PDMS DC (130 μm) PDMS DC (130 μm)	85 ppm, 25°C, 50 Pa 100 ppm, 25°C, 50 Pa, multi-component mixtures	2.69 2.69-3.87	2,023
- Ethyl 2-methyl butyrate	$C_7H_{14}O_2$	Green	PDMS GFT	1.3 ppm, 5°C, 500-600 Pa		122
- Ethyl propionate	$C_5H_{10}O_2$	Sweet,	PDMS (60 μm)	5,000 ppm, 35°C	35	134
- Hexyl acetate	$C_8H_{16}O_2$	Apple	PDMS GFT PDMS GFT PDMS GFT	5 ppm, 5°C, 500-600 Pa 2.2 ppm, 5°C, 600 Pa 2.2 ppm, 20°C, 600 Pa		83 65-120 26-39
- Isoamyl acetate	$C_7H_{14}O_2$	Banana	PDMS GFT PDMS GFT	1 ppm, 33°C, 250 Pa, 10 % ethanol 9 ppm, 5°C, 500-600 Pa	0.0306	508 112
- Methyl anthranilate	$C_8H_9NO_2$	Grape	PDMS-PC PDMS-PC PDMS 1070 PEBA (1mm)	50 ppm, 33-60°C, 660 Pa 50 ppm, 33°C, 660 Pa, 0-20 % ethanol 50 ppm, 33°C, 400 Pa 50 ppm, 33°C, 400 Pa	0.028-0.144 0.02-0.022 0.026 0.078	11-19 9-4 9.3 15.3
- Methyl benzoate	$C_8H_8O_2$	Fruity	PDMS GFT PDMS GFT PDMS GFTz PDMS DC (130 μm)	100-900 ppm, 25°C, 60 Pa 100 ppm, 25°C, 35-60 Pa 100 ppm, 25°C, 35-60 Pa 100 ppm, 25°C, 35-60 Pa	2.1-18.3 1.92 1.75 1.63	267-222 251 539 1,228
- Methyl lactate	$C_4H_8O_3$		PDMS 1060	60 ppm, 6-35°C, 100 Pa, 9.6 % ethanol	0.011-0.09	1.7-2.9

Table 2.1 Continued

Aroma compound	Formula	Flavor	Membrane (thickness)	Process conditions ([feed], T_F, P_P)	Organic flux ($g/m^2.h$)	Separation factor (α)
Alcohols:						
- Benzyl alcohol	C_7H_8O	Burning, Fruity	PDMS GFT	100 ppm, 25°C, 60 Pa	0.02	2.5
			PDMS DC (100 μm)	120-790 ppm, 25°C, 200 Pa		7.5-2.4
			PDMS GE	43.4 ppm, 24°C, 66.7-900 Pa	0.034-0.001	12.2-0.694
			PDMS GE	43.4 ppm, 24-40°C, 66.7 Pa	0.034-0.51	12.2-83
			PDMS GE	43.4-1,020 ppm, 24°C,66.7 Pa	0.034-0.47	12.2-5.9
- o-cresol	C_7H_8O	Musty	PEBA GKSS (46 μm)	100 ppm, 50°C, 50-200 Pa	2.8	152
- Hexanol	$C_6H_{14}O$	Alcoholic	PDMS GFT	29 ppm, 5°C, 500-600 Pa		10
			PDMS GFT	13 ppm, 5°C, 600 Pa		4-10
			PDMS GFT	13 ppm, 5°C, 600 Pa		4-22
			PDMS 1060	3 ppm, 6-35°C, 100 Pa, 9.6 % ethanol	0.008-0.09	25-55
- 3-Hexene-1-ol	$C_6H_{12}O$	Fresh, green grass	PDMS GFT	1 ppm, 33°C, 250 Pa, 10 % ethanol	0.00178	29.6
- Isoamyl alcohol	$C_5H_{12}O$	Whisky	PDMS GFT	100 ppm, 33°C, 250 Pa, 10 % ethanol	0.174	29
			PDMS	17 ppm, 5°C, 500-600 Pa		11
			PDMS 1060	214 ppm, 6-35°C, 100 Pa, 9.6 % ethanol	0.3-1-1	17-29
- Isobutanol	$C_4H_{10}O$	Medicinal	PDMS 1060	44 ppm, 100 Pa, 6-35°C, 10 % ethanol	0.06-0.3	13-18
- Linalool	$C_{10}H_{18}O$	Light floral	PDMS GFT	1 ppm, 33°C, 250 Pa, 10 % ethanol	0.0745	124
			PDMS GFT	50 ppm, 25°C, 200 Pa, 10 < Re < 10000	0.28-0.78	
			PDMS 1060	50 ppm, 20°C, 100 Pa, 0-12 % ethanol	0.47	129-58

Table 2.1 Continued

Aroma compound	Formula	Flavor	Membrane (thickness)	Process conditions ([feed], T_F, P_P)	Organic flux ($g/m^2.h$)	Separation factor (α)
- Linalool	$C_{10}H_{18}O$	Light floral	PDMS SEMPAS	600-900 ppm, 25°C, 50 Pa	6-5	74
			PDMS DC (170 µm)	800 ppm, 25°C, 50 Pa	11	6,557
			PDMS DC (250 µm)	800 ppm, 25°C, 50 Pa	14.5	2,500
			PDMS DC (510 µm)	800 ppm, 25°C, 50 Pa	16.5	3,050
			SBR SEMPAS	600-900 ppm, 25°C, 50 Pa	7.5-5.6	120
- Octene 3-ol	$C_8H_{16}O$	Mushroom	PDMS GFT	50-1,700 ppm, 30°C, 5 Pa	1-23	101-280
			PDMS GFT	100 ppm, 30°C, 5 Pa	1.85	163
			PDMS GFT	100 ppm, 25°C, 35-60 Pa	1.87	195
			PDMS GFTz	100 ppm, 30°C, 5 Pa	1.5	386
			PDMS GFTz	100 ppm, 25°C, 35-60 Pa	1.90	406
			PDMS GFTz	100 ppm, 30°C, 300-2,000 Pa, Re = 100	0.80-0.40	204-195
			PDMS GFTz	100 ppm, 30°C, 300-2,000 Pa, Re = 600	1.79-0.97	171-99
			PDMS DC (130 µm)	87 ppm, 25°C, 50 Pa	1.77	1,430
			PDMS DC (130 µm)	100 ppm, 25°C, 35-60 Pa	1.73	1,317
			PDMS BRAUN	31 ppm, 30°C		95
			PDMS BRAUN	31 ppm, 45°C	0.32	209-258
- 1-Pentene 3-ol	$C_5H_{10}O$	Butter green	PDMS 1060	10 ppm, 20°C, 100 Pa, 0-12 % ethanol	0.06	40-20
			PDMS 1060	10 ppm, 25°C, 100 Pa, 10 < Re < 10,000	0.06	
- 2-Phenylethanol	$C_8H_{10}O$	Rose	PDMS DC (150 µm)	1,000 ppm, 25°C, 60 Pa	0.04	38
			PDMS GFT	100 ppm, 33°C, 250 Pa, 10 % ethanol	0.00163	2.72
			PDMS GFT	2.89 g/L, 30°C	3.79	5.5
			PDMS GFT	2.86 g/L, 30°C	3	5.73
- Thymol	$C_{10}H_{14}O$	Woody, burnt	PEBA GKSS (46 µm)	100 ppm, 50°C, 50-200 Pa	8.4	395
- 2,5-Xylenol	$C_8H_{10}O$	Creosote, sweet	PEBA GKSS (46 µm)	100 ppm, 50°C, 50-200 Pa	3.5	215

Table 2.1 Continued

Aroma compound	Formula	Flavor	Membrane (thickness)	Process conditions ([feed], T_F, P_P)	Organic flux ($g/m^2.h$)	Separation factor (α)
Aldehydes:						
- Benzaldehyde	C_7H_6O	Almond	PDMS GFT	75-1,400 ppm, 25°C, 60 Pa	1-15	101-277
			PDMS GFT	100 ppm, 25°C, 35-60 Pa	1.04	116
			PDMS GFT	100 ppm, 25°C, 70 Pa	1.04	280
			PDMS GFTz	100 ppm, 25°C, 35-60 Pa	0.71	291
			PDMS DC (30 μm)	87 ppm, 25°C, 60 Pa	1.75	498
			PDMS DC (60 μm)	100 ppm, 25°C, 60 Pa	1.48	521
			PDMS DC (100 μm)	78-132 ppm, 25°C, 200 Pa		24-90
			PDMS DC (130 μm)	100 ppm, 25°C, 60 Pa	0.91	591
			PDMS DC	100 ppm, 25°C, 35-60 Pa	0.94	637
			PDMS DC (150 μm)	100 ppm, 25°C, 60 Pa	0.93	1,074
- Furaldehyde	$C_5H_4O_2$	Woody, almond	PDMS 1060	50 ppm, 100 Pa, 6-35°C, 9.6 % ethanol	0.0001-0.01	<1
- Hexanal (C_6-aldehyde)	$C_6H_{12}O$	Green	PDMS GFT	1 ppm, 33°C, 250 Pa, 10 % ethanol	0.0125	207
- trans 2 Hexenal	$C_6H_{10}O$	Green, almond	PEBA GKSS (50 μm)	110 ppm		142
			PEBA GKSS (25 μm)	110 ppm		98
			PEBA GKSS (5 μm)	110 ppm		4
			PDMS GKSS (10 μm)	110 ppm		26
			PDMS GFT	5 ppm, 5°C, 500-600 Pa		44
			PDMS GFT	10 ppm, 5°C, 600 Pa		38-57
			PDMS GFT	10 ppm, 20°C, 600 Pa		19-36
			PDMS 1060	20 ppm, 20°C, 0-12 % ethanol	0.5	368-189
			PDMS 1060	87 ppm, 25°C, 10 < Re < 10,000	0.12-0.61	
- 2-Methyl butanol	$C_5H_{12}O$	Cocoa, coffee	PDMS 1060	7 ppm, 25°C, 200 Pa, 10 < Re < 10,000	0.03-0.24	
			PDMS 1060	7 ppm, 20°C, 200 Pa, 0-12 % ethanol	0.21	389-283

Table 2.1 Continued

Aroma compound	Formula	Flavor	Membrane (thickness)	Process conditions ([feed], T_F, P_P)	Organic flux ($g/m^2.h$)	Separation factor (α)
- Methyl propanal	C_4H_8O	Pungent	PDMS 1060	9 ppm, 25°C, 200 Pa, 10 < Re < 10,000	0.06-0.13	
			PDMS 1060	9 ppm, 20°C, 200 Pa, 0-12 % ethanol	0.14	171-108
- Octanal	$C_8H_{16}O$	Citrus	PDMS GFT	100 ppm, 25°C, 35-60 Pa	2.85	379
			PDMS GFTz	100 ppm, 25°C, 35-60 Pa	3.22	1,082
			PDMS GFTz	100 ppm, 30°C, 300-2,000 Pa, Re = 100	0.91-0.59	232-285
			PDMS GFTz	100 ppm, 30°C, 300-2,000 Pa, Re = 600	5.03-3.46	495-364
			PDMS DC (130 μm)	100 ppm, 25°C, 35-60 Pa	2.97	2,145
S compounds:						
- Furfuryl mercaptan	C_5H_6OS	Fishy, oily	PDMS (1 μm)	46 ppm, 29°C	1.3	36
- Isobutyl thiazole	$C_7H_{11}NS$	Tomato leaves	PDMS GFT	100 ppm, 25°C, 35-60 Pa	1.38	189
			PDMS GFT	30°C, 70 Pa	1.86	179
			PDMS GFTz	100 ppm, 25°C, 35-60 Pa	1.26	460
			PDMS DC (130 μm)	100 ppm, 25°C, 35-60 Pa	1.31	1,249
- p-Mentha-8-thiol-3- one	$C_{10}H_{18}OS$	Black current	PDMS (60 μm)	30 ppm, 48°C	1.15	427
- S-methyl thiobutyrate	$C_5H_{10}OS$	Putrid, cabbage	PDMS 1070	15 ppm, 30°C, 285-2,490 Pa	0.17-0.03	292-96
			PEBA GKSS (70 μm)	15 ppm, 30°C, 285-2,490 Pa	0.3-0.14	1,227-707
			PEBA GKSS (70 μm)	50 ppm, 30°C, 260-2,200 Pa	1.01-0.63	841
			PEBA GKSS (70 μm)	50 ppm, 30°C, 260-2,200 Pa, culture medium	0.98-0.53	747
Ketones:						
- Acetoin	$C_4H_8O_2$	Buttery	PEBA	17 g/L, 50-95°C, 2,000-3,000 Pa		1.2-1.5
			PEBA	17 g/L, 50-70°C,2,000-3,000 Pa, fermentation broth		2-2.3
			PDMS GFT	17 g/L, 25-85°C, 2,500 Pa		0.6

Table 2.1 Continued

Aroma compound	Formula	Flavor	Membrane (thickness)	Process conditions ([feed], T_F, P_P)	Organic flux ($g/m^2.h$)	Separation factor (α)
- Diacetyl	$C_4H_6O_2$	Butter	PDMS 1070	70 ppm, 30°C, 240-2,500 Pa	0.144-0.072	15
			PDMS 1070	70 ppm, 50°C, 240-2,500 Pa	0.408-0.352	19
			PDMS-PC	200 ppm, 33°C, 650-3,000 Pa	0.15-0.4	38-35
			PDMS-PC	200 ppm, 25-43°C, 650 Pa	0.22-0.74	33-41
			PDMS-PC	20-2,000 ppm, 33°C, 650 Pa	0.044-63	40-38
			PEBA GKSS (70 μm)	70 ppm, 30°C, 220-2,500 Pa	0.038-0.019	17
			PEBA GKSS (70 μm)	70 ppm, 30°C, 220-2,500 Pa	0.087-0.060	18
- 2-Heptanone	$C_7H_{14}O$	Banana, fruity	PDMS DC (150 μm)	100 ppm, 25°C, 60 Pa	1.92	3,333
- 2-Nonanone	$C_9H_{18}O$	Rose, tea	PDMS DC (150 μm)	100 ppm, 25°C, 60 Pa	2.4	4,705
- 2-Octanone	$C_8H_{16}O$	Floral, acid	PDMS DC (150 μm)	100 ppm, 25°C, 60 Pa	2.1	3,947
- 3-Octanone	$C_8H_{16}O$	Spicy	PDMS DC (130 μm)	20 ppm, 60°C	0.1	1,561
			PDMS DC (130 μm)	60°C, oven emanation	0.8	3,203
			PDMS DC (130 μm)	20 ppm, 60°C, cooking meat water	0.7	2,118
Pyrazines:						
- 2,3 Diethyl pyrazine	$C_8H_{12}N_2$	Baked potato	PEBA GKSS (30 μm)	250 ppm		82
- 2,5 Dimethyl pyrazine	$C_6H_8N_2$	Nutty	PDMS GFT	100 ppm, 25°C, 35-60 Pa	0.13	15
- 2,5 Dimethyl pyrazine	$C_6H_8N_2$	Nutty	PDMS GFTz	100 ppm, 25°C, 350-600 Pa	0.06	14
			PDMS DC (130 μm)	100 ppm, 25°C, 35-60 Pa	0.03	21

Table 2.1 Continued

Aroma compound	Formula	Flavor	Membrane (thickness)	Process conditions ([feed], T_F, P_P)	Organic flux ($g/m^2.h$)	Separation factor (α)
Pyrazines:						
- 2,3,5,6 Tetra methyl pyrazine	$C_8H_{12}N_2$	Musty, chocolate	PDMS GFT	100 ppm, 25°C, 35-60 Pa	0.13	15
			PDMS GFTz	100 ppm, 25°C, 35-60 Pa	0.13	28
			PDMS GFTz	100 ppm, 30°C, 300-2,000 Pa, Re = 100	0.10-0.03	25-7
			PDMS GFTz	100 ppm, 30°C, 300-2,000 Pa, Re = 600	0.08-0.04	7-4
			PDMS DC (130 μm)	100 ppm, 25°C, 35-60 Pa	0.09	35
Other hydrocarbons:						
- Limonene	$C_{10}H_{16}$	Citrus, orance	PDMS (60 μm)	2.8 ppm, 67°C	0.44	1,831
- Vanilin	$C_8H_8O_3$	Vanilla	PEBA GKSS (100 μm)	2,000 ppm		18

[feed] = feed concentration; T_F = feed temperature; P_P = permeate pressure; Re = Reynold number
PDMS = poly(dimethylsiloxane) ; PDMS-PC = PDMS-polycarbonate; PEBA = poly(ether block amide)
BRAUN = Braun company ; DC = Dow Corning ; GE = General Electric; GFT = Gesellschaft fur Trenntechnik
PDMS GFTz = silicalite-filled PDMS 1070; GKSS = Göteborgs Kungliga Segel Sällskap
SBR = styrene-butadiene rubber; SEMPAS = Sempas Membran-technik, Germany

As a follow up of prior studies, in 1998 Djebbar *et al.* also used PEBA and PDMS membranes to concentrate some ester model aroma compounds from aqueous solutions. In their study, PDMS was shown to have better performance than PEBA; however, an increase in the polyether content in PEBA could improve the pervaporation performance substantially. Another membrane, poly(vinylidene fluoride-*co*-hexafluoropropene), has also been tested by Tian *et al.* (2004) for PV separation of ethyl acetate-water mixtures. It was found that the separation factor was higher than PEBA but lower than PDMS, and the permeation flux was relatively high. Meanwhile, Baudot *et al.* (1999) studied the pervaporation performance of three membranes for separation of different aroma compounds. The first membrane, a silicalite-filled silicone membrane, was found to be best suited for the selective extraction of small-sized organic permeants, or low-boilers (diacetyl and ethyl acetate). The other two membranes, PEBA and PDMS, were suitable for high-boiling aroma compounds (S-methylthiobutanoate and γ-decalactone). Similar to PDMS, another silicone based polymer, poly(octylmethyl siloxane) (POMS) was also found to have good pervaporation performance for aroma compound separation (Sampranpiboon *et al.*, 2000).

In order to resemble real applications of aroma compound recovery, instead of using aroma compound models, studies on pervaporation of actual aroma compounds from natural sources have been conducted, including wine must fermentation (Schafer *et al.*, 1999), apple juice (Borjesson *et al.*, 1996; Olsson and Tragardh, 1999; Alvarez *et al.*, 2000), grape juice (Rajagopalan and Cheryan, 1995), vanillin (Boddeker *et al.*, 1997), tropical fruit juice (Pereira *et al.*, 2005), cauliflower (Souchon *et al.*, 2002) and apple essence-orange aroma-black tea distillate (She and Hwang, 2006).

The most recent review on pervaporation separation of aroma compounds was by Pereira *et al.* (2006); it was reported that about 70 aroma compounds have been investigated for pervaporation separation. Among the membrane materials, PDMS was the most widely used membrane material (41 %), followed by zeolite-filled PDMS, PEBA, poly(octylmethylsiloxane) (POMS), ethylene-propylene-diene monomer (EPDM) and others.

2.3 Performance of Pervaporation

Generally speaking, the performance of pervaporation separation is characterized by two parameters, i.e., permeation flux and selectivity. The permeation flux represents the rate of permeation that can be achieved by the membrane and is expressed in term of amount of permeate collected (Q) per effective area (A_m) of the membrane through which the permeant passes per unit operating time (t) (Huang, 1991),

$$J = \frac{Q}{A_m t} \tag{2.1}$$

The selectivity describes the degree of separation attained in pervaporation. It can be measured by either the separation factor (α) or enrichment factor (β):

$$\alpha = \frac{c'(1-c)}{c(1-c')} \tag{2.2}$$

$$\beta = \frac{c'}{c} \tag{2.3}$$

where c' and c are the concentrations (in mass fraction) of the desired permeant in the permeate and feed, respectively. Obviously, if the target component concentration is very low in feed and permeate (i.e., $c << 1$, $c' << 1$), then the separation factor will approach the enrichment factor numerically.

2.4 Transport Mechanism

In order to explain how the permeant passes through the membrane during pervaporation, a model of mass transport may be used. The model is particularly useful for quantifying the pervaporation performance and for design applications such as simulation and scale up. Although pervaporation is a physical process, the mass transport through the membrane,

which is a solid phase, is not as easy to describe as the mass transport through liquid or gas phases.

The most widely accepted model is the solution-diffusion model (Long, 1965; Greenlaw *et al.*, 1977a; 1977b; Brun *et al.*, 1985; Heintz and Stephan, 1994). Based on this model, the movement of permeant from the feed (liquid phase) to the permeate (vapor phase) undergoes three consecutive steps, (i) Upstream partitioning of the feed-components based on their different affinities to the membrane surface (sorption step); (ii) Diffusion of the permeant through the unevenly-swollen permselective membrane (diffusion step); and (iii) Permeant desorption at the downstream surface of the membrane (desorption step). This mechanism is illustrated in Figure 2.2.

In principle, a mathematical expression to describe the solution-diffusion model can be derived by taking into account all these steps. However, since the first and the last steps are believed to occur very fast as compared to the second step, diffusion through the membrane is considered to be the controlling step that governs the mass transport of the whole process. If diffusion is the rate determining step, the Fick's law can be applied (Long, 1965),

$$J_i = -D_i \frac{dC_i}{dx} \tag{2.4}$$

where J_i is the flux of component i, D_i is the diffusivity of component i, and dC_i / dx is the concentration gradient of component i across the membrane. This equation can take into account of the diffusivity dependency on permeant concentration and the sorption equilibrium, which correlates the permeant concentration on the membrane surface at feed side to that in the bulk feed. A simple case in which the diffusivity is independent of concentration has been used by Lee (1975). However, constant diffusivity was found not valid for many pervaporation separation systems. Therefore, several studies also suggested the use of certain relationships to describe the concentration dependency of diffusivity, including linear (Greenlaw *et al.*, 1977) and exponential correlations (Greenlaw *et al.*, 1977a;

1977b; Rautenbach and Albrecht, 1985; Brun *et al.*, 1985; Aptel *et al.*, 1974; Huang and Lin, 1968).

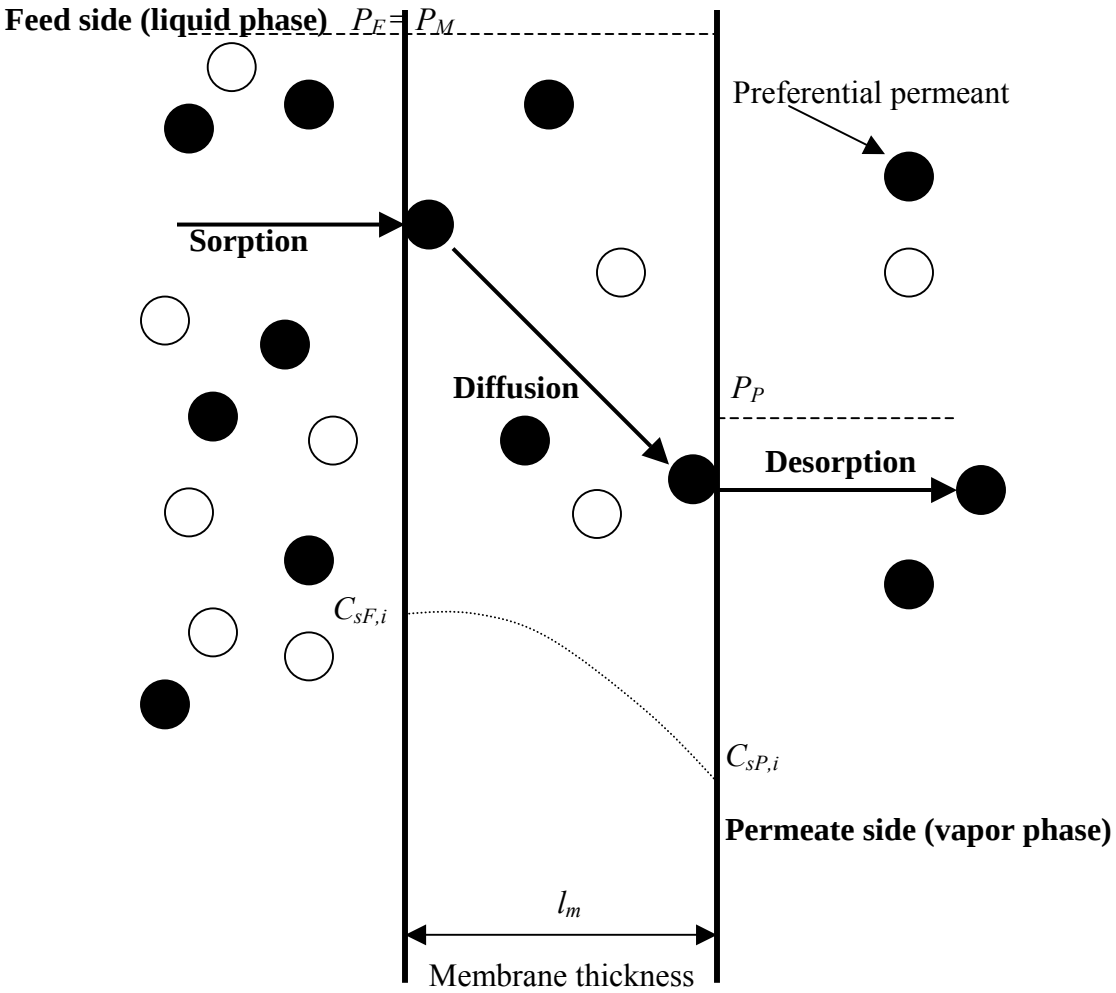

Figure 2.2 Schematic of solution-diffusion model in pervaporation.

In 1961, a modification of the solution-diffusion model by applying free volume theory was made by Fujita, and later by Huang and Rhim (1991); the involvement of volume fraction of liquid (permeant) inside the membrane was considered in the model. According to this modified model, at steady state the permeation flux can be expressed as follows,

$$J_i = -\frac{D_i}{(1-v_i)}\frac{dC_i}{dx} \tag{2.5}$$

where v_i is the volume fraction of liquid in the membrane. The volume fraction represents the free volume of the membrane that can be occupied by permeant. The model implies that a higher volume fraction in the membrane results in a higher permeation flux. In this model, the diffusivity may also be influenced by the volume fraction of permeant, the permeant activity and the thermodynamic diffusivity (D_T),

$$D_i = (D_T)_i(1-v_i)\frac{d\ln a_i}{d\ln v_i} \tag{2.6}$$

with

$$D_T = RTA_d \exp\left(\frac{-B_d}{f(1-\Phi_c)}\right) \tag{2.7}$$

where R is the gas constant, A_d and B_d are the parameters related to the shape and size of permeant, f is the fractional free volume which is a function of temperature (T), and Φ_c is the crystallinity of the membrane. a_i is the activity of component i that can be obtained from the Flory-Huggins thermodynamics correlation (Flory, 1953),

$$\frac{d\ln a_i}{d\ln v_i} = 1-\left(1-\frac{v_i}{v_m}\right)v_i - 2\chi_{im}v_i v_m \tag{2.8}$$

$$\frac{d\ln a_j}{d\ln v_j} = 1-\left(1-\frac{v_j}{v_m}\right)v_j - 2\chi_{jm}v_j v_m \tag{2.9}$$

where v_i, v_j and v_m are the molar volumes of solvent i, j and the membrane, respectively. χ_{im} is the Flory-Huggins interaction parameter between pure liquid i and the polymer. χ is mainly

affected by the molar volume of polymeric membrane (v_m), and can be evaluated using a simplified equation:

$$\chi = -\frac{\ln(1 - v_m) + v_m}{v_m^2} \tag{2.10}$$

This model tries to correlate diffusivity to such parameters as free volume, effective concentration (activity) and the permeant-membrane interaction.

Another modified model is the pseudophase-change solution-diffusion model (PCSD) proposed by Shieh (1996) to combine liquid and vapor permeation in series. The main differences between the PCSD and the original solution-diffusion model are the pressure profile across the membrane and the location at which the phase change takes place. The original solution-diffusion model considers that there is no pressure drop along the membrane and the phase change occurs on the membrane surface at the permeate side when desorption takes place. The PCSD model, on the other hand, notes the pressure inside the membrane changes in a certain trend and the phase change occurs somewhere inside the membrane. The PCSD model tried to describe the phase change inside the membrane with some quantitative parameters, i.e., the pressure and concentration profiles across the membrane and the phase change interface (boundary). The phase change interface is identified when the pressure of the system equals to the saturated vapor pressure of the mixture (P_0). Two zones of permeation with different driving forces can be distinguished. The driving force in the liquid permeation zone is a linear pressure gradient ($P_F - P_0$), whereas the permeation rate is proportional to a squared pressure gradient ($P_0^2 - P_P^2$) in the vapor permeation zone.

Other models for pervaporation transport include the pore flow model (Sourirajan *et al.*, 1987), non-equilibrium thermodynamics (Baranowski, 1991), and carrier facilitated transport model (Shimidzu and Yoshikawa, 1991). The pore flow model was initially proposed by Sourirajan *et al.* (1987) and then developed by Okada and Matsuura (1991). It is assumed that the permeant moves from the upstream to the downstream side through pores in the

membrane. Similar to the PCSD model, the primary difference between the pore flow model and the solution-diffusion model is that this model clearly states the existence of the phase change boundary inside the membrane. The driving force for permeation is considered to be pressure gradient across the membrane, and the permeation and separation of liquid mixtures are mainly determined by the physical properties of the membrane (such as membrane structure). Because of the existence of the liquid-vapor phase boundary inside the membrane, the mass transport in the pore flow model also consists of three consecutive steps: liquid transport from the pore inlet to the liquid-vapor interface, phase change (i.e., liquid evaporation) at the phase boundary, and vapor transport from the phase boundary to the pore outlet. The non-equilibrium thermodynamics, on the other hand, is derived merely from an irreversible thermodynamic standpoint without considering the details how the permeant passes through the membrane, whereas the carrier facilitated transport model describes the movement of permeant facilitated by specific functional groups in the membrane (e.g., carboxyl groups) as a carrier, similar to ion exchange processes. Depending on the mobility of the carrier in the membrane, the carrier can be considered as a non-fixed carrier or a fixed carrier. For the non-fixed carrier, a permeant-carrier complex is formed. The permeant is then separated from the carrier on the membrane surface at the permeate side. On the other hand, the fixed carriers undergo repetition processes of adsorption and desorption and as such the permeant is transported between the fixed carriers towards the permeate side.

In addition to the above mentioned models, other approaches such as the Maxwell-Stefan theory (Schaetzel *et al.*, 2001) and molecular simulation (Hofmann *et al.*, 1998) are also proposed, but they are not widely used.

2.5 Transport Properties in Pervaporation

Considering the solution-diffusion model, there are two important aspects that control the mass transport in pervaporation, i.e., solubility and diffusivity. Inside the membrane, the permeant swells the membrane. It is essentially a dissolvation process where the permeant is a dispersed component (solute) and the membrane is a dispersing agent (solvent). The maximum amount of permeant that can be dispersed defines the solubility of the permeant in

the membrane. While swelling the membrane, the permeant moves under the concentration gradient of the permeant to a direction where spaces are available. From this standpoint, the molecular diffusion inside the membrane is an important step and diffusivity is an important parameter characterizing the diffusion rate.

Generally speaking, the diffusivity of a permeant in a polymeric membrane also measures the ability of the polymer to physically accommodate the permeant, and to continually provide randomly-generated voids for the permeant to diffuse through the membrane (Watson *et al.*, 1990). The permeant molecules occupy the inter-chain space (or free volume) among the macromolecules of the polymer. The molecular size and shape of the permeant affect the diffusivity. However, Watson *et al.* (1990; 1992) showed that in silicone rubber the diffusion was not dominated by the permeant size, but was affected to a large extent by the permeant-polymer interactions. They expressed the diffusivity as follows,

$$D = \frac{\lambda^2}{2\tau_p} \tag{2.11}$$

with

$$\tau_p = \tau_0 \exp\left(\frac{E}{RT}\right) \tag{2.12}$$

where τ_p is the dwell time determined by the strength of permeant-polymer interactions, E is the activation energy describing the permeant-polymer physisorption bond, $1/\tau_0$ is the vibration frequency of the bond, and λ is the jump length. Other researchers (e.g., Brookes and Livingston, 1995; LaPack *et al.*, 1994) found that the two factors above (molecular size of permeant and its interaction with polymeric membrane) often affect the diffusivity; some studies even noted that the diffusivity might also be influenced by the molecular interactions of permeant-permeant or coupling effect (Heintz *et al.*, 1991; Chen and Chen, 1998).

Both the solubility and diffusivity are often found to be dependent on permeant concentration. Heintz *et al.* (1991) classified the general cases of these properties in pervaporation into three categories: (i) Both the solubility coefficient S_i and diffusivity coefficient D_i are independent of concentration C_i. This is an ideal case where the Henry's

law applies to the sorption process. (ii) Both S_i and D_i are a function of C_i only, and there are no interactions between permeating components. (iii) S_i is dependent on C_i and the concentrations of other components, D_i is dependent on C_i but not on the concentrations of other components (Heintz and Stephan, 1994). In addition, as mentioned previously, three different correlations have been suggested to describe concentration dependency of diffusivity, i.e., constant diffusivity, linear concentration dependent, and exponential concentration dependent.

2.5.1 Time-Dependent Sorption Method

To measure the diffusivity of a permeant through a membrane either for pure components or in a mixture, various techniques have been developed. One method is the time-dependent sorption, which allows the diffusivity (D) to be evaluated from the sorption data, which essentially correlate the mass of permeant sorbed by the membrane as a function of time, as illustrated in Figure 2.3.

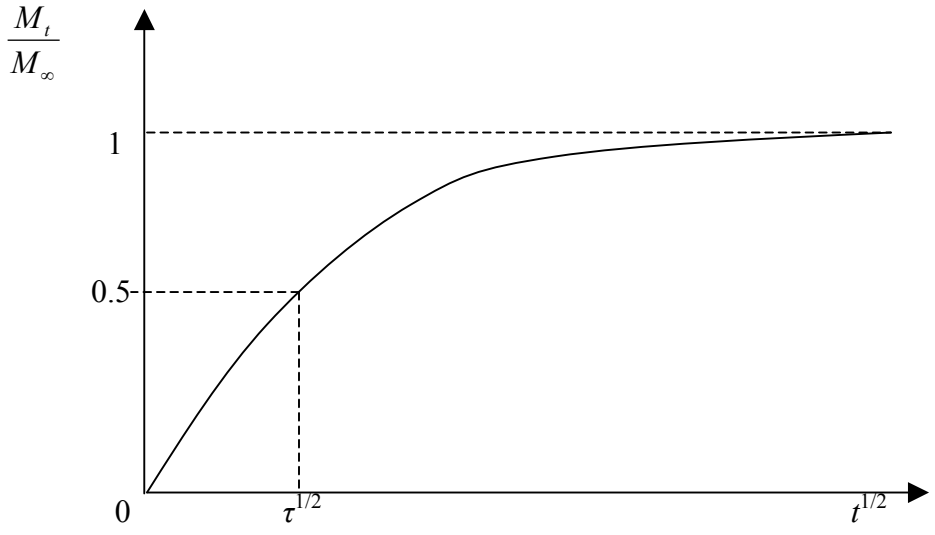

Figure 2.3 The time-dependent sorption method.

According to Crank (1975), the mass sorbed at a given time, where the two sides of membrane surfaces have same concentrations, follows the following relationship,

$$\frac{M_t}{M_\infty} = 1 - \sum_{n=0}^{\infty} \frac{8}{(2n+1)^2 \pi^2} \exp\left(- \frac{(2n+1)^2 \pi^2 Dt}{l_m{}^2} \right) \tag{2.13}$$

where M_t and M_∞ are the mass of permeant sorbed by the membrane at time t and at equilibrium, respectively; and l_m is the membrane thickness. Eqn. (2.13) is an analytical solution of the second Fick's law for unsteady state diffusion through a slab of membrane. For long times, the summation for $n = 1$ to ∞ in Eqn. (2.13) is relatively small as compared to the first term ($n = 0$), and thus can be simplified,

$$\frac{M_t}{M_\infty} = 1 - \frac{8}{\pi^2} \exp\left(- \frac{\pi^2 Dt}{l_m{}^2} \right) \tag{2.14}$$

For short times ($(Dt/l_m{}^2) \leq 0.13$), a more useful analytical solution for unsteady state diffusion can be used (Crank, 1975),

$$\frac{M_t}{M_\infty} = 4 \left(\frac{Dt}{l_m{}^2} \right)^{1/2} \left[\pi^{-1/2} + 2 \sum_{n=1}^{\infty} (-1)^n \, ierfc\left(\frac{n l_m}{2\sqrt{Dt}} \right) \right] \tag{2.15}$$

Eqn. (2.15) can also be simplified by ignoring the value of summation in the second term,

$$\frac{M_t}{M_\infty} = 4 \left(\frac{Dt}{\pi l_m{}^2} \right)^{1/2} \tag{2.16}$$

Based on Eqn. (2.13), a simplified correlation, the so-called half-time method, can also be used.

$$D = \frac{0.04919}{\left(\frac{\tau}{l_m^{\,2}}\right)} \tag{2.17}$$

where τ is the half time, which is the time needed for the membrane to attain a half of equilibrium sorption amount (or $M_t/M_\infty = 0.5$).

2.5.2 Time-Lag Method

The measurement of diffusivity can also be done based on the permeation rate using the time-lag method. Initially, the permeation is at unsteady state, and during this period the permeation rate varies with time. When the steady state of permeation is achieved, the permeation rate becomes constant, as indicated by the linear relationship between Q (amount of permeant passing through the membrane at time t) and t (Figure 2.4).

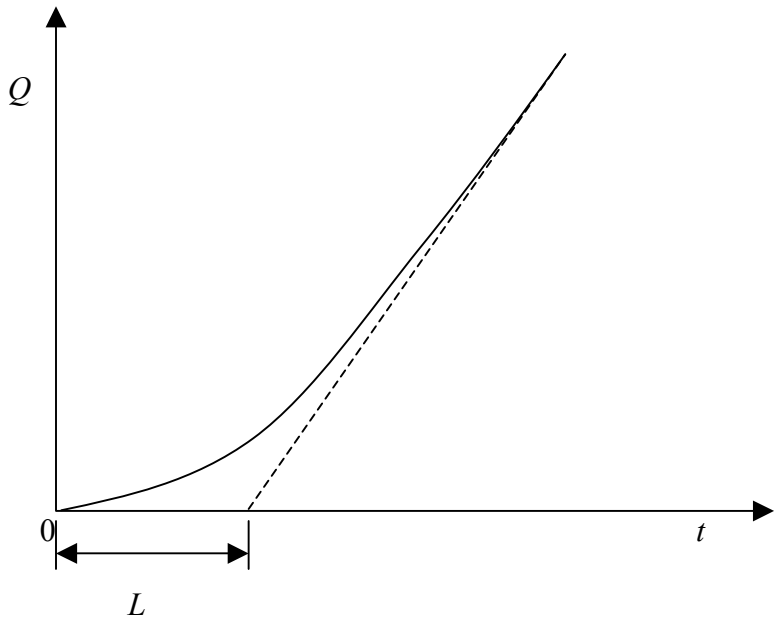

Figure 2.4 The time-lag method.

A transient permeation (unsteady state) is observed from the moment that permeant enters the membrane initially until steady state is reached. The time interval L obtained by extrapolating the steady state permeation rate to the time axis, is the time-lag. For concentration independent diffusivity and solubility, the following relation applies (Comyn, 1985),

$$L = \frac{l_m^{\,2}}{6D} \tag{2.18}$$

Under steady state condition (normally $t > 3\ L$), the Q versus t curve becomes linear. In case of constant diffusivity and ideal sorption while ignoring the concentration of permeant in the permeate side (due to vacuum), if the simple solution-diffusion model applies, the permeation flux can be expressed as,

$$\frac{1}{A_m}\frac{dQ}{dt} = DS\frac{C_F}{l_m} \tag{2.19}$$

and

$$P_m = DS \tag{2.20}$$

where A_m is the area of the membrane for permeation, S is the solubility coefficient, C_F is the concentration of permeant in the bulk feed, and P_m is the permeability. Both P_m and D can be determined from a single experiment using the steady state permeation rate and the time-lag of the unsteady state permeation.

In addition, Watson *et al.* (1990) evaluated the diffusivity of permeant in a silicone rubber membrane based on the data of permeation flux versus time, using the following correlation,

$$\frac{J}{J_S} = 1 + 2\sum_{n=1}^{\infty}(-1)^n \exp\left(\frac{-n^2\pi^2 Dt}{l_m^{\,2}}\right) \tag{2.21}$$

where J and J_S are the fluxes at a given time and at steady state, respectively. However, it must be pointed out that both methods are restricted to cases where the concentration dependences of D and S are insignificant.

2.5.3 Inverse Gas Chromatography Method

In case of very slow diffusion or the quantity of the sorbed permeant is small, the conventional methods become unreliable. An alternative, inverse gas chromatography (IGC) might be able to overcome the challenge. The principle of diffusivity measurement using IGC is based on partitioning of a substance between a mobile gas phase and a stationary polymer phase. IGC has been used to determine such physicochemical properties as solubility (Baltus *et al.*, 1993), activity coefficient (Bonifaci *et al.*, 1994), enthalpy of interaction, Flory-Huggins interaction parameter, crystallinity (Gray and Guillet, 1971), sorption isotherm (Kontominas *et al.*, 1994), degree of fusion (Qin *et al.*, 1995), and degree of cross-linking (Tan *et al.*, 1994). Due to the accuracy of IGC, some complex correlations on diffusivity have also been formulated (Vrentas and Duda, 1977a; 1977b; Pawlisch *et al.*, 1987; 1988). Thus, this method has the potential to be used in determining the diffusivity of permeant in membranes.

In addition, the diffusivity can also be determined by data fitting of permeation flux into a mass transport model (Bell *et al.*, 1988). The diffusivity obtained by this method is an apparent diffusivity unless the model is really applicable for the system. In case of solution-diffusion model, for instance, the diffusivity can be calculated from the steady state permeation flux and equilibrium sorption (solubility).

2.6 Process Variables in Pervaporation

The separation performance of pervaporation is determined by the physicochemical nature of the membrane material and the species to be separated, the structure and the morphology of the membrane, and the process conditions (Feng and Huang, 1996). Pervaporation is a rate process that occurs under a driving force of chemical potential gradient. The chemical

potential can be formulated as a function of temperature (T), activity, and pressure (P) (Baker, 2004),

$$d\mu_i = \mu_i^0 + RTd\ln(\gamma_i y_i) + v_i dP \tag{2.22}$$

where μ_i is the chemical potential of component i, μ_i^0 is the chemical potential of pure i at a reference pressure, whereas γ_i, y_i and v_i are the activity coefficient, mole fraction and molar volume of component i, respectively. The process variables, including feed concentration, temperature, and pressures at feed and permeate sides, can directly affect the chemical potential, and thus pervaporation performance will change when the process conditions vary.

2.6.1 Feed Concentration

In addition to its effect on the mass transfer driving force, the feed concentration also affects the membrane permeability. Based on the solution-diffusion model, the movement of a permeant through a membrane is started with sorption onto the membrane surface, followed by diffusion and desorption. In the sorption step, the amount of permeant uptake in the membrane is affected by the feed concentration. In the diffusion step, the diffusivity is affected by the local permeant concentration (Greenlaw *et al.*, 1977; Binning *et al.*, 1961; Huang and Lin, 1968; Mulder and Smolders, 1984). The local permeant concentration relates to the amount of permeant sorbed by the membrane. Clearly, a change in feed concentration will affect both the solubility and diffusivity of the components inside the membrane, and ultimately influence the permeability of the membrane.

2.6.2 Operating Temperature

Both solubility and diffusivity are temperature dependent. Since the pervaporation transport involves these two properties, the separation performance is significantly affected by the temperature. Generally speaking, the permeation flux as a function of temperature follows the Arrhenius type of relationship, $J = Jo\ exp(-E_P/(RT))$ (Huang and Lin, 1968; Huang and

Jarvis, 1970; Cabasso *et al.*, 1974), and the apparent activation energy for permeation, E_P, is generally in the range of 17-63 kJ/mole.

2.6.3 Permeate Pressure

As mentioned above, the driving force in pervaporation is the chemical potential difference between the feed and permeate side, which is influenced by the pressure. In order to maximize the driving force, a high pressure on the feed side and a low pressure (vacuum) on the permeate side are used. Lee (1975) showed that theoretically a very high feed pressure in reverse osmosis could have similar effect as in pervaporation in terms of flux and selectivity, and this has been confirmed experimentally by Greenlaw *et al.* (1977). On the other hand, an increase in vapor pressure in the downstream side will result in a quick decline in permeation flux. Shelden and Thompson (1984) and Neel *et al.* (1986) showed experimentally that an increase in downstream pressure (P_2) from zero to a pressure about 30 % of its saturated vapor pressure can decrease the permeation flux by 90 %. Studies by Greenlaw *et al.* (1977) and Shelden and Thompson (1984) also showed that a variation in permeate pressure could influence the selectivity as well. The selectivity could increase or decrease, depending on the relative volatility of the permeating permeant.

2.6.4 Feed Flow Rate

Concentration polarization is a phenomenon that takes place due to selective mass transfer. The selective permeation results in accumulation of the slow component on the membrane surface. In microfiltration, ultrafiltration and reverse osmosis, concentration polarization is a serious problem that causes a reduction in flux and degree of separation. Spitzen (1988) investigated the effect of concentration polarization on pervaporation performance and concluded that in general concentration polarization would decrease the permeation flux and selectivity as well. Psaume *et al.* (1988) also found that in very dilute organic solutions, concentration polarization at the liquid-membrane interface may be significant enough to control the mass transfer for the organic compound permeation. In order to measure the

extent of concentration polarization on the membrane surface, Feng and Huang (1994) introduced a concentration polarization index (X_s/X_f), which was defined as

$$\frac{X_s}{X_f} = \frac{1}{\beta - (\beta - 1)\exp(-u/k_l)} \tag{2.23}$$

where X_s and X_f represent the mol fractions of the more permeable component on the membrane surface and in the bulk feed, respectively. β is the intrinsic enrichment factor, u is the molar average velocity for mass transport, which is proportional to the feed flow rate, and k_l is the mass transfer coefficient in the boundary layer. Obviously, an increase in feed flow rate will decrease the ratio of (X_s/X_f), indicating a decrease in concentration polarization effect.

2.7 Selection of Membrane Material

Generally speaking, the membranes used in pervaporation can be classified into two types, hydrophilic and organophilic. Hydrophilic membranes absorb water preferentially, whereas organophilic membranes absorb organic compounds preferentially. In general, glassy polymers have a good interaction with water, while rubbery (elastomeric) polymers are more appropriate to attract organic compounds. In addition, ionic polymeric membranes have also attracted attention (Feng, 1994). They contain ionic groups (cations or anions) that are neutralized by counter ions, and they are hydrophilic since water is a good solvent for electrolyte.

In order to predict the preferential permeation among liquids in contact with a given membrane, which helps the selection of appropriate membranes, some theoretical approaches have been developed. In principle, the prediction is based on the different interactions between the components to be separated with the membrane. One way to measure the interaction between a permeant and a membrane qualitatively is to use the solubility parameter. There are three vectorial components that influence the molecular interaction, i.e., dispersion forces (δ_d), polar forces (δ_p), and hydrogen bonds (δ_h). The solubility parameter is

represented by the end-point of the vector which is composed of the above three components (Hannsen and Beerbower, 1971),

$$\delta^2 = \delta_d{}^2 + \delta_p{}^2 + \delta_h{}^2 \tag{2.24}$$

A qualitative assessment dealing with the preferential interaction between the permeant and membrane can be seen from the distance (Δ) between the end-points of the solubility vectors of the polymeric membrane and the solvent (permeant) (Ravindra *et al.*, 1999),

$$\Delta_{Pm} = \left[\left(\delta_{d,P} - \delta_{d,m}\right)^2 + \left(\delta_{p,P} - \delta_{p,m}\right)^2 + \left(\delta_{h,P} - \delta_{h,m}\right)^2\right]^{1/2} \tag{2.25}$$

where subscripts *P* and *m* refer to the permeant and the membrane, respectively. The swelling of membrane due to sorption increases with decreasing Δ_{Pm} values. Lloyd and Meluch (1985) used the ratio Δ_{Pm} for each permeant to assess the preferential sorption. For example, for a system of permeant (*i* and *j*) and a membrane (*m*), $\Delta_{im}/\Delta_{jm} < 1$ means *i* is preferentially sorbed on the membrane *m* over *j*. However, this approach does not always work well especially for non-polar systems (Mulder, 1991). In order to improve the prediction of preferential sorption based on the solubility parameters, Zellers (1993) introduced the use of weighing factors,

$$\Delta_{Pm} = \left[\omega_0\left(\delta_{d,P} - \delta_{d,m}\right)^2 + \omega\left(\delta_{p,P} - \delta_{p,m}\right)^2 + \omega\left(\delta_{h,P} - \delta_{h,m}\right)^2\right]^{1/2} \tag{2.26}$$

where ω_0 and ω are the weighing factors, and their values depend on the functional group. With the weighing factors, Zellers succeeded in explaining the sorption behavior of 40 liquids (alcohols, amides, aliphatic hydrocarbons, aromatic hydrocarbons, etc.) on a fluorinated polymer.

Another approach, based on the surface thermodynamics, has also been proposed by van Oss *et al.* (1983). This approach used thermodynamic parameters (i.e., Gibbs free energy and interfacial tension) to evaluate the surface interaction between permeant and membrane. The

phase separation between two different solvents (*i*, *j*) sorbed in a polymeric membrane (*m*) can be explained from the total Gibbs free energy ΔG_{imj},

$$\Delta G_{imj} = \sigma_{ij} - \sigma_{im} - \sigma_{jm} \tag{2.27}$$

where σ refers to the interfacial tension. The value of σ for a solvent / polymer system can be evaluated using an empirical equation proposed by Neumann *et al.* (1974),

$$\sigma_{ij} = \frac{\left(\sigma_i^{0.5} - \sigma_j^{0.5}\right)^2}{1 - 0.015\sigma_i^{0.5}\sigma_j^{0.5}} \tag{2.28}$$

A large value of ΔG_{imj} means there would be a good separation among the solvents in the polymer phase. Lee *et al.* (1987) applied this approach in the selection of membrane materials, but they found that the prediction did not work for some cases.

Mulder (1991) recommended the use of polarity in term of Dimroth's solvent polarity value (E_T(25^{o}C)) as a parameter to determine the preferential sorption of permeant. Based on this approach, a particular component that will be removed from a liquid mixture must have a polarity close to that of the membrane. For instance, in separation of ethanol-water mixtures utilizing polystyrene membranes, because the polarity of polystyrene (31.7 kcal/mol) was closer to the polarity of ethanol (30 kcal/mol) than that of water (63.1 kcal/mol), the membrane preferentially permeates ethanol over water. However, because the polarity values of polymers are not well documented, the use of this approach is limited.

An alternative approach based on chromatographic measurement, was introduced by Matsuura and Sourirajan (1978). They applied liquid chromatography in which the carrier or mobile phase was a liquid and the stationary phase was the membrane material. The affinity among components to membrane was measured from the retention volume. If the solute injected to the mobile phase had a strong affinity to the stationary phase (membrane), the elution of the solute would be delayed. Similarly, Pawlish *et al.* (1987, 1988) and Bonifaci *et al.* (1994) tried to apply this method using a gas carrier (i.e., inverse gas chromatography)

and used the retention time and eluted peak to determine the degree of interaction between the solute and the membrane.

Nabe *et al.* (1997) used a contact angle approach. It was essentially a simplification of the surface thermodynamics method. The affinity between a permeant and a membrane can be judged from its contact angle, and a smaller contact angle on the membrane surface means a better permeant-membrane affinity.

2.8 Process Design in Pervaporation

As mentioned before, the driving force for mass transfer is affected by activity (or effective concentration), temperature and pressure. In order to maximize the driving force and thus to achieve the maximum permeation flux, a high feed pressure and a low permeate pressure are required. However, the feed pressure does not affect the permeation flux significantly, and lowering the permeate pressure is the most effective way to increase the driving force. In laboratory the low permeate pressure is usually achieved with a vacuum pump. However, in industrial applications the utilization of vacuum pump represents a significant operating cost. In the early days of pervaporation research, vacuum pump size was sometimes considered to hinder pervaporation from commercial applications.

The utilization of vacuum pump may also be replaced by other means, and some potential alternatives have been suggested by Baker (2004). One is to condense the permeate vapor into liquid, and the condensation of vapor will generate vacuum. A combination of cooling the permeate and heating the feed may be more interesting if the cost of a vacuum pump is an issue, provided that the membrane is still stable at an elevated temperature. Another possibility is to sweep the permeate side of membrane with a carrier gas. If the permeate is valuable and to be recovered, the permeate vapor must be condensed in a condenser and the carrier gas can thus be reused. In case that the permeate is invaluable (e.g., solvent dehydration process), the permeate can be swept out without any condensation if it can be discharged directly without further treatment (Yuan and Schwartzberg, 1972). Sometimes, a low grade steam may be used as a sweep gas (Robertson, 1949; Friesen *et al.*, 1995). If, after

permeate condensation, the permeate is immiscible with water, it can be recovered by decantation, and the condensed water that may contain a small amount of dissolved permeate can then be reused to produce steam.

In the recovery of low solubility organic compounds from dilute aqueous solutions, another issue should be considered. In most cases, the concentration of the organic compounds in the permeate stream obtained by pervaporation separation is much higher than the solubility limit. As a result, a phase separation takes place in the permeate resulting in an organic phase and a water phase. Baker (2004) and Liu *et al.* (2005) suggested recycling the water phase into the system to enhance the recovery of the organic compounds.

CHAPTER 3
Pervaporation Separation of Binary Aroma–Water Solutions by a PEBA Membrane

3.1 Introduction

There are many studies on pervaporation of aroma compound recovery from aqueous solution. Organophilic membranes, particularly PEBA and PDMS, are suitable for this separation. The separation performance depends on the types of aroma compounds, membranes used, and process conditions. Prior studies showed that PDMS also had a permselectivity in aroma compound recovery from aqueous solutions. However, it must be noticed that a successful pervaporation process is also measured from other aspects including productivity and stability. PEBA is not only a good organophilic membrane but also has a good mechanical stability. Moreover, the permselectivity of PEBA could be improved by adjusting the polyether and polyamide composition of PEBA. This chapter presents the results of pervaporation separation of three binary aroma-water solutions using PEBA 2533 membranes. PEBA 2533 is a block copolymer comprising 80 wt.% poly(tetramethylene oxide) and 20 wt.% nylon 12 (Liu *et al.*, 2005). It has the general formula of (Cen *et al.*, 2002),

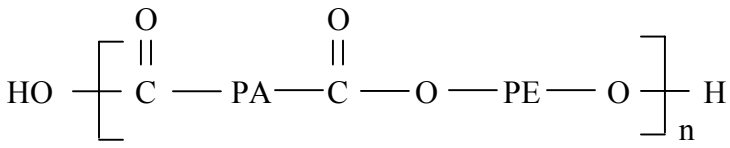

Figure 3.1 The general formula of PEBA.

where PA and PE denote polyamide and polyether segments, respectively. The good selectivity of PEBA to aroma compound permeation derives from the strong affinity between

the polyether segments and aroma compounds. As a matter of fact, PEBA polymers with a high polyether content can be used as a potential fragrance carrier for long lasting release of fragrance (Pougalan and Holzner, 1988). Therefore, PEBA 2533 was chosen as the membrane material in the present study because of its exceptional organophilic properties and mechanical and chemical stabilities. It may be mentioned that compared to PEBA 4033 membranes reported previously (as listed in Baudot and Marin, 1997), PEBA 2533 has a higher content of polyether segment (80 wt.%), which as expected resulted in a better permselectivity for aroma compound separation.

Three model aroma compounds were selected to represent ester (propyl propionate), aldehyde (C_6-aldehyde) and aromatic (benzaldehyde) groups. They have different functional groups but similar number of carbons. Table 3.1 lists the physical properties of these aroma compounds.

Table 3.1 Properties of the model aroma compounds (Perry and Green, 1999).

	Aroma compound		
Property	**Propyl propionate**	**C_6-aldehyde**	**Benzaldehyde**
Molecular formula	$C_6H_{12}O_2$	$C_6H_{12}O$	C_7H_6O
Molecular weight, g/mol	116.16	100.16	106.12
Density, g/cm^3	0.883	0.814	1.050
Boiling point, ^{0}C	122.3	121.5	178.0
Solubility in water, ppm	5,600[a]	1,190[b]	3,000[a]
Natural source	Apple, banana, bilberry, cider, cranberry, durian, grape, olive, pear	Apple, banana, carrot, tomato, coconut, strawberry	Apple, apricot, almond bitter, cinnamon leaf

[a] at 25^{o}C ; [b] at 100^{o}C (Hertel *et al*., 2007)

Their presence in natural sources is another important consideration in selecting them as model compounds. These aroma compounds are only slightly soluble in water (less than 6,000 ppm). As such, flash distillation is apparently not energy-efficient to recover these compounds from dilute aqueous solutions. A literature search showed that among these

aroma compounds, the recovery of propyl propionate from water has not been studied, whereas the recoveries of C_6-aldehyde and benzaldehyde were only tested using different membranes.

The effects of feed aroma concentration and operating temperature on the separation performance (i.e., permeation flux and selectivity) of PEBA 2533 membranes were studied.

3.2 Experiments

3.2.1 Materials and Membrane Preparation

Reagent grade propyl propionate (99 wt.%), C_6-aldehyde (98 wt.%) and benzaldehyde (99.5 wt.%), were purchased from Aldrich. They were dissolved in de-ionized water to form feed solutions at various concentrations. PEBA 2533 polymer was kindly provided by Arkema. The solvent used for membrane preparation was *N*,*N*-dimethyl acetamide (DMAc).

The membrane was prepared using the solution-casting technique. The PEBA polymer was first dissolved in DMAc to form a homogeneous solution of 15 wt.%. In order to facilitate the dissolvation, the polymer solution was kept at 70^{o}C under constant stirring. The solution was then cast on a flat glass plate at 70^{o}C. The solvent was removed from the membrane by evaporation for 2 h, followed by drying in an oven at 55^{o}C for about 24 h. The dry membrane so obtained had a thickness of ~25 μm. The procedure of the membrane preparation is schematically shown in Figure 3.2.

3.2.2 Pervaporation

The pervaporation setup consisted of a feed tank, a circulation pump, a membrane cell, a pair of cold traps and a vacuum pump. The apparatus was also equipped with appropriate control and monitoring devices (e.g., thermometer and pressure gauge) for measurement of process conditions. The effective area of the membrane was 20.43 cm^2. A narrow space was designed in the feed side of the membrane chamber so as to achieve a high feed flow velocity minimizing the concentration polarization. A porous-metal support was used to support the

membrane. Because this investigation was concerned with quite low feed concentrations of aroma compounds, a Shimazu-500 total organic carbon (TOC) analyzer was used to analyze the composition of the samples. The repeatability in measurements by this TOC has a standard deviation of 1.5 % for a range not less than 5 ppm and 3 % for a range less than 5 ppm. A schematic diagram of the experimental setup is shown in Figure 3.3. Pervaporation experiments were initiated by circulating the feed from the feed tank to the membrane cell for 1-2 h to condition the membrane. Then vacuum was provided on the permeate side to induce the permeation. The permeate sample was collected in a cold trap immersed in liquid nitrogen (around -196^{o}C). The permeation rate was determined gravimetrically by weighing the permeate sample collected over a given period of time. This work was concerned with steady state permeation, and the quantity of permeate removed by the membrane during each pervaporation run was kept below 0.1 % of the initial feed loading so as to retain an essentially constant feed composition. Pervaporation was considered to have reached steady state when the permeation rate and permeate composition become constant. To determine the composition of the permeate, which was highly enriched in aroma compound, the permeate sample was diluted with de-ionized water before analysis with a TOC analyzer. In studying the effect of feed aroma concentration on the pervaporation performance, other process conditions (i.e., operating temperature, permeate pressure, feed flow rate, and thickness of membrane) were all kept constant. The permeate pressure was kept at around 400 Pa (3 mmHg) and the feed pressure was atmospheric. The feed flow rate and membrane thickness were 1.6 L/min and ~25 μm, respectively. The feed aroma concentration varied in the range of 390-3,210 ppm for propyl propionate-water mixtures, 420-1,120 ppm for C_6-aldehyde-water mixtures, and 430-2,380 ppm for benzaldehyde-water mixtures. The pervaporation data reported represent an average of 2-3 measurements, and the average experimental error was found to be within 5 %. The experimental error was calculated from the deviation of each measurement to the corresponding average measurements, as follows,

$$E_{rr} = \left| \frac{Y - \bar{Y}}{\bar{Y}} \right| x100\% \qquad (3.1)$$

where E_{rr}, Y and $\bar{Y}$ are the experimental error percentage, the measured points and the average value of corresponding measurements, respectively. As demonstration, the experimental errors are shown in the measurements of propyl propionate-water permeation (Figure 3.4), which was the first experimental work investigated in this study.

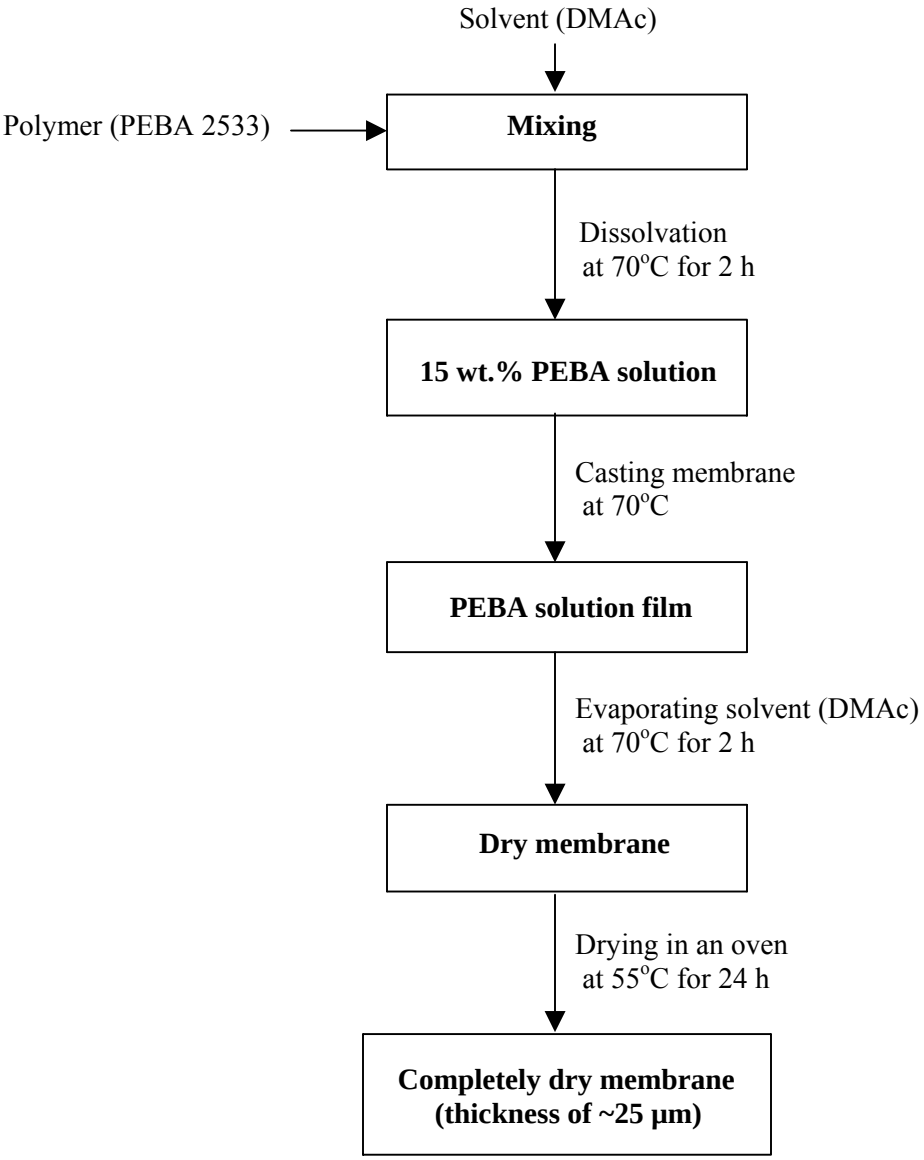

Figure 3.2 Schematic illustrating steps in preparing PEBA membranes using the solvent-casting technique.

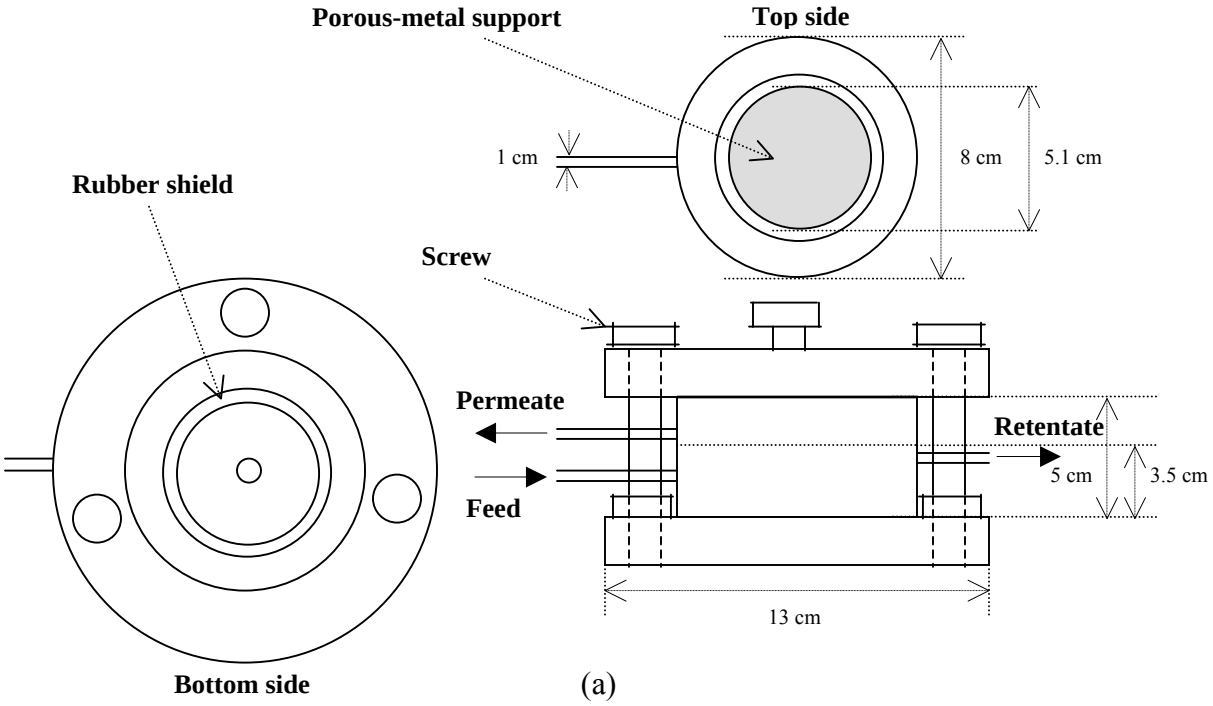

(a)

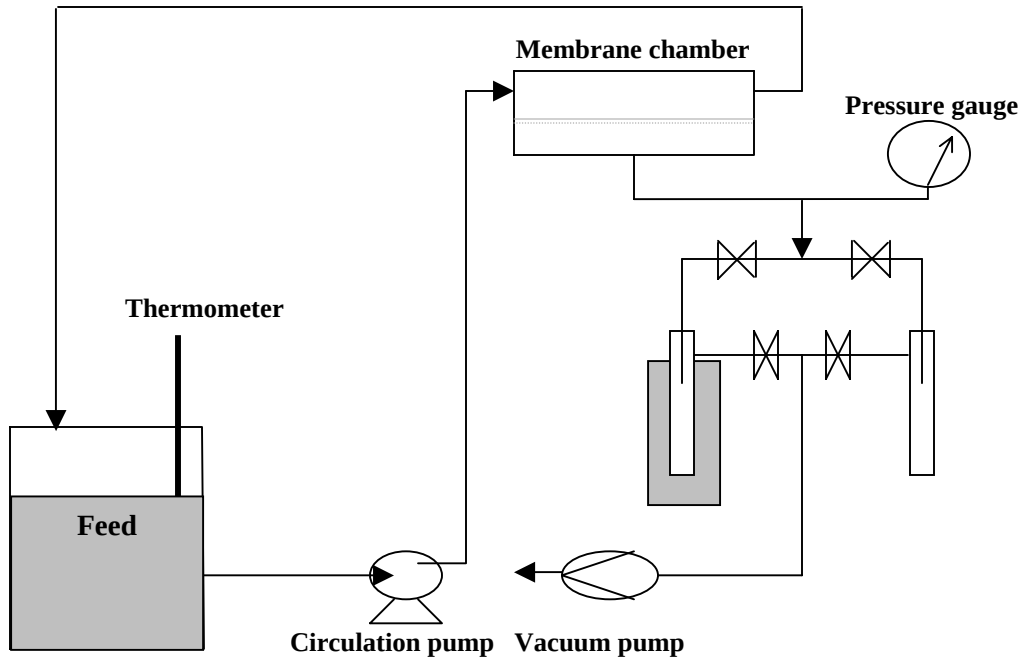

(b)

Figure 3.3 Schematic membrane chamber design (a) and diagram of pervaporation experiment (b).

3.3 Results and Discussion

3.3.1 Effect of Feed Concentration

Pervaporation of the three binary aroma-water solutions on PEBA membrane was studied at various feed aroma concentrations. Figures 3.4 and 3.5 show the effects of the feed aroma concentration on the total and partial permeation fluxes, respectively. Both the total and partial fluxes increase as the feed aroma concentration increases. However, the increase in aroma fluxes through the membrane is more significant than the water flux. This phenomenon can be explained from the organophilicity of the membrane, the driving force for permeation and the transport property of the membrane. PEBA is organophilic and thus the aroma compounds are preferentially sorbed in the membrane over water. As discussed in Chapter 2, pervaporation is a rate controlled process under the driving force of chemical potential gradient. The chemical potential of a permeant is directly affected by its concentration. An increase in the feed aroma concentration will raise the chemical potential of aroma in the feed. On the permeate side, on the other hand, due to its vapor state, the chemical potential is mainly influenced by the permeate pressure. The permeate side was maintained at vacuum. Increasing feed aroma concentration will increase the chemical potential gradient across the membrane, thereby increasing the permeation flux. In addition, the concentration of permeant will affect the mass transport behavior since the solubility and diffusivity are normally dependent on the permeant concentration in the membrane. In the sorption step, a higher feed aroma concentration will increase sorption uptake of aroma compounds in the membrane. Consequently, the concentration of permeant inside the membrane will also increase. Generally speaking, a high concentration of permeant inside the membrane causes membrane swelling. Membrane swelling will increase the free volume in the polymeric matrix of the membrane, making it easier for aroma compound to diffuse through the membrane. It is generally observed that the membrane swelling by a permeant increases its diffusivity through the membrane (Feng and Huang, 1996). In a swollen polymer, the mobility of the polymer segments is promoted, and the space available for diffusion is increased. This has been found to be the case in selective removal of organic compounds from aqueous solutions using organophilic membranes and dehydration of organic solvents using hydrophilic membranes (Lamer *et al.*, 1994; Feng and Huang, 1996).

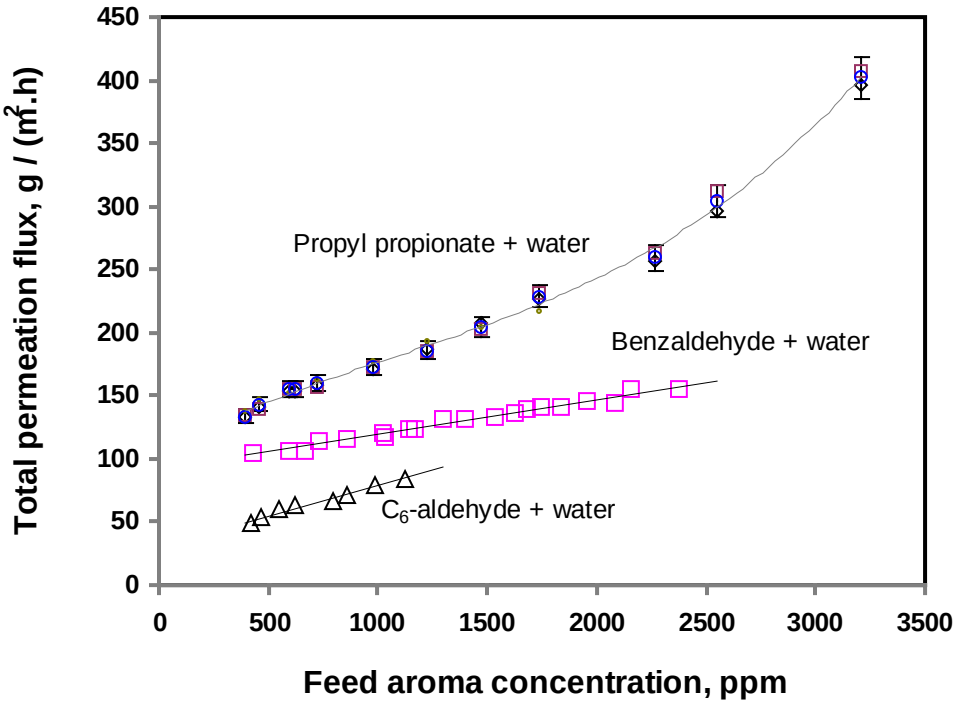

Figure 3.4 Effect of feed aroma concentration on the total permeation flux for binary aroma-water solutions using PEBA membranes (T = 30°C; P_P = ~3 mmHg; feed flow rate = 1.6 L/min; membrane thickness = ~25 μm). The error bars are also shown for propyl propionate-water system.

For water permeation, however, the driving force tends to decrease as the feed aroma concentration increases, but the decrease is relatively insignificant over the feed concentration range studied because of the low concentrations of aroma compounds in the feed. It can thus be concluded that when the feed aroma concentration increases, the enhanced permeability of the membrane causes an increase in water flux as well, as shown in Figure 3.5.

Among the three aroma compounds, within the same range of feed concentrations, propyl propionate has the highest permeation flux, followed by C_6-aldehyde and benzaldehyde. Interestingly, the water flux for each binary aroma-water systems shows different order

compared to the aroma flux. This seems to justify that the permeant-permeant and permeant-membrane interactions affect the pervaporation performance.

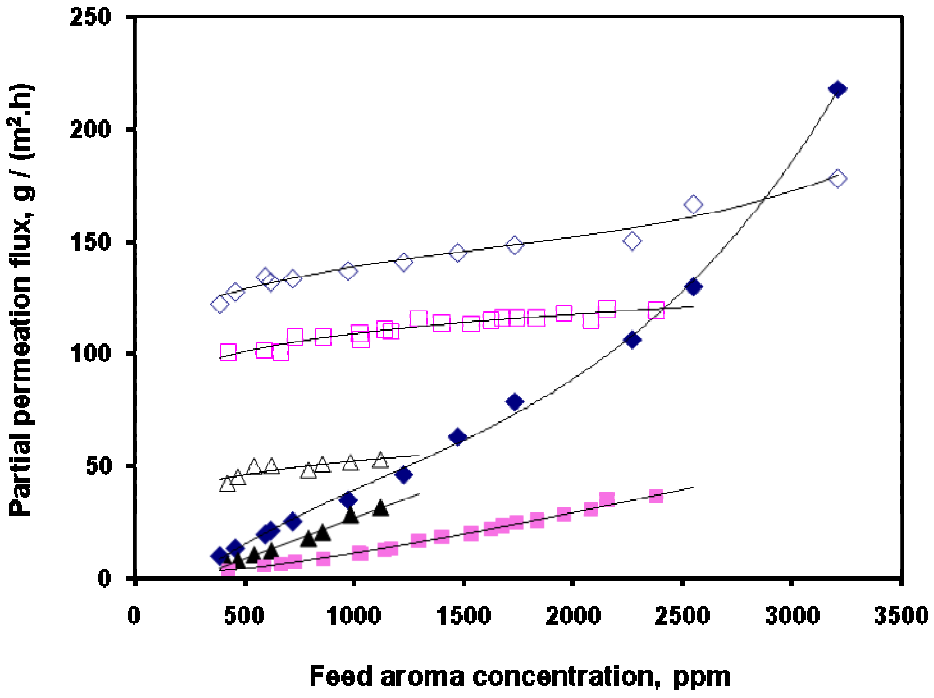

Figure 3.5 Effect of feed aroma concentration on the partial fluxes of aroma compounds and water for binary aroma-water permeation through PEBA membranes (♦ = propyl propionate (pp); ■ = benzaldehyde (bzd); ▲ = C_6-aldehyde (ald); ◊ = water in pp; □ = water in bzd; Δ = water in ald).

Figure 3.6 shows the effect of feed aroma concentration on the overall concentration of aroma compound in the permeate for binary aroma-water separations. The concentration of permeate aroma increases as the feed aroma concentration increases. Among the three aroma compounds, C_6-aldehyde is the most selective permeant to separate from aqueous solutions by the PEBA membrane, followed by propyl propionate and benzaldehyde. The concentration of the permeate attained can reach up to around 23-55 wt.% for all three aroma compounds, corresponding to an enrichment factor of 225-170 for propyl propionate, 327-360 for C_6-aldehyde and 90-105 for benzaldehyde. It should be pointed out that the permeate

concentration shown in Figure 3.6 represents the overall aroma concentration in the permeate stream. They are much higher than the solubility limit at the ambient temperature for all three aroma compounds, and phase separation took place in the permeate stream resulting in two phases: an organic phase and an aqueous phase. In practice, these two phases can be separated by a decanter so that nearly pure aroma (i.e., organic phase) can be obtained. However, not all the aroma in the permeate stream can be recovered since some still exist in the aqueous phase. In order to improve the aroma compound recovery, recycling of the aqueous phase can be utilized, and this will be studied in details later (Chapter 6).

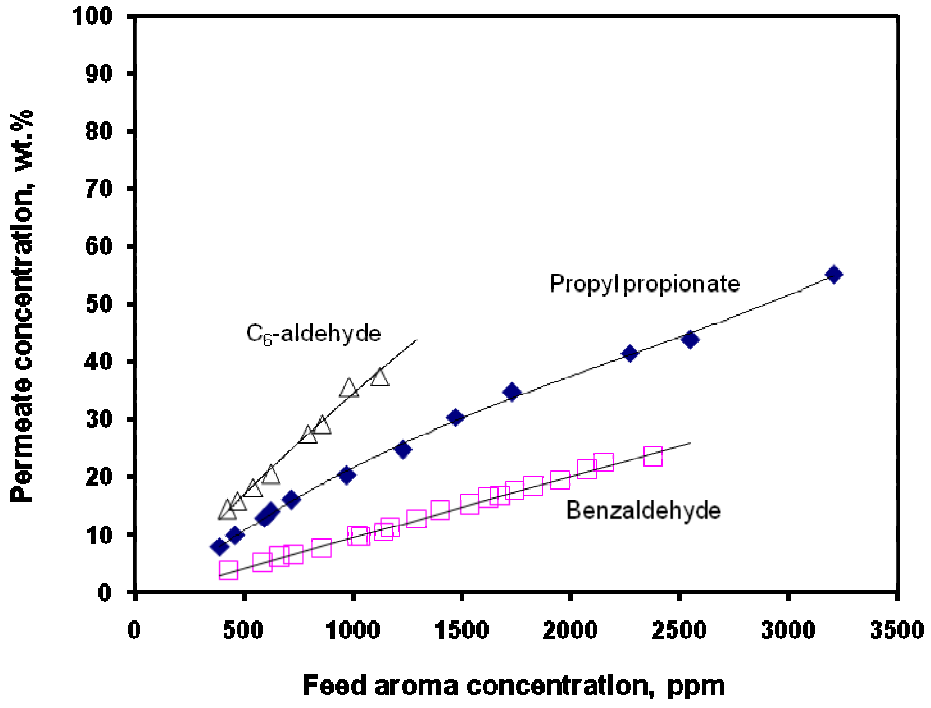

Figure 3.6 Effect of feed aroma concentration on the permeate concentration attained. Operating conditions same as those given in Figure 3.4.

Based on the overall permeate concentrations given in Figure 3.6, the separation factor can be evaluated using Eqn. (2.2) and the results are shown in Figure 3.7. As it can be seen, the selectivity goes up gradually as the feed aroma concentration increases. The permselectivity

of the membrane to the aroma compound permeation follows the order of C_6-aldehyde > propyl propionate > benzaldehyde.

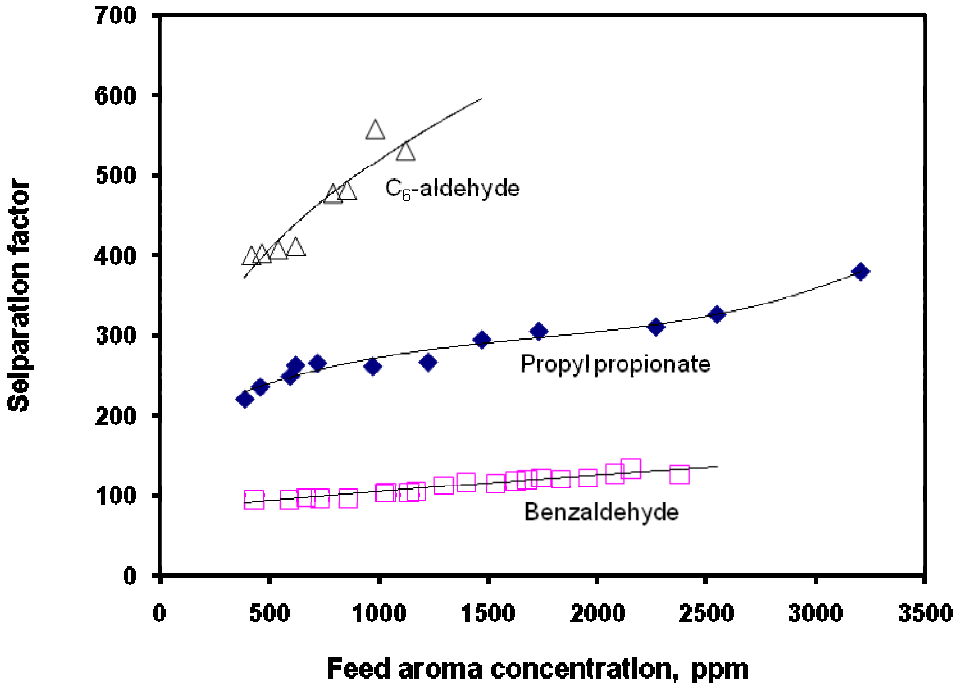

Figure 3.7 Effect of feed aroma concentration on the separation factor.

In the range of feed aroma concentrations investigated, the membrane exhibits a separation factor of 220-380 for propyl propionate, 400-558 for C_6-aldehyde and 95-135 for benzaldehyde. The separation factor would be much higher than these values if the concentrations of aroma compounds in the organic phase of the permeate decanter were used. For example, at 23^{o}C the solubility of water in propyl propionate is 0.86 wt.% (Stephenson and Stuart, 1986); this means the organic phase contains about 99.9 wt.% of propyl propionate. Thus, a 1,000 ppm of propyl propionate in the feed can be concentrated by the PEBA membrane to reach 99.9 wt.% corresponding a separation factor of up to 990,000. In this sense, PEBA is indeed a very promising membrane for pervaporation separation of aroma compounds from aqueous solutions.

3.3.2 Effect of Operating Temperature

Operating temperature is known to have a significant influence on the pervaporation performance. Prior studies showed strong temperature dependence of solubility and diffusivity. In this study, experiments were also carried out at different temperatures while maintaining other process conditions constant. The binary feed solutions of aroma-water had a concentration of 700, 435 and 745 ppm for propyl propionate, C_6-aldehyde and benzaldehyde, respectively. The temperatures tested (25-55^{o}C) was well below the boiling point. Relatively low temperatures are preferred considering energy cost and retaining aromas' natural properties.

Figure 3.8 shows the effects of temperature on the total and partial permeation fluxes. The total permeation flux is almost tripled when the temperature increases from 27 to 55^{o}C. However, the partial fluxes of aroma compounds increase less significantly as the operating temperature increases. The significant increase in the total flux is mainly caused by the significant increase in water flux. In general, the permeation flux increases as temperature increases. This is understandable considering the permeation mechanism and the nature of the membrane. Based on the solution–diffusion model, sorption and diffusion are the two major steps in the mass transport that control the permeation. An increase in temperature generally increases the diffusivity of the permeant exponentially (Liu et al., 2005), and this will be discussed later. The operating temperature also affects the characteristics of the membrane. An increase in temperature enhances thermal motion of the polymer chains, which facilitates the movement of permeant. In pervaporation, the permeant diffuses through the free volumes of the membrane. The free volume is produced by random thermal motion of the polymer chains in the amorphous region (Tian *et al.*, 2005). As the temperature increases, the frequency and amplitude of the polymer chain motion increase, and thus increasing the free volume.

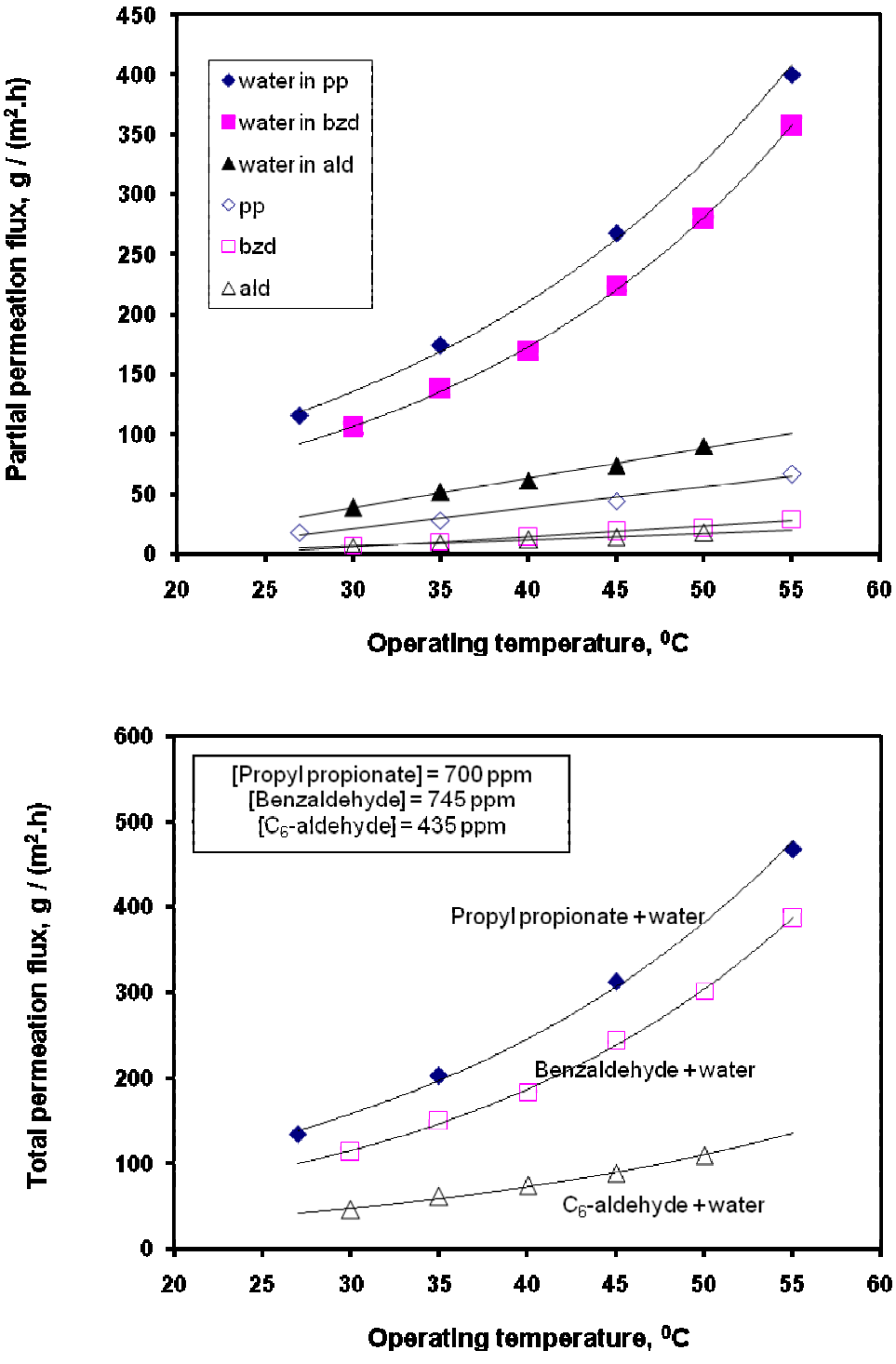

Figure 3.8 Effect of operating temperature on the total and partial fluxes for the permeation of binary aroma-water mixtures (membrane thickness = ~25 μm).

Another explanation is in conjunction with the phase change of permeant in pervaporation. During pervaporation, the permeant changes in phase from liquid to vapor so that a certain amount of energy is needed to vaporize. The energy to vaporize is taken from the system itself, which causes a localized cooling of the membrane (Neel, 1991). An increase in temperature will help supply the energy needed for the phase change.

Figure 3.9 shows the relationship between the permeation (i.e., total and partial) fluxes and *1/T*. It is shown that the temperature dependence of the total permeation flux follows an Arrhenius type of correlation. The same has also been observed for the partial fluxes of aroma compounds and water. This is consistent with other studies reported in the literature (Huang and Lin, 1968; Huang and Jarvis, 1970; Cabasso *et al.*, 1974). According to Feng and Huang (1996), there were two ways to evaluate the activation energy for permeation, one was evaluated from a ln(*J*) versus *1/T* plot, the other from a ln(*J/ΔP*) versus *1/T* plot. The activation energy determined from ln(*J*) vs *1/T* accounts for the heat of evaporation, which is required for the liquid-vapor phase change. On the other hand, the activation energy derived from ln(*J/ΔP*) vs *1/T* is based on the permeability coefficient in which the vapor pressure difference across the membrane (*ΔP*) is used to represent the driving force. Thus, the activation energy obtained this way consists of the activation energy for diffusion and the heat of sorption, excluding the heat of evaporation. Based on the ln(*J*) vs *1/T*, the activation energies for the permeation of propyl propionate, C_6-aldehyde and benzaldehyde are determined to be 37.4, 39.7, 45.0 kJ/mol, respectively. The activation energy for water to permeate in the three binary aroma-water systems is 36.4, 33.0 and 40.2 kJ/mol, respectively. The different values of activation energy for water permeation also show that the permeant-permeant molecular interactions influence the mass transport during pervaporation.

Compared to their evaporation heats at normal boiling points, i.e., 36.4 kJ/mol for propyl propionate, 37.1 kJ/mol for C_6-aldehyde, 42.7 kJ/mol for benzaldehyde, and 40.7 kJ/mol for water, the activation energy for aroma permeation is higher, whereas water permeation activation energy is lower. Generally speaking, the sorption of permeant into the membrane is an exothermic process, and the solubility decreases with an increase in temperature (Liu *et al.*, 2005).

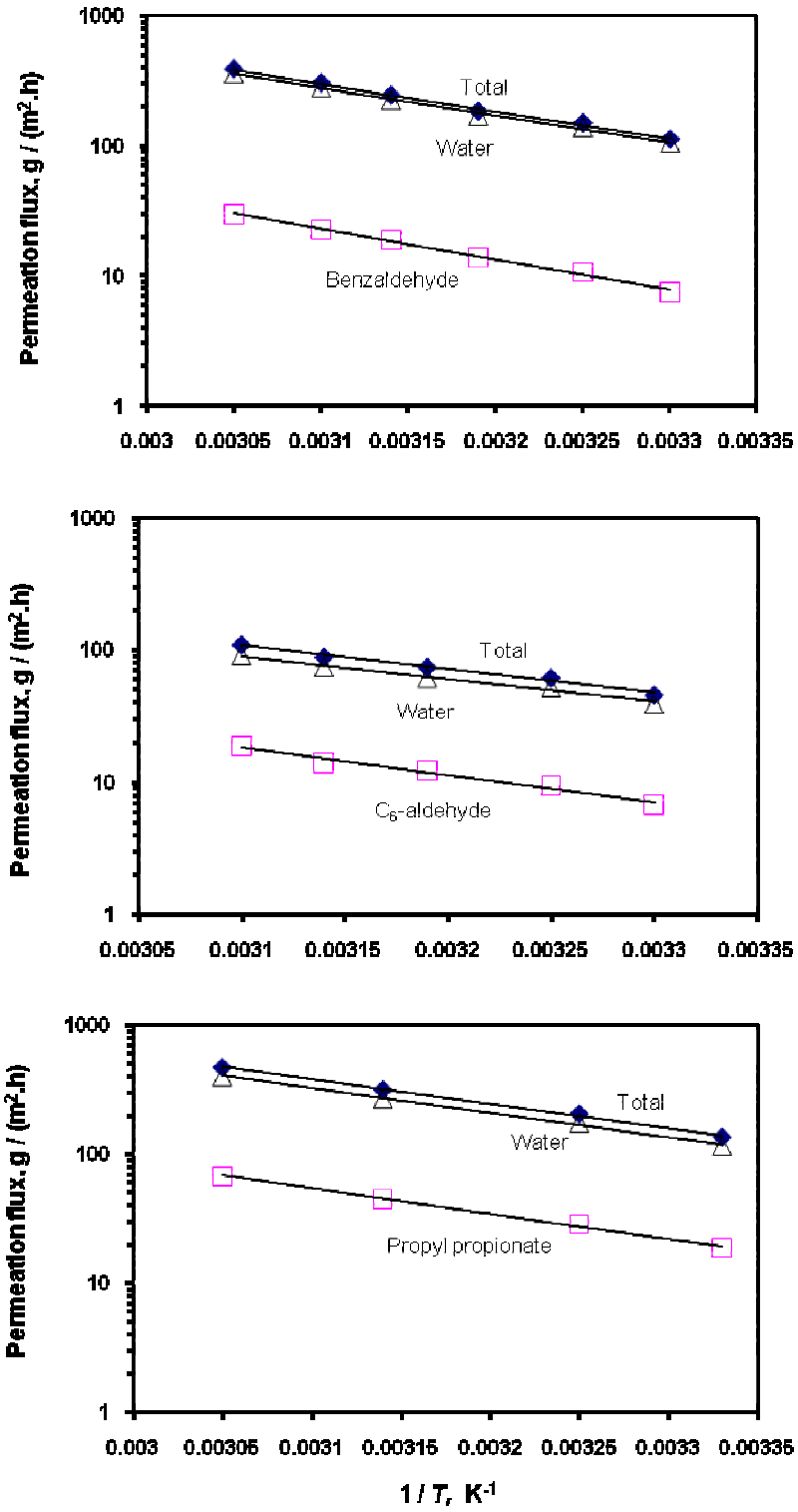

Figure 3.9 Correlation between permeation flux and 1/*T* ([propyl propionate] = 700 ppm, [benzaldehyde] = 745 ppm, [C_6-aldehyde] = 435 ppm).

In contrast, the diffusivity is positively influenced by temperature and an increase in temperature will augment the diffusivity. The above data imply that for the permeation of the three aroma compounds, with an increase in temperature, increases the diffusivity more significantly than the solubility, and this is not the case for water permeation.

Because of the relatively small difference in the activation energy of permeation between aroma compounds and water, only a small change in permeate composition was observed when the operating temperature increases, as shown in Figures 3.10. It can be seen that although the operating temperature has a significant influence on the total permeation flux, the permeate concentration increases only slightly as the operating temperature increases. This indicates that an increase in temperature facilitates, to a similar extent, the permeation of both aroma compounds and water through the membrane.

It may be mentioned again that the concentrations of permeate shown in Figure 3.10 represent the overall concentration of aroma compound in the permeate. Under the experimental conditions (i.e., 435-745 ppm of feed aroma concentration; 27-55^{o}C of operating temperature), the permeate obtained had a concentration that was much higher than their solubility limits, and a phase separation took place in the permeate collector, resulting in a substantially higher aroma concentration in the organic phase. Figure 3.11 shows the effect of operating temperature on the separation factor based on the overall permeate concentration. Since the separation factor is calculated from the permeate composition, an increase in temperature also increases the separation factor, as expected from the temperature dependence of permeate composition shown in Figure 3.10.

In comparison to other membranes reported in the literature, it is not easy to tell which membrane has the best pervaporation performance because of the different process conditions used. Nevertheless, a general trend can be observed, that is, the pervaporation performance of the PEBA membrane achieved in this work is better than most other membranes for separations of propyl propionate and C_6-aldehyde from their aqueous solutions; however, for benzaldehyde-water separation, the PEBA membrane has a higher permeation flux but a lower selectivity.

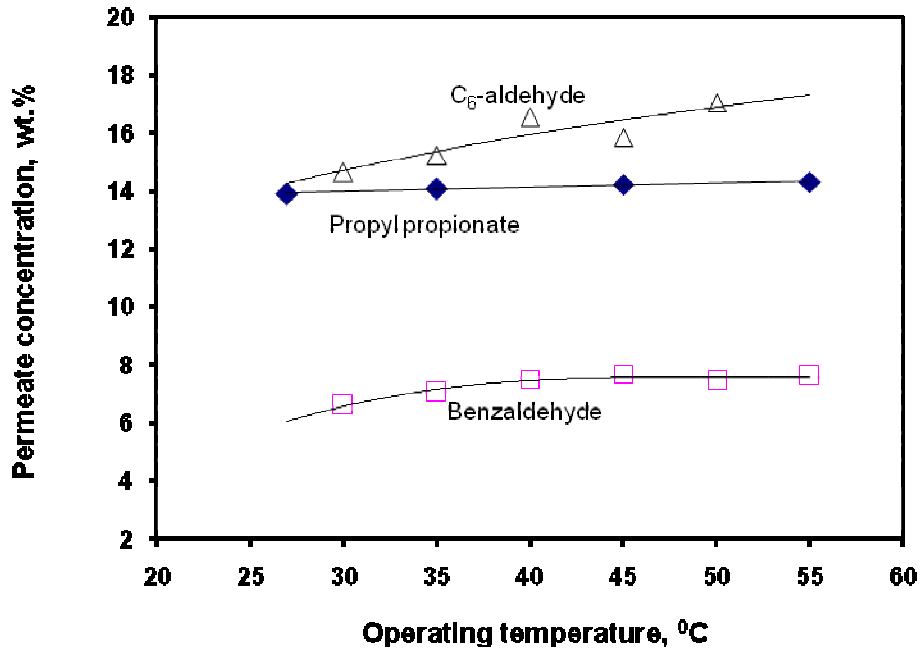

Figure 3.10 Effect of operating temperature on the permeate concentration for binary aroma-water separations ([propyl propionate] = 700 ppm, [benzaldehyde] = 745 ppm, [C_6-aldehyde] = 435 ppm).

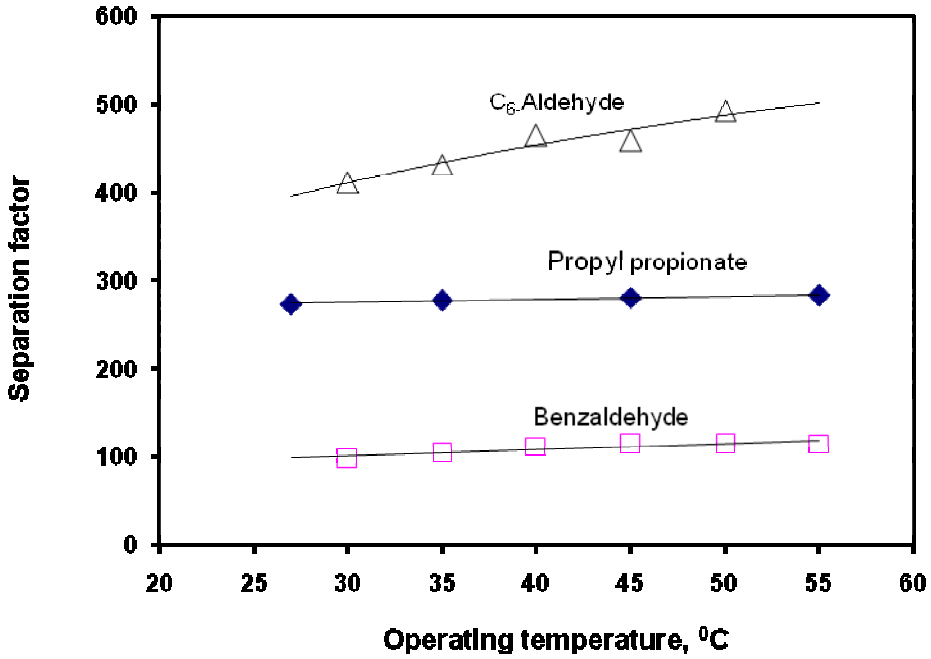

Figure 3.11 Effect of operating temperature on the separation factor for binary aroma-water separations.

Some results of pervaporation performance for the same or similar aroma compounds using different membranes reported in the literature (including some that were shown in Table 2.1) are summarized in Table 3.2. Of particular interest is the work of Djebbar *et al.* (1998), who used different PEBA membranes with varying contents of polyether and polyamide segments (where the number code represents the relative polyamide (nylon 12) content). For instance, PEBA 2 consists of 75 wt.% polyether and 25 wt.% polyamide, whereas PEBA 3 contains 67 wt.% polyether and 33 wt.% polyamide. The PEBA membrane used in this study is close to PEBA 2 used by Djebbar *et al.* in terms of the membrane composition. The partial fluxes of ester compounds (ethyl butyrate and ethyl propionate) from Djebbar *et al.*'s work are very high and even higher than the permeation flux of water. This is not surprising since the feed aroma concentration used by Djebbar *et al.* was very high (i.e., at saturated concentrations of organic phase which is nearly pure organic compounds). This high permeation flux of aroma than water is actually consistent with the data shown in Figure 3.5 for the separation of propyl propionate-water solutions by PEBA 2533 membrane used in this study. As the feed propyl propionate concentration approaches saturation (i.e., solubility limit), the partial flux of propyl propionate is expected to be higher than water flux based on the data in Figure 3.5.

Table 3.2 Comparison of pervaporation performance in aroma compound recovery from aqueous solutions between this work and other investigations (same or very close aroma compounds).

Aroma compound	**Formula**	**Membrane (thickness)**	**Exp. conditions ([feed], T_F, P_P)**	**Organic flux ($g/m^2.h$)**	**Separation factor (α)**	**Ref.**
Esters:						
- Propyl propionate	**$C_6H_{12}O_2$**	**PEBA 2533 (25 µm)**	**400-3,207 ppm, 30°C, 3 mBar**	**10.47-217.92**	**220-380**	**This work**
		PEBA 2533 (25 µm)	**700 ppm, 27-55°C, 3 mBar**	**18.57-66.86**	**273-283**	**This work**
- Butyl acetate	$C_6H_{12}O_2$	PDMS GFT	11.2 ppm, 5°C, 500-600 Pa		112	Bengtsson *et al.*, 1989
		PDMS GFT	12 ppm, 5°C, 600 Pa		91-133	Bengtsson *et al.*, 1992
		PEBA 2533 (100 µm)	50-2,125 ppm, 30-60°C	1-168	195-545	Liu *et al.*, 2005
- Ethyl butyrate	$C_6H_{12}O_2$	PDMS GFT	100 ppm, 5°C, 500-600 Pa	3-5	114	Bengtsson *et al.*, 1989
		PDMS GFT	500 ppm, 32-45°C, 700 Pa 10 % ethanol	3-3.5		Beaumelle *et al.*, 1992
		PDMS GFT	500 ppm, 31°C, 2,700 Pa		151	Beaumelle *et al.*, 1992
		PDMS GFT	500 ppm, 31°C, 2,700 Pa, 10 % ethanol		56	Beaumelle *et al.*, 1992
		PDMS GFT	500 ppm, 36°C, 0-10 % ethanol	22-28.2	1,215-694	Beaumelle *et al.*, 1992
		PDMS GFT	100 ppm, 30°C, 5 Pa	3.2	253	Lamer and Voilley, 1991
		PDMS GFT	100 ppm, 25°C, 35-60 Pa	2.53	299	Lamer, 1993
		PDMS GFTz	100 ppm, 25°C, 35-60 Pa	2.62	735	Lamer, 1993
		PDMS GFTz	100 ppm, 30°C, 300-2,000 Pa, Re = 100	1.50-0.52	375-253	Lamer *et al.*, 1992
		PDMS GFTz	100 ppm, 30°C, 300-2,000 Pa, Re = 600	4.73-3.64	465-382	Lamer *et al.*, 1992
		PDMS DC (130 µm)	100 ppm, 25°C, 35-60 Pa	2.2	1,635	Lamer, 1993
		PDMS DC (130 µm)	100 ppm, 25°C, 50 Pa, Re = 10^5	2.61	2,413	Lamer *et al.*, 1994

Table 3.2 Continued

Aroma compound	Formula	Membrane (thickness)	Exp. conditions ([feed], T_F, P_P)	Organic flux ($g/m^2.h$)	Separation factor (α)	Ref.
- Ethyl butyrate	$C_6H_{12}O_2$	PDMS DC (130 µm)	100 ppm, 25°C, 50 Pa, multi-component	2.6-3.4		Lamer *et al.*, 1996
		PEBA 2	Saturated solution, 30°C	800	765	Djebbar *et al.*, 1998
		PEBA 3	Saturated solution, 30°C	660	954	Djebbar *et al.*, 1998
		PEBA 4	Saturated solution, 30°C	282	631	Djebbar *et al.*, 1998
		PEBA 5	Saturated solution, 30°C	86	548	Djebbar *et al.*, 1998
		PEBA 6	Saturated solution, 30°C	10	199	Djebbar *et al.*, 1998
		PDMS	Saturated solution, 30°C	5,000	3,020	Djebbar *et al.*, 1998
		PEBA 3533	100-900 ppm, 30°C	1-25	81-201	Sampranpiboon, 2000
- Ethyl isobutyrate	$C_6H_{12}O_2$	PDMS GFT	100 ppm, 25°C, 35-60 Pa	2.72	293	Lamer, 1993
		PDMS GFTz	100 ppm, 25°C, 35-60 Pa	1.65	549	Lamer, 1993
		PDMS DC (130 µm)	100 ppm, 25°C, 35-60 Pa	2.11	1,641	Lamer, 1993
		PDMS DC (130 µm)	85 ppm, 25°C, 50 Pa	2.69	2,023	Lamer *et al.*, 1994
		PDMS DC (130 µm)	100 ppm, 25°C, 50 Pa, multi-component mixtures	2.69-3.87		Lamer *et al.*, 1996
- Ethyl butanoate	$C_6H_{12}O_2$	PDMS (10 µm)	300 ppm, 30-40°C, 3 mmHg	14.31-21.42	158-93	Sampranpiboon, 2000
		PDMS (10 µm)	300 ppm, 30°C, 3-15 mmHg	14.31-12.15	158-151	Sampranpiboon, 2000
		POMS (10 µm)	300 ppm, 30-40°C, 3 mmHg	14.69-18.81	165-83	Sampranpiboon, 2000
		POMS (10 µm)	300 ppm, 30°C, 3-15 mmHg	14.69-9.19	165-157	Sampranpiboon, 2000
- Ethyl 2-methyl Butyrate	$C_7H_{14}O_2$	PDMS GFT	1.3 ppm, 5°C, 500-600 Pa		122	Bengtsson *et al.*, 1989
- Ethyl propionate	$C_5H_{10}O_2$	PDMS (60 µm)	5,000 ppm, 35°C	35	134	Sluys *et al.*, 1992
		PEBA 2	Saturated solution, 30°C	1,180	209	Djebbar *et al.*, 1998
		PEBA 3	Saturated solution, 30°C	1,000	278	Djebbar *et al.*, 1998
		PEBA 4	Saturated solution, 30°C	295	174	Djebbar *et al.*, 1998
		PEBA 5	Saturated solution, 30°C	88	114	Djebbar *et al.*, 1998
		PEBA 6	Saturated solution, 30°C	20	100	Djebbar *et al.*, 1998

Table 3.2 Continued

Aroma compound	Formula	Membrane (thickness)	Exp. conditions ([feed], T_F, P_P)	Organic flux ($g/m^2.h$)	Separation factor (α)	Ref.
- Ethyl propionate	$C_5H_{10}O_2$	PDMS	Saturated solution, 30°C	2,810	328	Djebbar *et al.*, 1998
		PDMS GFT	1 ppm, 33°C, 250 Pa, 10 % ethanol	0.0306	508	Beaumelle, 1994
		PDMS GFT	9 ppm, 5°C, 500-600 Pa		112	Bengtsson *et al.*, 1989
Aldehydes:						
- C_6-aldehyde	**$C_6H_{12}O$**	**PEBA 2533 (25 µm)**	**420-1,120 ppm, 30°C, 3 mBar**	**7.07-31.52**	**400-558**	**This work**
		PEBA 2533 (25 µm)	**435 ppm, 30-50°C, 3 mBar**	**6.67-18.52**	**411-493**	**This work**
		PDMS GFT	1 ppm, 33°C, 250 Pa, 10 % ethanol	0.0125	207	Beaumelle, 1994
- trans 2 Hexenal	$C_6H_{10}O$	PEBA GKSS (50 µm)	110 ppm		142	Bengtson and Boddeker, 1995
		PEBA GKSS (25 µm)	110 ppm		98	
		PEBA GKSS (5 µm)	110 ppm		4	Bengtson and Boddeker, 1995
		PDMS GKSS (10 µm)	110 ppm		26	
		PDMS GFT	5 ppm, 5°C, 500-600 Pa		44	Bengtsson *et al.*, 1989
		PDMS GFT	10 ppm, 5°C, 600 Pa		38-57	Bengtsson *et al.*, 1992
		PDMS GFT	10 ppm, 20°C, 600 Pa		19-36	Bengtsson *et al.*, 1989
		PDMS 1060	20 ppm, 20°C, 0-12 % ethanol	0.5	368-189	Karlsson and Tragardh, 1994
		PDMS 1060	87 ppm, 25°C, 10 < Re < 10,000	0.12-0.61		Karlsson and Tragardh, 1993

Table 3.2 Continued

Aroma compound	Formula	Membrane (thickness)	Exp. conditions ([feed], T_F, P_P)	Organic flux ($g/m^2.h$)	Separation factor (α)	Ref.
Aromatic:						
- Benzaldehyde	**C_7H_6O**	**PEBA 2533 (25 µm)**	**430-2,378 ppm, 30°C, 3 mBar**	**4.07-36.16**	**95-135**	**This work**
		PEBA 2533 (25 µm)	**745 ppm, 30-55°C, 3 mBar**	**7.42-29.41**	**97-115**	**This work**
		PDMS GFT	75-1,400 ppm, 25°C, 60 Pa	1-15	101-277	Lamer, 1993
		PDMS GFT	100 ppm, 25°C, 35-60 Pa	1.04	116	Lamer, 1993
		PDMS GFT	100 ppm, 25°C, 70 Pa	1.04	280	Lamer *et al.*, 1996
		PDMS GFTz	100 ppm, 25°C, 35-60 Pa	0.71	291	Lamer, 1993
		PDMS DC (30 µm)	87 ppm, 25°C, 60 Pa	1.75	498	Lamer *et al.*, 1996
		PDMS DC (60 µm)	100 ppm, 25°C, 60 Pa	1.48	521	Lamer *et al.*, 1996
		PDMS DC (100 µm)	78-132 ppm, 25°C, 200 Pa		24-90	Lamer *et al.*, 1996
		PDMS DC (130 µm)	100 ppm, 25°C, 60 Pa	0.91	591	Lamer *et al.*, 1996
		PDMS DC	100 ppm, 25°C, 35-60 Pa	0.94	637	Lamer, 1993
		PDMS DC (150 µm)	100 ppm, 25°C, 60 Pa	0.93	1,074	Souchon *et al.*, 1997

3.4 Summaries

The following conclusions can be drawn from the studies on pervaporation separation of three binary aroma-water solutions using the PEBA membrane:

- PEBA was very selective for the separation of propyl propionate, C_6-aldehyde and benzaldehyde from their aqueous solutions.
- The feed aroma concentration affected significantly the aroma permeation flux and selectivity.
- At 30^{o}C and in the range of feed aroma concentrations investigated (390-3,207 ppm), the aroma compound fluxes were 10.5-218, 7.1-31.5 and 4.1-36.2 g/m^2.h for propyl propionate, C_6-aldehyde and benzaldehyde, respectively. The corresponding separation factors were in the range of 220-380, 400-558 and 95-135, respectively.
- The operating temperature strongly affected the total flux, but the selectivity was only slightly affected.
- The temperature dependence of permeation flux followed an Arrhenius type of relationship, and the activation energy for permeation was 37.4, 39.7, 45.0 kJ/mol for propyl propionate, C_6-aldehyde and benzaldehyde, respectively.
- The permeant-membrane and permeant-permeant interactions were found to affect the mass transport of permeant across the membrane.

CHAPTER 4

Solubility and Diffusivity Aspects for Binary Aroma– Water Permeation through PEBA membrane

4.1 Introduction

Among the three steps of mass transport in pervaporation, desorption is the only step that can be assumed to be neglected, and diffusion inside the membrane is widely accepted to be the rate controlling step. While the diffusivity measures how fast the permeant moves in the membrane, the solubility determines how many permeant molecules are accommodated inside the membrane. Therefore, the permeation rate (i.e., the quantity of permeant molecules that permeate through the membrane) is determined by both the solubility and diffusivity. Solubility is an equilibrium property that represents the ability of the membrane to absorb the permeant, and the diffusivity, on the other hand, is a kinetic property describing how the permeant can diffuse through the membrane. Solubility and diffusivity in pervaporation are often dependent on permeant concentration (Greenlaw *et al.*, 1977; Binning *et al.*, 1961; Huang and Lin, 1968; Mulder and Smolders, 1984). This chapter attempts to study the solubility and diffusivity in PEBA 2533 membrane for the separation of the three model aroma-water solutions studied in Chapter 3. The dependency of solubility and diffusivity on permeant concentration was evaluated from both pervaporation and sorption-desorption experiments. The diffusivity was evaluated from data fitting of permeation flux versus concentration using the solution-diffusion model, and based on the time-dependent sorption method. Since the local concentration of the permeant inside the membrane is difficult to determine, the overall diffusivity through the membrane at given feed solution concentrations were determined, although in theory the diffusivity in the membrane during pervaporation varies from the feed side to the permeate side because of the concentration gradient across the membrane.

4.2 Experiments

The solubility as a function of permeant concentration was determined from sorption and desorption experiments. The sorption experiments were conducted by immersing dried membrane samples into aqueous solutions of aroma compounds at various known concentrations maintained at 30^{o}C. The concentration of aroma compound in the solution varied in the range of 0-2,332 ppm for propyl propionate-water, 0-1,024 ppm for C_6-aldehyde-water, and 0-1,655 ppm for benzaldehyde-water. All measurements were carried out at 30^{o}C. The equilibrium sorption uptake was determined after the membrane sample submerged in the liquid for a sufficiently long time (at least 24 h) until no further increase in the sorption uptake was observed. The quantity of the sorption uptake was measured from the weight change of the membrane before and after sorption in the liquid. In order to determine the quantity of both aroma compound and water inside the membrane, desorption experiments were carried out immediately after the swollen membrane was weighed using a digital balance. Caution was exercised to minimize evaporative loss of the sorbate from the membrane prior to the desorption measurements. The desorption was carried out under vacuum using the same pervaporation setup with a slight modification, and the desorbed sorbate was collected in the cold trap. The composition of the sorbate was analyzed using the TOC analyzer. To ensure that the sorbate sample was homogeneous and not phase-separated (considering the limited solubilities), the sample was diluted with de-ionized water prior to TOC analysis. The sorption uptake of individual components (i.e., aroma compound and water) was calculated from the total mass uptake and the composition of the sorbate. In this study, the membrane thickness used for sorption/desorption experiments was purposely made thicker (~50 μm) than the membrane used for pervaporation experiments (~25 μm) in an attempt to obtain a sufficiently large amount of sorbate inside the membrane for more accurate measurements in the weight and composition of the sorbate samples. The sorption/desorption experiments were repeated at least twice to establish the reproducibility of the measurements, and the experimental error in the sorption uptake was shown to be within 5-8 %.

The diffusivity was also determined based on the solution-diffusion model. With given solubility and permeation flux from the sorption and pervaporation experiments, the diffusivity can be evaluated by data fitting. In addition, another method (i.e., time-dependent sorption) was used to determine the diffusivity for the permeation system of propyl propionate-water. The latter method also required sorption/desorption experiments, but were carried out at various times of sorption. To determine the time-dependent sorption uptake in the membranes, the membrane sample was taken from the aroma-water solutions at various times of sorption (including at equilibrium), blotted quickly with Kimwipes to remove excess liquid on membrane surfaces, and then placed immediately in a glass tube that was fitted to the desorption setup. The determination of sorption uptake and the experimental steps for the desorption run were the same as performed in the abovementioned evaluation of solubility. The sorption uptake at various times was normalized with the sorption uptake at equilibrium (M_t/M_∞), and was plotted with their corresponding times. The diffusivity was determined from the sorption kinetics by data fitting with Eqn. (2.13) where n was taken as 7 because the extra terms in Eqn. (2.13) using larger n values did not have any effect on the diffusivity values obtained. On the other hand, if the value n was taken as zero, the maximum error could be 10 %.

The diffusivity of pure aroma compound (i.e., propyl propionate) and pure water in the PEBA membrane was also evaluated. The diffusivity of pure propyl propionate was determined from the rate of evaporation (i.e., desorption) data at 30^{o}C, 1 atm. A certain mass of dry membrane sample was immersed in the pure propyl propionate. Once the membrane was fully saturated (equilibrium) by propyl propionate, the saturated membrane was taken out from the solution. The free liquid on the membrane surfaces was carefully wiped with Kimwipes; then, the membrane sample was immediately put on a digital balance. The change in mass of membrane sample due to evaporation at any times (so-called desorption kinetics) was observed until a constant mass of membrane sample was achieved. The diffusivity was determined from the desorption kinetics data using the modified Eqn. (2.13). The diffusivity of pure water through PEBA membrane was evaluated based on the time-dependent sorption method.

4.3 Results and Discussion

4.3.1 Solubility

Figure 4.1 shows the effect of aroma compound concentration in the liquid solution on the solubility of the aroma compound in PEBA membrane. The trend is consistent with the feed concentration dependency of permeation flux. An increase in feed aroma concentration causes more aroma compounds to be absorbed by the PEBA membrane. In the range of aroma concentration investigated, the aroma compound sorption can be approximated by the Henry's law (i.e., linear correlation). Among the three aroma compounds, benzaldehyde is the most selectively sorbed permeant by the PEBA membrane, followed by C_6-aldehyde and propyl propionate, with solubility coefficients (from the slopes of lines) of 13.6 x 10^{-6}, 8.35 x 10^{-6} and 4.60 x 10^{-6} g / (g membrane.ppm), respectively. This trend is different from their permeation fluxes shown in Chapter 3. Clearly, the molecular interactions between permeant-membrane and permeant-permeant have a significant effect on the pervaporation performance. A high solubility does not guarantee to give a high permeation flux because the diffusivity, which also affects the permeation rate, is affected by the molecular size of the permeant. Propyl propionate, for instance, has the lowest solubility in PEBA membrane but has the highest permeability. The membrane selectivity for propyl propionate-water separation, on the other hand, is between the selectivities for binary C_6-aldehyde-water and benzaldehyde-water separations.

As a matter of fact, because of the permeant-permeant interactions, the more swollen membrane also gives more spaces for water uptake. Consequently, an increase in aroma compound concentration in liquid solution also increases the solubility of water in the PEBA membrane, as shown in Figure 4.2. It can be observed that the presence of C_6-aldehyde and benzaldehyde strongly affects the solubility of water in the PEBA membrane, whereas propyl propionate does not influence the water solubility significantly. The similar trend in the effects of C_6-aldehyde and benzaldehyde on water solubility in PEBA membrane may be attributed to their similar functional groups (i.e., aldehyde) in these two compounds.

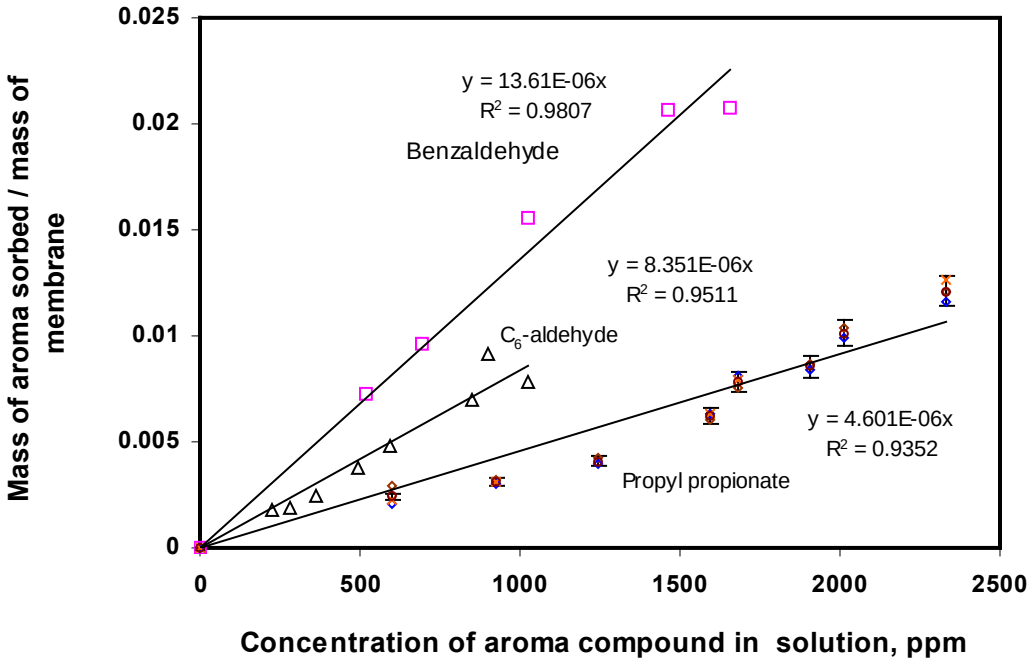

Figure 4.1 Effect of aroma compound concentration in binary aroma-water mixtures on its solubility in PEBA membrane (T = 30°C). The error bars are also shown for propyl propionate sorption uptake.

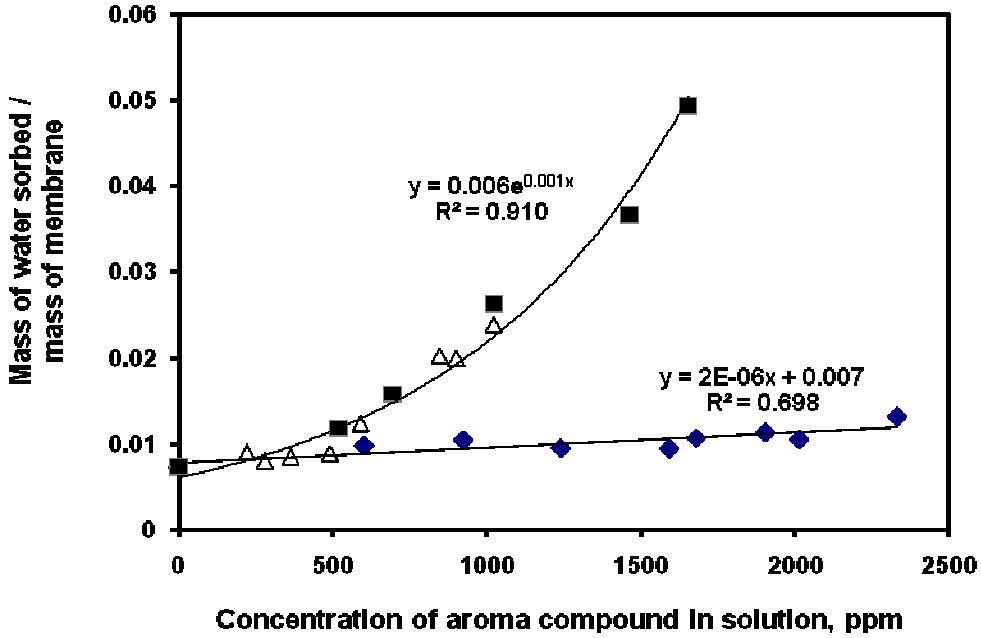

Figure 4.2 Effect of aroma compound concentration in binary aroma-water mixtures on water solubility in the PEBA membrane (T = 30°C; ♦ = water in propyl propionate; Δ = water in C_6-aldehyde; ■ = water in benzaldehyde).

The different behavior in solubility between the aroma compounds and water in the PEBA membrane may also relate to the degree of separation that can be achieved by pervaporation. In analog to the selectivity given in Eqn. (2.2) for pervaporation separation, a selectivity based on solubility (i.e., the solubility selectivity, α_S), can be defined as,

$$\alpha_S = \frac{c''(1-c)}{c(1-c'')} \tag{4.1}$$

where *c''* is the mass fraction of aroma compound in the sorbate taken up by the membrane. Using the solubility data of aroma compounds and water in PEBA membrane given in Figures 4.1 and 4.2, the solubility selectivity of the PEBA membrane can be determined, as shown in Figure 4.3. It can be seen that the solubility selectivity of aroma-water solutions in PEBA membrane tends to be higher than the selectivity for pervaporation separation. This again confirms that the mass transport of permeant from the feed side to the permeate side in pervaporation is controlled not only by the sorption step but also influenced by the diffusion through the membrane. In this sense, the permeation of water, which has a smaller molecular size and weaker interaction with the organophilic PEBA material than the aroma compounds studied, will be easier to diffuse through the membrane, resulting in a lower selectivity in pervaporation (permselectivity) than the solubility selectivity. Based on the solution-diffusion model, the permselectivity (α) may be expressed in terms of solubility selectivity (α_S) and diffusivity selectivity (α_D),

$$\alpha = \alpha_S \alpha_D \tag{4.2}$$

Experimental data show that as the feed aroma concentration increases, the permselectivity of aroma compounds also increases (Figure 3.7), but the solubility selectivity decreases (Figure 4.3). This implies that the diffusivity selectivity α_D increases with an increase in feed aroma concentration. Generally speaking, the α_D tends to decrease as the membrane becomes more swollen. Such a discrepancy could be caused by the fact that the simplest solution-diffusion model does not always work properly for pervaporation systems.

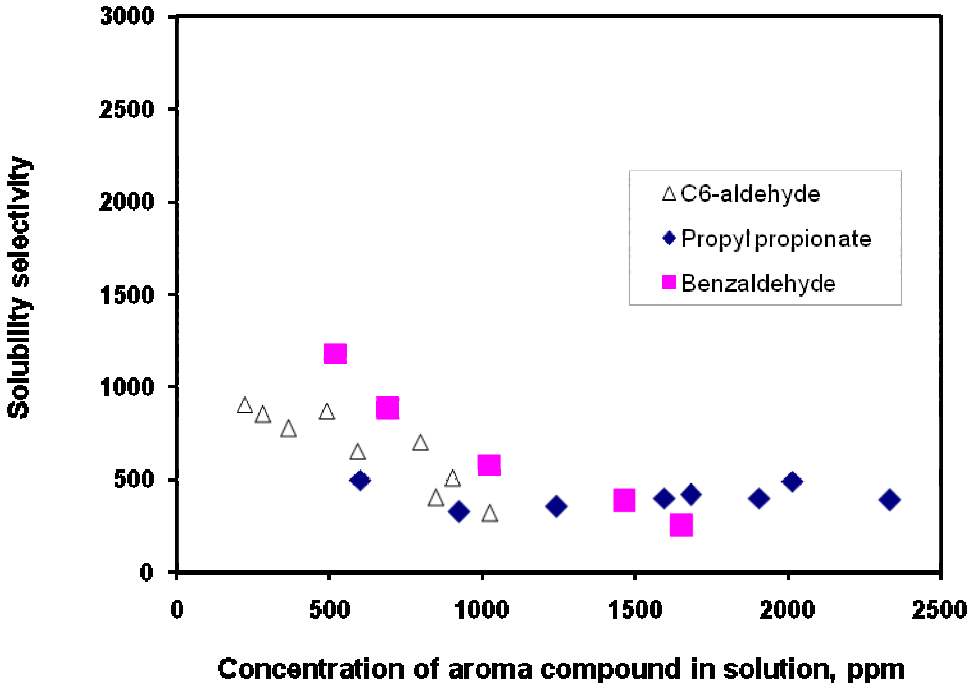

Figure 4.3 Solubility selectivity for binary aroma compound/water in PEBA membrane at different aroma concentrations in the solution.

4.3.2 Diffusivity

The diffusivity can be evaluated from the experimental data of pervaporation by data fitting using a mass transport model. Based on the simplest solution-diffusion model and considering that diffusion controls the permeation rate, the diffusivity (D_i) can be evaluated using Eqn. (2.4). At steady-state, the permeation flux (J_i) is constant and thus integrating Eqn. (2.4) with the boundary conditions of the permeant concentrations on both membrane surfaces, gives

$$J_i l_m = -\int_{C_{sF,i}}^{C_{sP,i}} D_i dC_i \qquad (4.3)$$

where $C_{sF,i}$ and $C_{sP,i}$ are the concentrations of permeant i on the membrane surfaces of feed and permeate sides, respectively. The concentrations of permeant on the membrane surfaces are difficult to measure. However, the concentration on the membrane surface of the feed side can be expressed in terms of permeant concentration in the bulk feed using solubility coefficient.

$$X_{m,i} = S_i x_{F,i} \tag{4.4}$$

where $X_{m,i}$ is the mass of permeant i per unit mass of dry membrane (g permeant / g membrane), S_i is the solubility coefficient, and $x_{F,i}$ is the feed concentration (g / g solution). The mass fraction of permeant in the membrane phase can be expressed in term of permeant concentration in the membrane (C_i, g permeant / volume of swollen membrane).

$$C_i = X_{m,i}\rho_m = S_i x_{F,i}\rho_m \tag{4.5}$$

where the density of swollen membrane may be considered to be the same as dry membrane (ρ_m) because of the similar densities of the PEBA and the aqueous solutions. On the permeate side, the permeant concentration on the membrane surface can be considered to be zero because of the vacuum applied.

The equations to determine diffusivity are obtained from further integration of Eqn. (4.3), and the types of equations depend on the dependency of diffusivity on permeant concentration. Three types of diffusivity dependencies on permeant concentration were examined here, i.e., (i) constant diffusivity ($D_i = D_0$), (ii) linear concentration dependency ($D_i = D_0 + \kappa C_i$), and (iii) exponential concentration dependency ($D_i = D_0\, exp(\gamma C_i + \kappa)$). Substituting Eqn. (4.5) into Eqn. (4.3) and then to be integrated with a constant diffusivity gives,

$$J_i = \frac{D_0 S_i x_{F,i}\rho_m}{l_m} \tag{4.6}$$

In the same way, the correlations between permeation flux and diffusivity based on linear and exponential concentration dependencies of diffusivity can be obtained (Eqns. (4.7) and (4.8)).

$$J_i = \frac{\left(D_0 + \frac{\kappa S_i x_{F,i} \rho_m}{2}\right) S_i x_{F,i} \rho_m}{l_m} \tag{4.7}$$

where D_0 is the diffusivity at infinite dilute solution, and κ is the proportional constant.

$$J_i = \frac{D_0}{l_m \gamma}\left[\exp\left(\gamma S_i x_{F,i} \rho_m + \kappa\right) - 1\right] \tag{4.8}$$

where γ is the plasticization parameter.

The diffusivity, if it is constant, can be directly calculated from Eqn. (4.6). In case that the diffusivity is linearly or exponentially dependent on permeant concentration, the parameters D_0, κ and γ can be determined by regressing Eqns. (4.7) and (4.8) using experimental data of pervaporation (i.e., permeation flux) and sorption (i.e., solubility). The regression results are shown in Table 4.1. For convenience of comparison, the solubility coefficients for the three aroma-water permeations are also shown. Considering the R^2 values of the regression, it can be seen that the linear concentration dependency is the most appropriate relationship to correlate diffusivity as a function of feed aroma concentration. To further verify this, the diffusivity as a function of feed concentration can be calculated from the given diffusivity correlations using the values of D_0, κ and γ so obtained, and they are shown in Figures 4.4, 4.5 and 4.6, respectively.

Table 4.1 Diffusivity parameters and solubility coefficient obtained from data fitting (T = 30°C).

	Aroma compound		
Parameter	**Propyl propionate**	**C_6-aldehyde**	**Benzaldehyde**
Solubility coefficient:			
- Solubility coefficient (S_i), g / (g membrane.ppm)	4.601×10^{-6}	8.351×10^{-6}	13.61×10^{-6}
Diffusivity parameter:			
A. Constant diffusivity, $D = D_0$			
- D_0, $cm^2.s^{-1}$	7.881×10^{-7}	2.051×10^{-7}	7.024×10^{-8}
Regression, R^2	0.899	0.887	0.942
B. Linear concentration dependent, $D = D_0 + \kappa C$			
- D_0, $cm^2.s^{-1}$	2.961×10^{-7}	8.726×10^{-8}	4.135×10^{-8}
- κ, $cm^5.g^{-1}.s^{-1}$	8.997×10^{-5}	3.201×10^{-5}	2.402×10^{-6}
Regression, R^2	0.990	0.990	0.994
C. Exponential concentration dependent, $D = D_0 \exp(\gamma C + \kappa)$			
- D_0, $cm^2.s^{-1}$	9.569×10^{-7}	2.847×10^{-7}	8.575×10^{-8}
- γ, $cm^3.g^{-1}$	1.10	1.10	1.10
- κ	6.13×10^{-5}	4.02×10^{-5}	9.54×10^{-4}
Regression, R^2	0.789	0.079	0.552

Figure 4.4 shows the diffusivity of the three aroma compounds calculated from Eqn. (4.6) based on constant diffusivity. Clearly, the diffusivity is shown to change as the feed aroma concentration increases. This implies that the diffusivity of the aroma compounds must be concentration dependent. Figure 4.5 shows the diffusivity of the aroma compounds in the PEBA membrane calculated from Eqn. (4.7) based on linear dependency of diffusivity on the permeant concentration. It can be seen that there is very good agreement between the profiles shown in the figure and the assumption used in the derivation of Eqn. (4.7). The diffusivity indeed increases linearly as the feed aroma concentration increases.

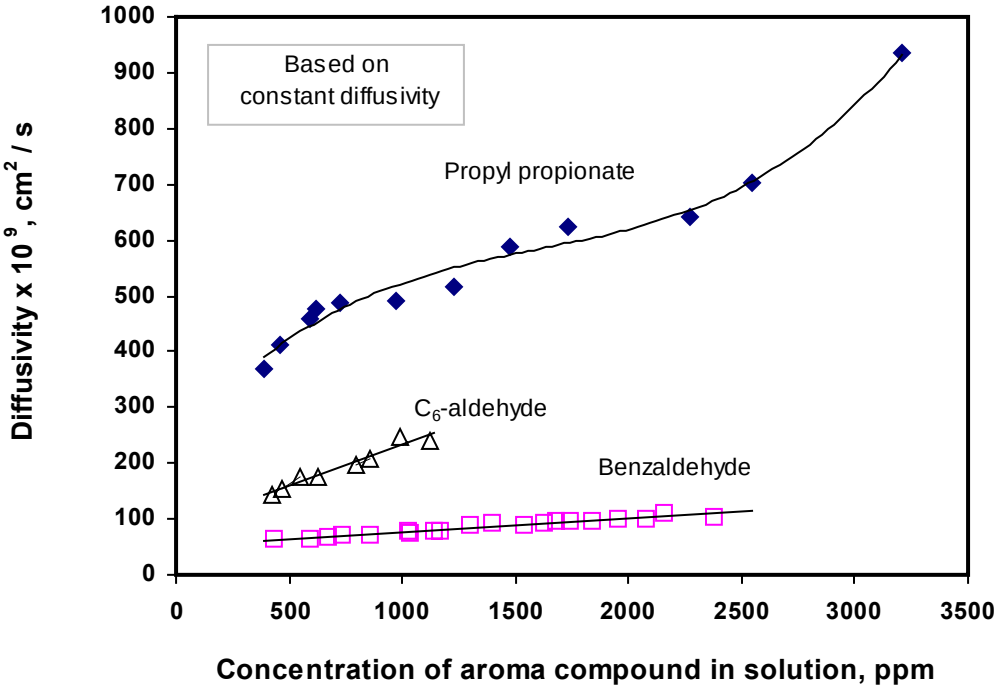

Figure 4.4 Diffusivity of aroma compounds in PEBA membrane calculated from Eqn. (4.6) based on constant diffusivity (i.e., independent on permeant concentration).

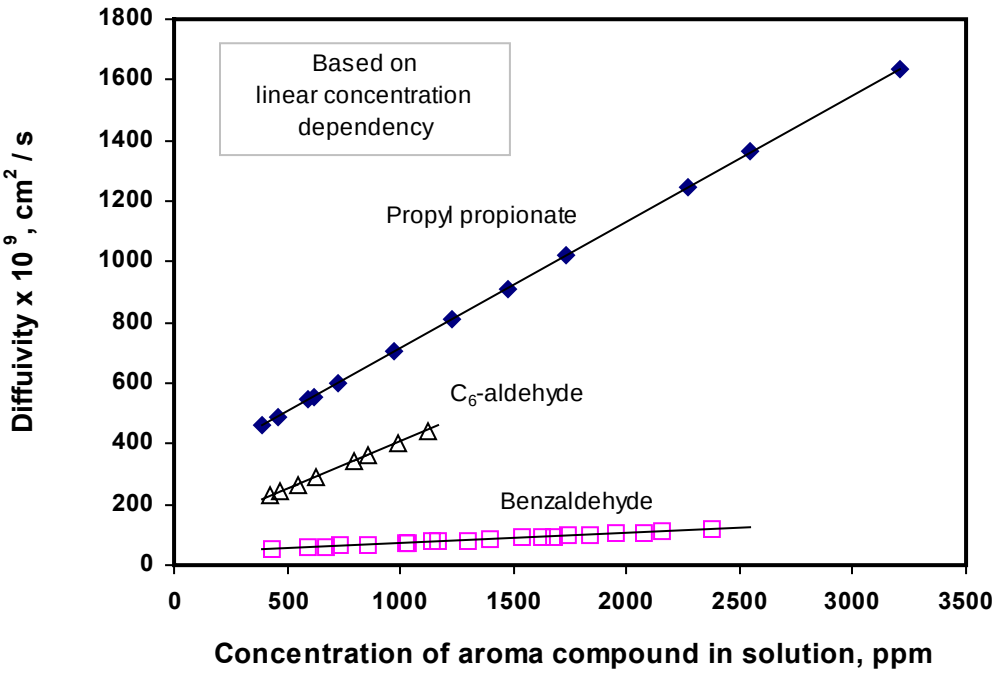

Figure 4.5 Diffusivity of aroma compounds in PEBA membrane calculated from Eqn. (4.7) based on linear concentration dependency.

Figure 4.6 shows the calculated diffusivity assumed to be exponentially dependent on concentration, which is clearly not the case. It is now clear that according to the data of sorption equilibrium and permeation rate, the diffusivity of the aroma compounds in the PEBA membrane follows a linear relationship with the feed aroma concentration. Propyl propionate was found to be the most diffusivity selective permeant in the PEBA membrane, followed by C_6-aldehyde and benzaldehyde.

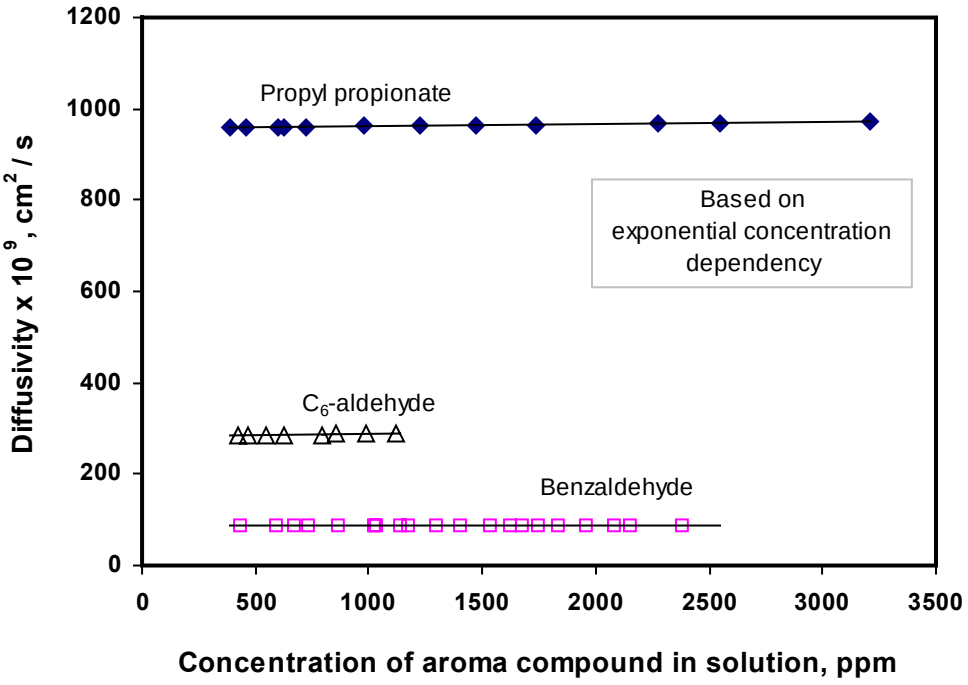

Figure 4.6 Diffusivity of the three aroma compounds in PEBA membrane calculated from Eqn. (4.8) which assumes exponential concentration dependency of the diffusivity.

As a comparison, the time-dependent sorption was also used to determine the diffusivity for the permeation system of propyl propionate-water mixtures. Figure 4.7 shows the typical sorption kinetics of propyl propionate on the PEBA membrane at three solution concentrations (i.e., 603, 926 and 2,014 ppm). Obviously, the sorption kinetics is affected by the concentration of propyl propionate in the solution. The sorption curve at a higher concentration before equilibrium is sharper than that at a lower concentration, which means

that the time for sorption to reach equilibrium at a higher concentration is shorter. Rapid sorption means a higher diffusivity. This further confirms that the diffusivity is dependent on the permeant concentration; a higher permeant concentration gives a higher diffusivity. To find out the numerical values of the diffusivity, the sorption kinetics data at various propyl propionate concentrations are fitted into Eqn. (2.13) by a non-linear regression method using Polymath.

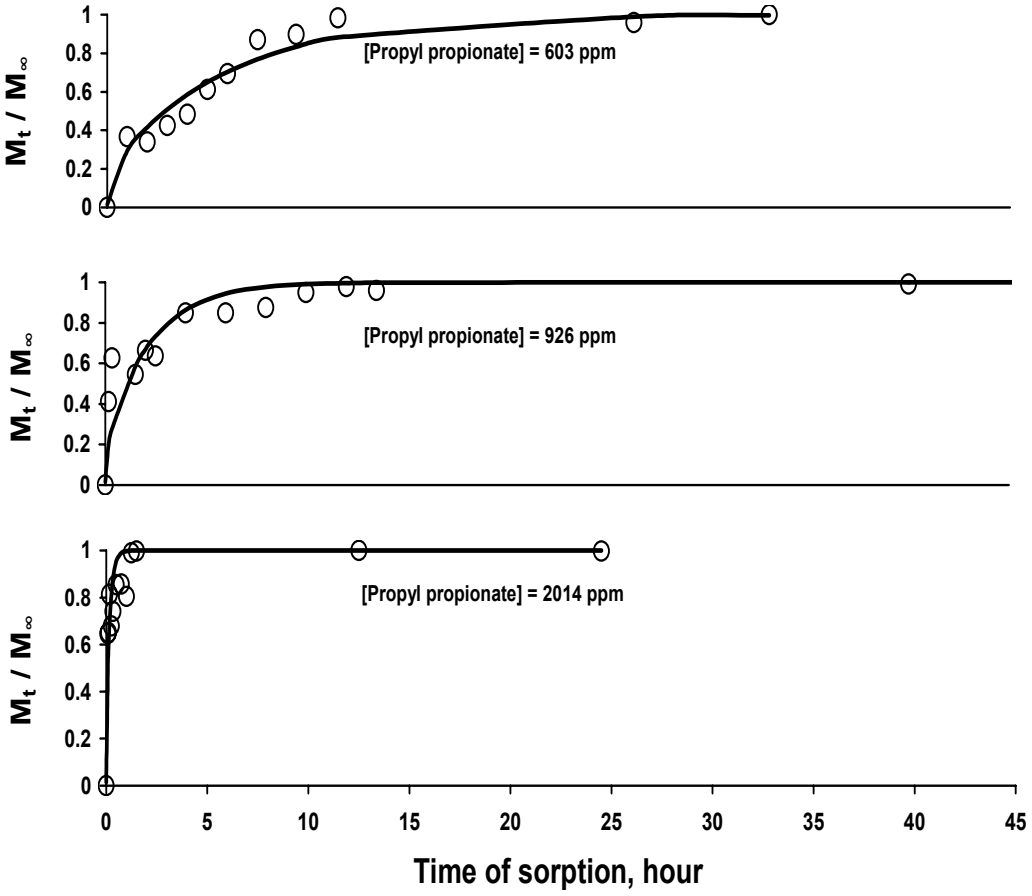

Figure 4.7 Sorption kinetics of propyl propionate in PEBA membrane (T = 30°C). Symbols represent experimental data and the solid lines represent the calculated values with the parameters obtained by the regression.

Figure 4.8 shows the diffusivity coefficient of propyl propionate through the membrane at different concentrations in the solution (600–2,330 ppm). It is shown that an increase in the

propyl propionate concentration will increase its diffusivity significantly, and the concentration dependence of the diffusivity follows an exponential relation. This confirms that membrane swelling due to propyl propionate sorption will enhance the diffusivity through the membrane. It may be mentioned that strictly speaking, Eqn. (2.13) is valid for Fickian diffusion with diffusivity being independent on the local concentration inside the membrane, and the diffusivity evaluated here is essentially an apparent mean values that enable us to see how the concentrations of propyl propionate in the feed influence the diffusivity.

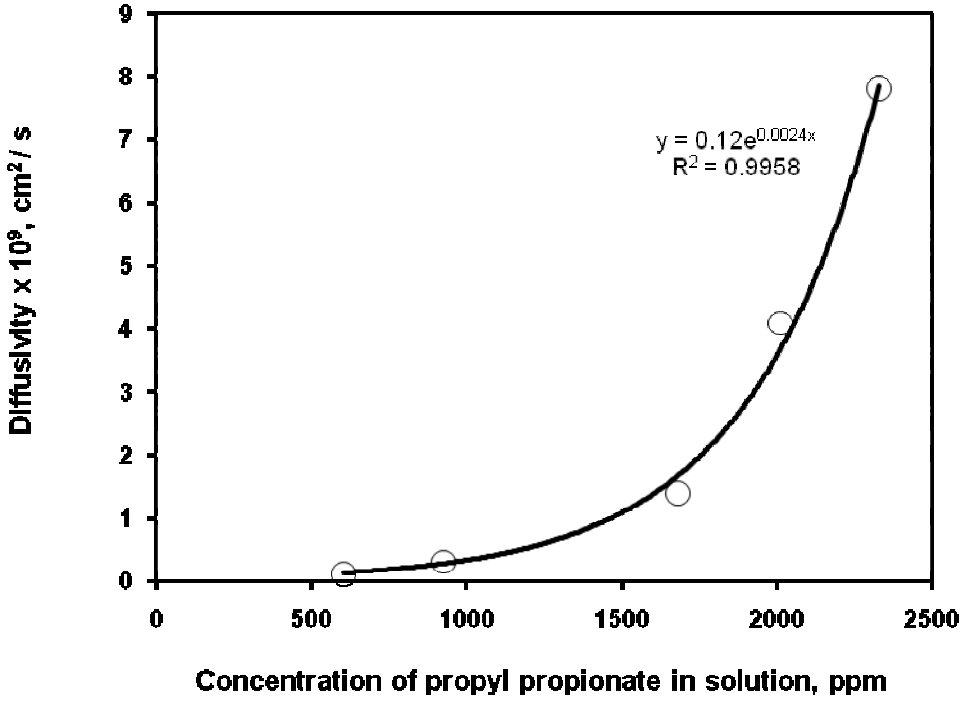

Figure 4.8 Diffusivity of propyl propionate in PEBA membrane evaluated from the time-dependent sorption method (T = 30°C).

Compared to the diffusivity obtained from the combination data of solubility and permeation flux (Figure 4.5), the time-dependent sorption method gives a much lower diffusivity. This is not surprising because the membranes are at different states during the course of

pervaporation and sorption experiments. Pervaporation experiments are considered to proceed at steady state. On the permeate side, vacuum is applied so that the pressure imposed on the two membrane surfaces is significantly different. In the time-dependent sorption experiments, the membrane is saturated by the permeant gradually (transient process) from both sides of membrane surfaces. Thus, the two membrane surfaces are in contact with liquid, and at the same pressure condition. It must be noticed that the diffusivity obtained from the first method represents an apparent diffusivity, which may vary depending on the mass transport model used. In this sense, the difference in diffusivity obtained from the two methods may be due to the weak applicability of the simplest solution-diffusion model to be applied in these pervaporation systems.

4.4 Transport Properties of Pure Component

In principle, the diffusivity of water in the binary mixture through the membrane can be determined in the same way. However, water is the major component in the solution (> 99.6%) and has poor affinity to the membrane, and a small variation in the composition analysis of the sorbate sample would lead to a large uncertainty in the measurements of water sorption uptake (which was done by subtracting the quantity of propyl propionate from the total quantity of the sorbate). As a result, the diffusivities of water in the dilute solutions at various concentrations (600–2,330 ppm propyl propionate) through the membrane cannot be well distinguished. Consequently, the diffusivity of pure water through the membrane was measured instead, by the same token, from a sorption experiment for which the sorption uptake could be simply determined gravimetrically and composition analysis of the sorbate was no longer needed. The diffusivity of pure water in the PEBA membrane was found to be 1.29×10^{-9} cm^2/s. Similarly, the diffusivity of pure propyl propionate in the membrane can also be determined. However, considering that the ambient air is free of propyl propionate, the diffusivity of pure propyl propionate can be more conveniently determined from the rate of evaporation (i.e., desorption) of propyl propionate from the membrane saturated with the sorbate.

Figure 4.9 shows the representative desorption kinetics of pure propyl propionate from the PEBA membrane. It can be seen that the evaporation of propyl propionate from the membrane surface to the surrounding air was initially fast and then became gradually slower. By fitting the desorption kinetics data to Eqn. (2.13), the diffusivity of pure propyl propionate in the membrane was found to be 1.48 x 10^{-7} cm^2/s, which is about 115 times greater than the diffusivity of pure water. The validity of using the desorption data to evaluate the diffusivity is verified by the straight line in a plot of $\ln((W_t - W_\infty)/(W_0 - W_\infty))$ versus t (shown in Figure 4.10, where W_0 and W_t are the weights of the membrane sample at time zero and t, respectively, and W_∞ is the dried membrane weight) because for large diffusivities and/or in later stages of diffusion, only the first term in the series of Eqn. (2.13) needs to be considered and the graph of $\ln(W_t - W_\infty)$ against t approaches a straight line (Ji *et al.*, 1995; Crank and Park, 1968). It may be mentioned that pure water diffusivity could not be determined accurately from the desorption experiment because of the presence of water vapor in the atmosphere and the small sorption uptake in the membrane.

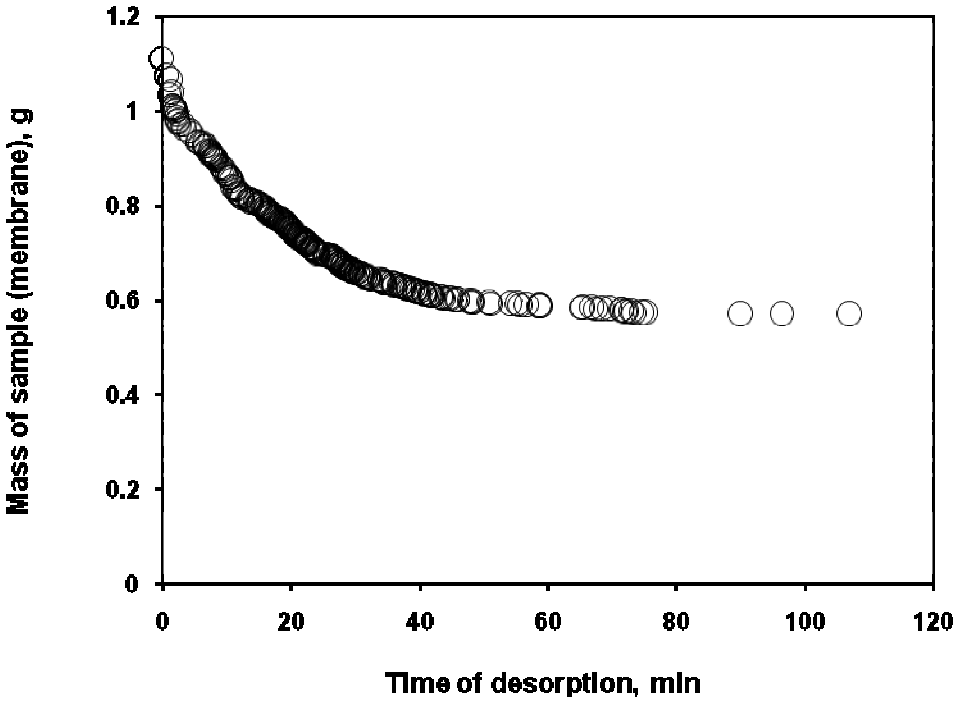

Figure 4.9 Desorption kinetics of pure propyl propionate on PEBA membrane (T = 30°C).

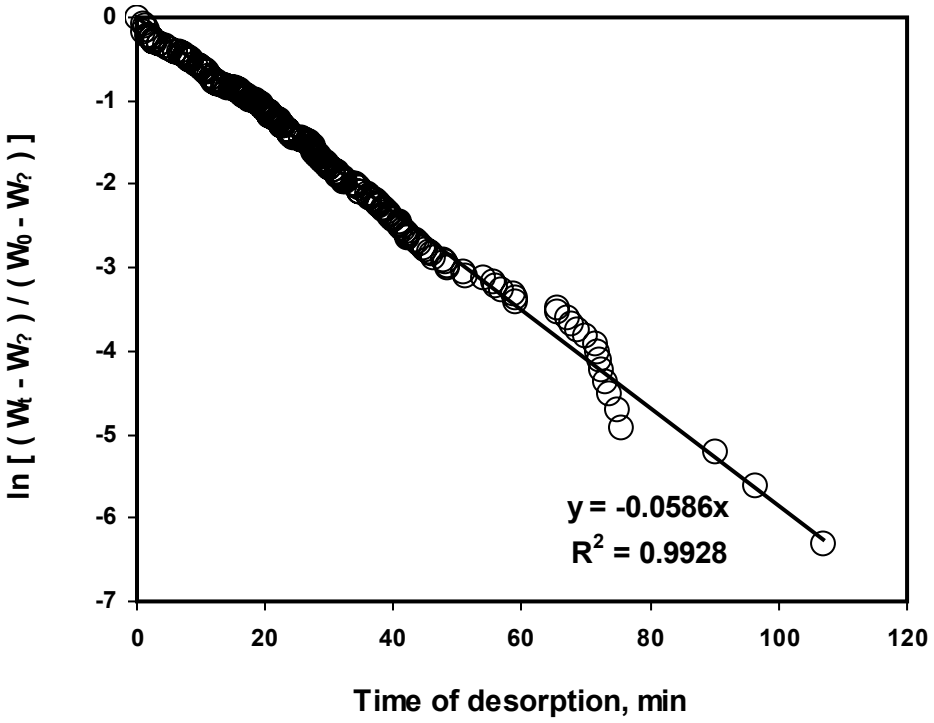

Figure 4.10 Correlation between $\ln\left[\frac{(W_t - W_\infty)}{(W_0 - W_\infty)}\right]$ and time of desorption.

The difference in mass of sample between that at initial time of desorption (1.112 g) to that at infinite time (dry membrane, 0.567 g) shown in Figure 4.9 actually represents the solubility of pure propyl propionate in PEBA membrane, i.e. 0.961 g propyl propionate / g membrane. The solubility of pure water on PEBA membrane, on the other hand, can be known from Figure 4.2 at zero concentration of aroma, i.e. 0.00729 g water / g membrane, almost 132 times lower than that of pure propyl propionate. Again, this confirms that PEBA is an organophilic membrane.

Compared to the experimental results reported in Chapter 3, there seem some contradictions. When the feed aroma concentration increases, the water flux also increases while the solubility selectivity of aroma compounds decreases. This indicates that the diffusivity of

water in the PEBA membrane in the presence of aroma compounds may be higher than that of aroma compounds. In fact, the diffusivity of pure propyl propionate in the PEBA membrane was found much higher than that of pure water. To the author's opinion, these findings confirm that the diffusivity of permeant through membrane is affected by not only the molecular size of permeant but also the permeant-membrane interactions, the permeant concentration inside the membrane, even the permeant-permeant interactions. Disregarding the effect of any molecular interactions, in normal condition a molecule having a smaller molecular size will be easier to diffuse. In fact, this is not the case for diffusion of pure water and pure propyl propionate through the PEBA membrane. The reason seems to be the different effect of molecular interactions between permeant and membrane. A strong interaction of permeant-membrane can facilitate the diffusion of permeant. The membrane will be more swollen and the free volume in the polymer matrix becomes larger. The interactions between permeant and permeant may also affect the diffusion. The permeants having strong interactions between one another may have similar ability to diffuse through the membrane. This seems to be the case for the propyl propionate-water system (highest solubility) where both have the highest permeation as compared to the other two systems. In particular to the permeant-permeant interaction effect, a qualitative justification can also be seen from the sorption behavior of water in the PEBA membrane (Figure 4.2). The sorption uptake of water in the presence of C_6-aldehyde differed from that in the presence of propyl propionate, but similar due to the presence of benzaldehyde. Both C_6-aldehyde and benzaldehyde have an aldehyde group and similar solubility parameters (19.55 and 19.2 $MPa^{1/2}$; van Krevelen and Hoftyzer, 1972) that can indicate the extent of molecular interactions. Briefly speaking, the molecular interactions of permeant-membrane and permeant-permeant affect the mass transport behavior (sorption and diffusion) of permeant across the membrane.

4.5. Summaries

The following conclusions can be drawn from the solubility and diffusivity studies for aroma-water solutions in the PEBA membrane:

- The solubilities of the aroma compounds and water in the PEBA membrane were affected by the aroma concentration in the solution. The sorption uptake of the aroma compounds was proportional to the solution concentration. Within the feed aroma concentration range investigated (0-2,332 ppm), the solubility of the aroma compounds in the PEBA membrane at 30^{o}C was 0-0.0121 g propyl propionate / g membrane, 0-0.0091 g C_6-aldehyde / g membrane and 0-0.0208 g benzaldehyde / g membrane.
- The membrane showed preferential sorption to the aroma compounds, the permselectivity of the membrane was mainly derived from its excellent sorption selectivity.
- The diffusivity of the three aroma compounds in the PEBA membrane was affected by the concentration of aroma compound in the solution. From the steady state pervaporation and equilibrium sorption data, the diffusivity was found to be linearly dependent on the feed aroma concentration; however, from the sorption kinetics data obtained from the time-dependent sorption experiments, the diffusivity was shown to be affected by the feed aroma concentration exponentially. This may be attributed to the different swelling states of the membrane during steady state pervaporation and transient sorption processes.
- The solubility of pure propyl propionate in the PEBA membrane was 0.961 g propyl propionate / g membrane, around 130 times that of pure water (0.00729 g water / g membrane). The diffusivity of pure propyl propionate was 148 x 10^{-9} cm^2/s, which is 115 times that of pure water (1.29 x 10^{-9} cm^2/s).
- The permeant-membrane and permeant-permeant interactions were found to affect the transport properties of permeant through the membrane.

CHAPTER 5
Evaporation–Permeation of Binary Aroma–Water Mixtures through PEBA Membrane

5.1 Introduction

As an alternative to pervaporation, which involves permeation and evaporation, evaporation-permeation (or evapermeation) was also studied for aroma-water separation. Unlike in pervaporation where the feed liquid is evaporized first and the vapor is in contact with membrane. Pervaporation and evapermeation are similar; only the place at which the vaporization takes place is different. Evapermeation must be distinguished from vapor permeation. The true feed in evapermeation is still the liquid phase as in pervaporation. A schematic of evapermeation is given in Figure 5.1. Evapermeation may be a promising alternative to pervaporation for aroma-water separation, in case that concentration polarization becomes an issue. As well, the transport properties of vapor permeant through membrane may be different from the liquid permeant. Generally speaking, the concentration polarization and the different degree of a membrane swelling in vapor and liquid phases are often used in literature for the explanation of differences between mass transport during evapermeation and pervaporation (Uchytil and Petrickovic, 2002).

This chapter will briefly discuss the performance comparison between evapermeation and pervaporation in aroma compound recovery. The evapermeation performance for the separation of propyl propionate-water mixtures using PEBA membrane was tested, and the effect of feed aroma concentration was investigated while the operating temperature was maintained at 30^{o}C. The solubility and diffusivity of vapor mixtures of propyl propionate-water in the PEBA membrane were also evaluated. The separation performance of evapermeation, defined the same way as in pervaporation, is measured by permeation flux and selectivity.

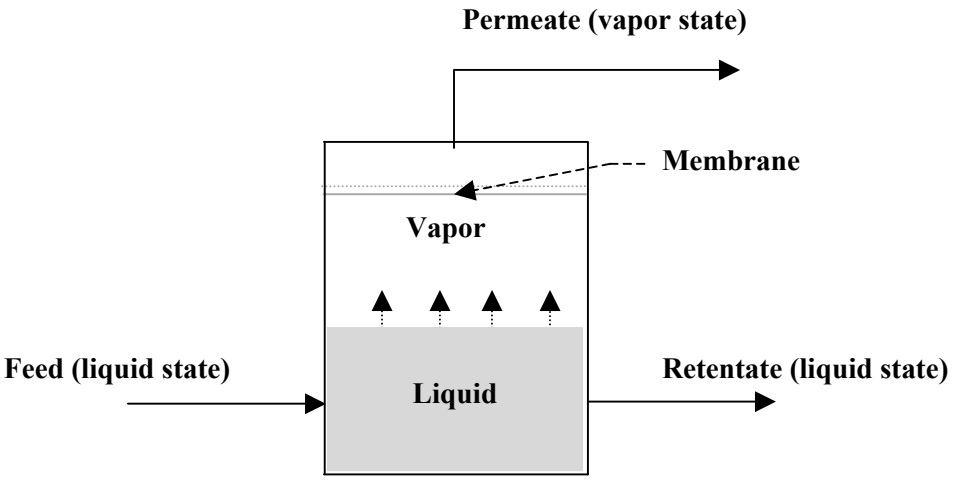

Figure 5.1 Simple schematic process of evapermeation.

5.2 Experiments

The model aroma compound (i.e., propyl propionate) and the membrane used in this work were the same as those used in pervaporation. The equipments setup for evapermeation is similar to that in pervaporation, except that the feed liquid must not be in contact with the membrane surface. The liquid was circulated to maintain the homogeneity of liquid phase, and the vapor phase was at equilibrium with liquid phase. Similar to pervaporation, evapermeation experiments were initiated by circulating the liquid feed for 1-2 h to condition the membrane, which was in contact with vapor. Then, vacuum was provided on the permeate side to induce the permeation. The permeate sample was collected in a cold trap immersed in liquid nitrogen. The collection of samples was conducted after the permeation reached steady state. The procedures for determining the permeation flux and permeate composition were the same as described previously for pervaporation. The feed concentration in the liquid phase was varied in the range of 400-3,900 ppm; other process conditions were all kept constant. The operating temperature and permeate pressure were kept at 30^{o}C and ~3

mmHg, respectively. The liquid feed was circulated at a flow rate of 1.6 L/min, and the membrane thickness used was ~25 μm.

The equilibrium compositions between liquid phase and vapor phase were measured experimentally. The feed liquid concentrations, which were in ppm levels, were analyzed using a TOC analyzer. The vapor sample was taken out by means of a-25 mL syringe, and was immediately diluted in a small amount of de-ionized water for further analysis. The aroma composition in the vapor phase was expressed in the unit of mass of vapor aroma per volume of vapor phase. The vapor mass of aroma compound in the syringe can be known from the TOC analysis results. Assuming that the pressure and temperature in the syringe and in the vapor feed are same, the concentration of vapor sample in the syringe (vapor mass of aroma compound / volume of syringe) is the same as that in the vapor feed.

5.3 Results and Discussion

5.3.1 Effect of Feed Aroma Concentration

Figure 5.2 shows a comparison of the permeation fluxes obtained in evapermeation and pervaporation at different feed aroma concentrations in the liquid solution. It can be seen that an increase in feed aroma concentration increases the permeation fluxes of both propyl propionate and water. However, in evapermeation, the feed aroma concentration does not affect the aroma permeation flux as strongly as in pervaporation. By contacting directly the liquid onto the membrane surface (pervaporation) results in higher permeation fluxes for both propyl propionate and water than evapermeation when the vapor is in contact with the membrane. Particularly, the aroma flux in pervaporation can be 100 times greater than in evapermeation. This is understandable since the concentration of propyl propionate in the vapor phase, which directly contacts with the membrane surface, is actually lower than that in the liquid phase. Water is more volatile than propyl propionate; therefore, at equilibrium, the composition of propyl propionate in the vapor phase is lower than that in the liquid phase. This can be seen in Figure 5.3, which shows the liquid-vapor equilibrium of propyl propionate-water solution at 30^{o}C and 1 atm. The concentration of propyl propionate in vapor phase is approximately 12-25 times lower than its concentration in the liquid phase.

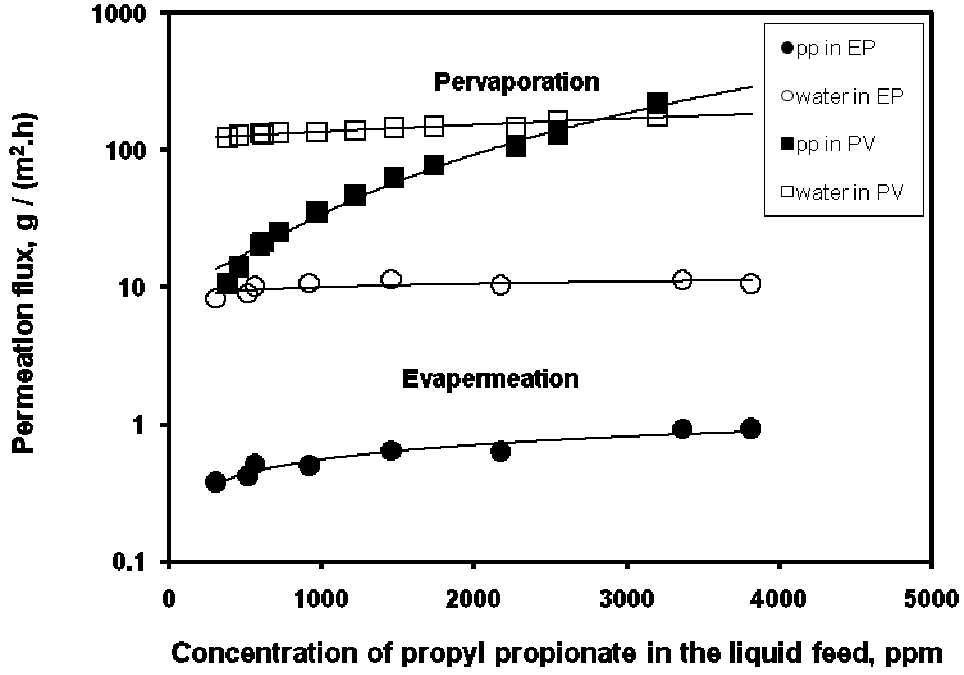

Figure 5.2 A comparison of permeation flux in evapermeation (EP) and pervaporation (PV) ($T = 30^{o}$C).

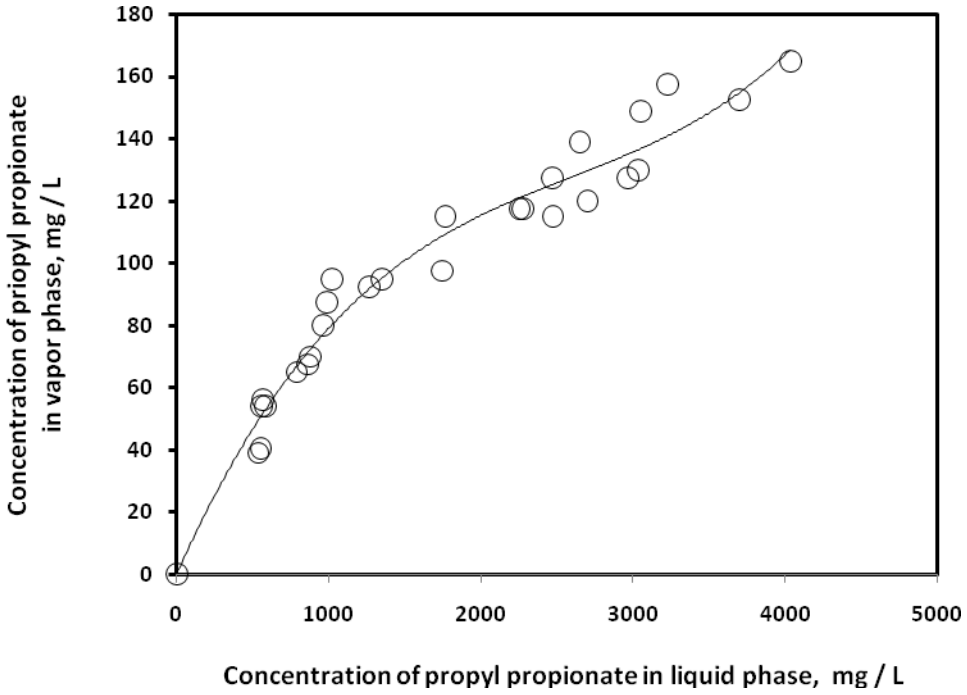

Figure 5.3 Liquid-vapor equilibrium of propyl propionate-water mixtures at 30^{o}C and 1 atm.

The lower concentration of propyl propionate in vapor phase causes the membrane to be less swollen. This helps maintain the hydrophobicity of PEBA membrane. It is expected that the water uptake in the PEBA membrane during evapermeation will be lower than water uptake during pervaporation.

Figure 5.4 shows the permeate concentration obtained in evapermeation and in pervaporation. The permeate concentration achieved by evapermeation increases slightly as the feed aroma concentration increases. However, they are extremely lower than that obtained by pervaporation, especially at higher feed aroma concentrations.

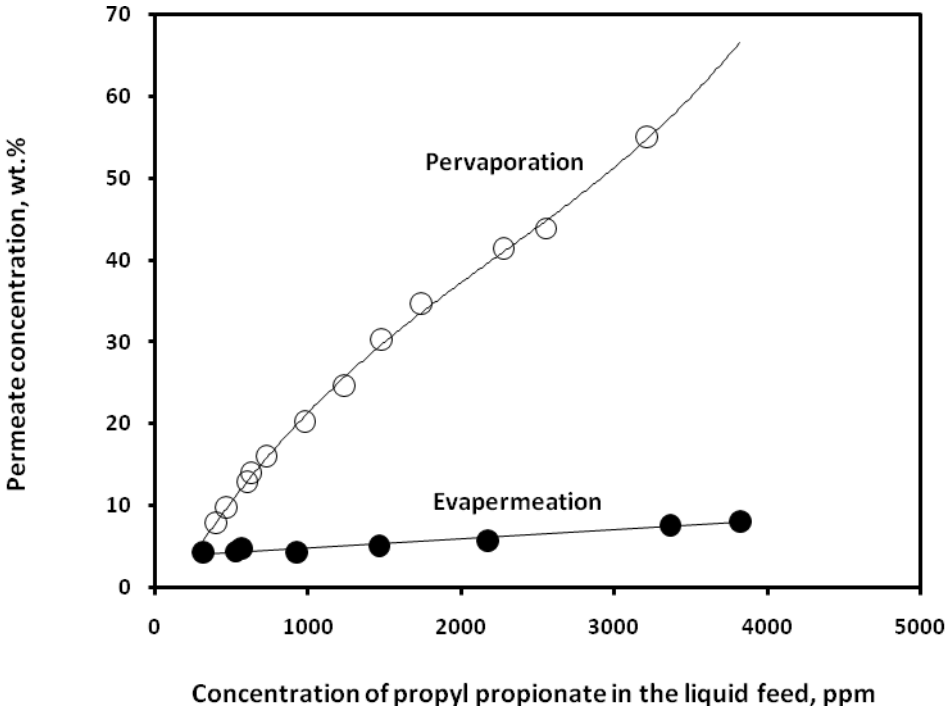

Figure 5.4 Permeate aroma concentration obtained in evapermeation and in pervaporation (T = 30^{o}C).

Pervaporation separation can concentrate dilute propyl propionate (concentration of 0.05-0.33 wt.%) to reach a concentration of 8-55 wt.%, whereas, evapermeation is only able to

produce up to 4-8 wt.% of propyl propionate in the permeate. As a matter of fact, when the propyl propionate concentration in the feed solution increases, the increase in the permeate concentration during evapermeation is less significant; therefore, the selectivity by evapermeation decreases gradually as the feed propyl propionate increases (Figure 5.5).

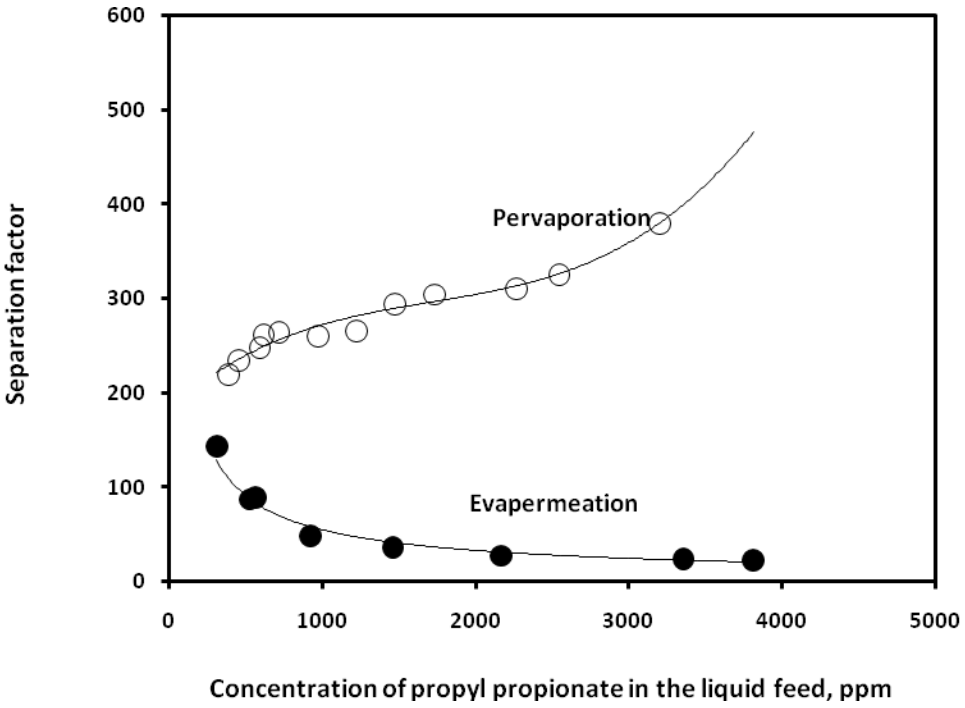

Figure 5.5 A comparison of separation factor for propyl propionate concentration by evapermeation and by pervaporation.

5.3.2 Solubility and Diffusivity of Vapor Aroma-Water Mixtures

Figure 5.6 and 5.7 show the solubility of vapor and liquid propyl propionate and water in the PEBA membrane as a function of the concentration of propyl propionate in the liquid phase. As in liquid sorption, the vapor sorption of propyl propionate follows an ideal sorption in which the sorption uptake increases linearly as the aroma concentration in the solution increases.

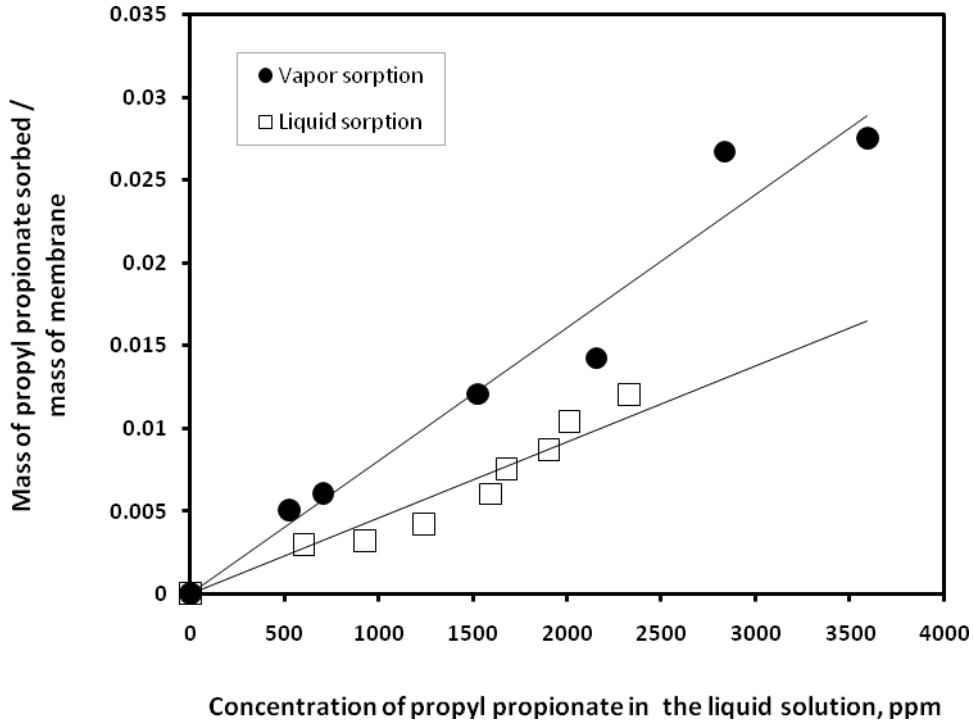

Figure 5.6 Sorption uptake of propyl propionate solubility in PEBA membrane from vapor and liquid phase as a function of liquid propyl propionate concentration.

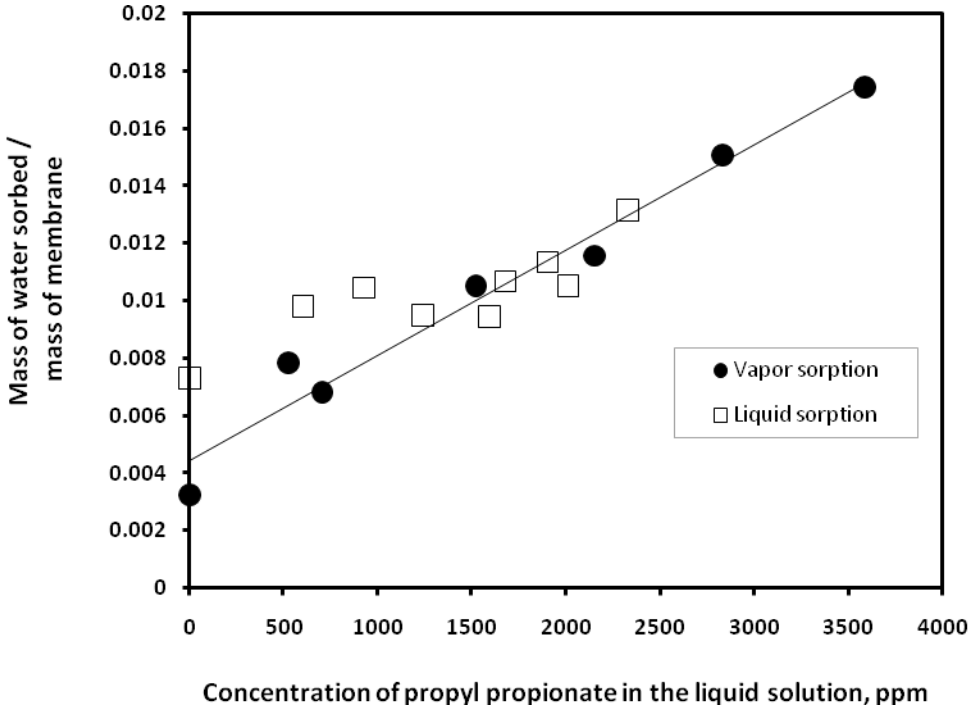

Figure 5.7 Water uptake by PEBA membrane from vapor and liquid phases.

Interestingly, more propyl propionate can be sorbed by PEBA membrane from the vapor phase than from the liquid phase. In other words, the solubility of propyl propionate vapor in the PEBA membrane is higher than that in liquid state. Detailed reasons for this are still unclear, and further studies are needed. Nonetheless, different behavior of pervaporation and evapermeation has also been reported for solvent dehydration using hydrophilic membranes.

It may be mentioned that unlike propyl propionate, the sorption uptake of water in PEBA membrane is not significantly affected by whether the sorption is from vapor or liquid phase. Only for pure water (zero concentration of propyl propionate), the sorption uptake from liquid phase is more than the sorption uptake from the vapor phase as shown in Figure 5.7.

From the given data of vapor permeation and vapor solubility, the diffusivity of vapor propyl propionate in the PEBA membrane can be evaluated using solution-diffusion model. Three types of diffusivity relationships as given in Chapter 4 (constant diffusivity, linear concentration dependency and exponential concentration dependency) were also examined for evapermeation. The regression results are shown in Table 5.1. Figure 5.8 shows the diffusivity of vapor propyl propionate through PEBA membrane, which is considered to be constant, linear concentration dependent and exponential concentration dependent. It may be stated that the diffusivity of vapor propyl propionate in the PEBA membrane within this particular range of vapor feed concentration (40-165 mg/L) is relatively independent on its concentration, around (3-8) x 10^{-9} cm^2/s. This value is lower than the diffusivity of liquid propyl propionate evaluated from the pervaporation and sorption data, but similar to that obtained by the time-dependent sorption method. Considering Figures 5.2 and 5.7, the diffusivity of vapor water in PEBA membrane was approximated 10 times lower than the liquid water. This infers that the selectivity diffusivity of propyl propionate relative to water in vapor state is lower than that in liquid state.

Based on the sorption uptake of vapor propyl propionate (Figure 5.5) and the diffusivity of vapor propyl propionate (Figure 5.8), one may wonder how can a higher sorption uptake in vapor phase than in liquid phase give a diffusivity in vapor phase much lower than in liquid

phase? This again appears to suggest that the simplest solution-diffusion model may not be fully applicable for the evapermeation separation of this system.

Table 5.1 Diffusivity parameters and solubility coefficient of vapor propyl propionate obtained from data fitting ($T = 30^{o}C$).

Parameter	Value
Solubility coefficient: - Solubility coefficient (S_i), g / (g membrane.(mg/L))	7.40×10^{-5}
Diffusivity parameter: A. Constant diffusivity, $D = D_0$ - D_0, $cm^2.s^{-1}$ Regression, R^2	 5.747×10^{-9} 0.750
B. Linear concentration dependent, $D = D_0 + \kappa C$ - D_0, $cm^2.s^{-1}$ - κ, $cm^2.s^{-1}.(mg/L)^{-1}$ Regression, R^2	 8.127×10^{-9} -4.858×10^{-7} 0.896
C. Exponential concentration dependent, $D = D_0 \exp(\gamma C + \kappa)$ - D_0, $cm^2.s^{-1}$ - γ, $cm^3.g^{-1}$ - κ Regression, R^2	 3.884×10^{-9} 1.99 9.69×10^{-3} 0.864

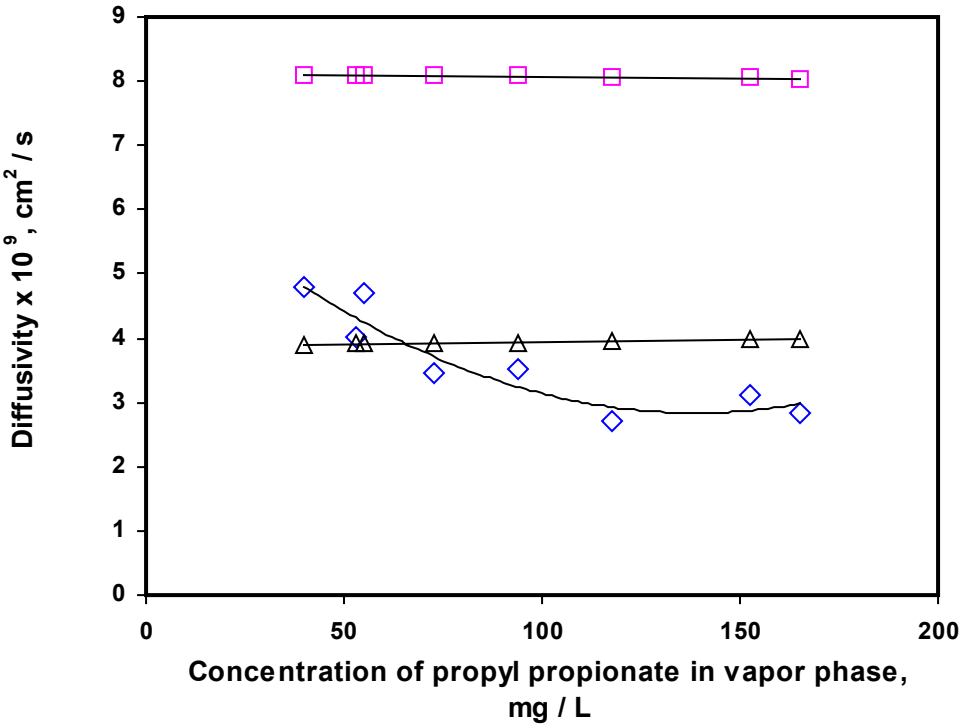

Figure 5.8 Diffusivity of vapor propyl propionate in the PEBA membrane evaluated from permeation flux and sorption uptake by assuming constant diffusivity (◊), linear concentration dependency of diffusivity (□), or exponential concentration dependency of diffusivity (Δ) (T = 30°C).

5.4. Summaries

The following conclusions can be drawn from the investigation of evapermeation of propyl propionate-water mixtures using PEBA membrane:

- The feed concentration had little effect on the permeation flux, and the permeation flux was lower than the permeation flux of pervaporation under the same operating conditions. The selectivity achieved by evapermeation was also lower than that by pervaporation. Thus, in terms of permeation flux and selectivity, evapermeation did not offer better separation performance for aroma compound recovery compared to pervaporation.

- The sorption uptake of propyl propionate in the membrane from vapor phase was higher than sorption uptake from liquid phase, but there was little difference for water uptake.
- The diffusivity of vapor propyl propionate through the membrane was slightly affected by its vapor feed concentration.
- The simplest solution-diffusion model was not adequate enough to describe the mass transport mechanism in the evapermeation separation of propyl propionate-water mixtures.

CHAPTER 6

Simulation of Recovery of Aroma Compound from Aqueous Solutions by Batch Pervaporation Coupled with Permeate Decantation and Water Phase Recycle

6.1 Introduction

Pervaporation has been well established for dehydration of alcohols (mainly ethanol and isopropanol) and removal of volatile organic compounds from contaminated water in wastewater treatment (Baker, 2004). Another potential application, which has not been exploited commercially, is the recovery of natural aroma compounds (particularly high-value aroma compounds) from aqueous solutions. The abundant and sustainable sources, large market demand and the high market prices of natural aroma compounds are apparently some of the driving factors to extend the application of pervaporation to aroma recovery processes.

As described in previous chapters, organophilic membranes exhibit a high selectivity in aroma compound from aqueous solutions. In case of recovery of low solubility aroma compounds, the permeate concentration attained can exceed the solubility limit and thus a phase separation takes place in the permeate stream, resulting in two phases: an organic phase and a water phase. In order to enhance the recovery of aroma compound where a phase separation takes place in the permeate collector, the recycle of the aroma compound from the water phase is important in order to achieve a high recovery. Such a process design has been proposed previously in our lab (Liu *et al.*, 2005), but no extensive study has been done yet to verify the modified pervaporation process. In this process, there are two streams recycled into the feed tank, i.e., one is the retentate stream from a membrane chamber like in a conventional pervaporation system, and the other is the water phase from the permeate decanter, as shown in Figure 6.1.

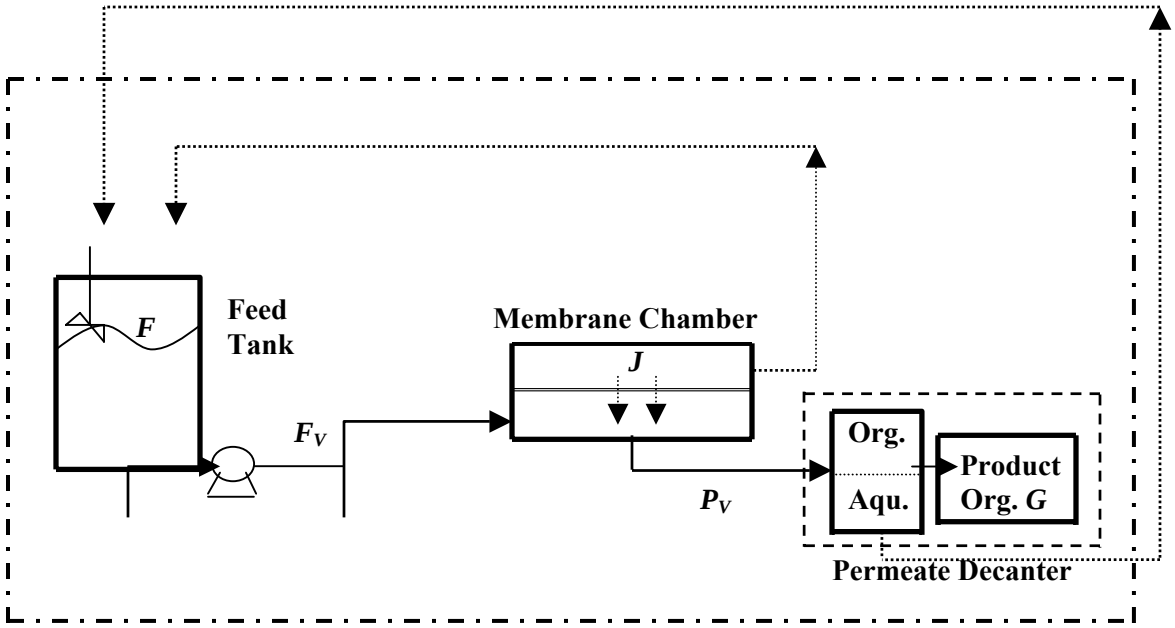

= conventional pervaporation system ; Org. = organic phase ; Aqu. = aqueous phase

Figure 6.1 Batch pervaporation of aroma compound recovery from aqueous solutions with permeate decantation and aqueous phase recycle.

In practical applications, the recovery of low solubility aroma compounds from aqueous solutions by pervaporation is most likely performed in a batch process due to its low processing capacities. The low processing capacity is mainly attributed to the very low concentration (ppm levels) of aroma compounds in natural sources. The dilute aqueous aroma solutions are obtained by extracting the aroma compounds from the natural sources using a large amount of water. Even though most industrial applications prefer continuous processes, a batch process is more advantageous in certain circumstances for the following reasons: low processing capacity, high fouling process that needs frequent cleaning (Walas, 1988). However, a batch process suffers from the disadvantage that it will never reach a steady state condition and all the process parameters will change with time.

This chapter aims to provide a mathematical model that can describe an operation of batch pervaporation process for recovery of low solubility aroma compounds from aqueous solutions where the water phase from permeate decantation is recycled to enhance aroma recovery. The model was derived from mass balances, followed by substitutions to obtain differential or algebraic equations. From the model, the extent of improvement in the recovery of aroma compounds and other advantages due to the recycle of the water phase as compared to the conventional pervaporation process, can be determined. The model is able to determine the process parameters as a function of time, including the permeation flux and aroma compositions in the feed tank, the quantity of permeate and retentate, and the quantity and composition of aroma produced recovered. The profiles of process parameters shown in this chapter are all from model simulation.

6.2 Model Derivation

Some major assumptions are considered in the derivation of model, i.e.: (i) isothermal operation, (ii) perfect mixing of feed solution, (iii) sorption equilibrium on the membrane surface, (iv) the permeation through the membrane follows Fick's law with a constant diffusivity, (v) the aqueous and organic phases are at equilibrium in the permeate decanter; and (vi) constant enrichment factor. The process may be divided into three sub-units: feed tank, membrane chamber and the permeate decanter. The derivation of the mathematical model is shown below.

Overall System

Considering the feed tank and the permeate decanter, it can be seen that a decrease in mass in the feed tank (F) will equal to the increase in mass of the organic phase (G) collected in the product collector,

$$-dF = dG \tag{6.1}$$

Since initially (t = 0) there is no organic phase collected in the permeate collector (G_0 = 0), integration of Eqn. (6.1) gives,

$$G = F_0 - F \tag{6.2}$$

where F_0 is the total mass in the feed tank initially. Eqn. (6.2) determines the mass of aroma product collected.

Feed Tank

Total mass balance (aroma compound and water) around the feed tank can be derived as follows,

Rate of input – Rate of output = Rate of accumulation

$$R_t + W - F_V = \frac{dF}{dt} \tag{6.3}$$

Similarly, in term of mass balance of aroma component,

$$x_R R_t + x_W W - x_F F_V = \frac{d(x_F F)}{dt} \tag{6.4}$$

Or,
$$x_R R_t + x_W W - x_F F_V = x_F \frac{dF}{dt} + F \frac{dx_F}{dt} \tag{6.5}$$

where R_t, W and F_V are the mass flow rates of the retentate, water phase recycle from the permeate decanter and the feed streams, respectively, and x_R, x_W and x_F are the aroma compositions (in mass fraction) in these streams, respectively. Substitution of Eqn. (6.3) into (6.5) and rearrangement gives,

$$\frac{dx_F}{dt} = \frac{R_t(x_R - x_F) + W(x_W - x_F)}{F} \tag{6.6}$$

Eqn. (6.6) expresses the composition of aroma compound in the feed tank as a function of time. The correlation between R_t and x_R and W is obtained from the mass balance on the membrane unit and the permeate decanter, respectively.

Membrane Unit

Mass balances on the overall and aroma component can be derived to determine the mass flow rate and composition of retentate stream (recycle 1),

$$R_t = F_V - P_V \tag{6.7}$$

where P_V is the mass flow rate of permeate stream leaving the membrane unit. The mass flow rate of the feed stream (F_V) is determined by the feed circulation rate, whereas the permeation rate (P_V) can be evaluated using the solution-diffusion model. As an approximation, P_V can be expressed as follows,

$$P_V = \sum J_i A_m = \frac{A_m}{l_m} \sum D_i C_{sF,i} = \frac{A_m \rho_m}{l_m} \sum S_i D_i x_{F,i} \tag{6.8}$$

where J_i is the permeation flux of permeant i, A_m is the effective area of the membrane, l_m is the thickness of the membrane, D_i is the diffusivity of component i through the membrane and $C_{sF,i}$ is the concentration of component i on the membrane surface at the feed side. ρ_m is the density of the membrane, S_i is the solubility coefficient of permeant i and $x_{F,i}$ is the mass fraction of permeant i in the bulk feed.

Similarly, the mass balance on aroma component in the membrane unit can be given by

$$x_R R_t = x_F F_V - x_P P_V \tag{6.9}$$

where x_P is the overall composition of the aroma component in the permeate stream. The permeate composition is determined by the membrane performance and x_P can be related to x_F and the enrichment factor (β).

$$x_P = \beta x_F \tag{6.10}$$

Substituting of Eqn. (6.10) into (6.9) and rearranging,

$$x_R = \frac{x_F\left(F_V - \beta P_V\right)}{R_t} \tag{6.11}$$

which gives the aroma component concentration in the retentate stream.

Permeate Decanter

The total and component mass balances on the permeate collector are described by Eqns. (6.12) and (6.13).

$$P_V - W = \frac{dG}{dt} \tag{6.12}$$

$$\beta x_F P_V - x_W W = \frac{d\left(x_G G\right)}{dt} \tag{6.13}$$

Or,
$$\beta x_F P_V - x_W W = x_G \frac{dG}{dt} + G\frac{dx_G}{dt} \tag{6.14}$$

The right-hand side term in Eqn. (6.13), i.e., $d(x_G G)/dt$, basically represents the mass of aroma compound that is recovered at a given time. In the permeate decanter where the overall permeate concentration is beyond the solubility limit, there will exist an equilibrium between the organic and aqueous phases, and the aroma concentrations in the organic phase (x_G) and water phase (x_W) are constant. Substitution of Eqn. (6.12) into (6.14) gives the mass flow rate of water phase stream (recycle 2):

$$W = \frac{(\beta x_F - x_G)P_V}{(x_W - x_G)} \tag{6.15}$$

The equations describing the pervaporation of low solubility aroma compound recovery from aqueous solutions with two recycle streams are summarized in Table 6.1. In order to compare this process to the conventional pervaporation process that does not involve recycle of water phase from the permeate decanter, the equations with only one recycle stream (i.e., retentate) are also provided in the table.

Table 6.1 Model equations for recovery of low solubility aroma compounds from aqueous solutions by pervaporation with two and one recycle streams.

Two Recycles	**Remarks**	**One Recycle**
Eqn. (6.3) Eqn. (6.6)	- to determine the mass in the feed tank as a function of time - to determine the concentration of aroma in the feed tank as a function of time	$\frac{dF}{dt} = R_t - F_V$ $\frac{dx_F}{dt} = \frac{R_t(x_R - x_F)}{F}$
Eqn. (6.8) Eqn. (6.10)	- to determine the mass flow rate of the permeate stream as a function of time - to determine the concentration of aroma in the permeate stream as a function of time	Same
Eqn. (6.7) Eqn. (6.11)	- to determine the mass flow rate of retentate stream as a function of time - to determine the concentration of aroma in the retentate stream as a function of time	Same
Eqn. (6.15)	- to determine the mass flow rate (or mass collected) of water phase in decanter as a function of time	$\frac{dW}{dt} = \frac{(\beta x_F - x_G)P_V}{(x_W - x_G)}$
Eqn. (6.2) or (6.12) Eqn. (6.13)	- to determine the mass of permeate (organic phase) collected in the decanter as a function of time - to determine the mass of aroma compound recovered as a function of time	$\frac{dG}{dt} = \frac{(\beta x_F - x_W)P_V}{(x_G - x_W)}$ or $G = F - F_0 - W$ $M_{org,\text{recovered}} = x_G G$

These equations can be solved numerically by means of Polymath provided that the values of F_V, F_0, S, D, A_m, ρ_m, l_m, β, x_G and x_W are all known. The changes in all the process parameters with time can be determined from the model equations; however, this study only highlights those that are considered important to compare the two modes of operation, including the mass in the feed tank and its composition, the permeation flux, the composition in the permeate stream, and the recovery of aroma compound that can be achieved.

It must be noticed that the above applies when the permeate concentration is beyond the solubility limit and phase separation occurs. If the feed aroma concentration is so low that the permeate aroma concentration is below the solubility limit, there will be no phase separation in the permeate.

6.3 Results and Discussion

6.3.1 Effect of F_0/A_m

For the purpose of illustration, the model was applied to pervaporation separation of propyl propionate-water mixtures using PEBA membrane (grade 2533) based on lab test conditions. Two parametric studies were conducted, i.e.: one was by varying the ratio of the initial feed mass over the membrane area used (F_0/A_m), and the other was by varying the values of aroma solubility in water phase to see how the solubility affect the recovery. The ratio of (F_0/A_m) is selected as a combined parameter instead of using F_0 or A_m individually, because it is this ratio that will affect the aroma compound recovery. For a given F_0/A_m ratio, any variations of F_0 and A_m will not change the values of performance in term of aroma recovery. The process conditions and other parameters (based on experimental data) used in the calculations are given in Table 6.2. Simulation with other aroma compounds are represented by the aroma solubility of 1 and 5 wt.%.

Figure 6.2 shows the profiles of mass in the feed tank and its composition during 50 h of operation with and without water phase recycle from the permeate decanter at various (F_0/A_m) values. A wide range of operating time was used on purpose in the calculation in order to get comprehensive descriptions about the process parameters that will be evaluated.

Table 6.2 Process conditions and other parameters used in model calculation for propyl propionate-water recovery.

Parameter	Quantity
- Initial mass of feed per membrane area, F_0/A_m	375, 150, 15 kg/m^2
- Initial feed concentration	1,000 ppm
- Solubility of propyl propionate in water phase	5,600 ppm (0.56 wt.%) (Perry and Green, 1999)
- Feed circulation, F_V	1.6 kg/min
- Solubility coefficient of propyl propionate in PEBA membrane, S_i	4.6014 g / (g membrane.ppm)
- Solubility of water in PEBA membrane as a function of mass fraction of propyl propionate	1.784 X_{pp} + 0.0078, g water / g membrane
- Diffusivity of propyl propionate in PEBA membrane (from pervaporation experiment data, average constant), D_i	6.5 x 10^{-11} m^2/s
- Diffusivity of water in PEBA membrane (from pervaporation experiment data, average constant)	1.4 x 10^{-10} m^2/s
- Enrichment factor, β	185
- Thickness of membrane, l_m	25 μm
- Solubility of water in propyl propionate phase	1 wt.% (Stephenson and Stuart, 1986)
- Density of PEBA membrane, ρ_m	1.010 kg/m^3 (Djebbar *et al.*, 1998)

X_{pp} = mass fraction of propyl propionate in the feed solution
All transport properties are evaluated at 25-30^{o}C

Clearly, the mass in the feed tank decreases with time increases a product stream (i.e., organic phase, G) is continuously withdrawn from the system. However, the two modes of operation have a different trend. The water phase recycle changed the mass in the feed tank only slightly for all the (F_0/A_m) values studied (15-375 kg/m^2). It may be mentioned that the variation of (F_0/A_m) has little effect on the mass change in the feed tank when the permeate stream is dominated by the water phase; in this case, most permeate stream will be recycled again into the feed tank.

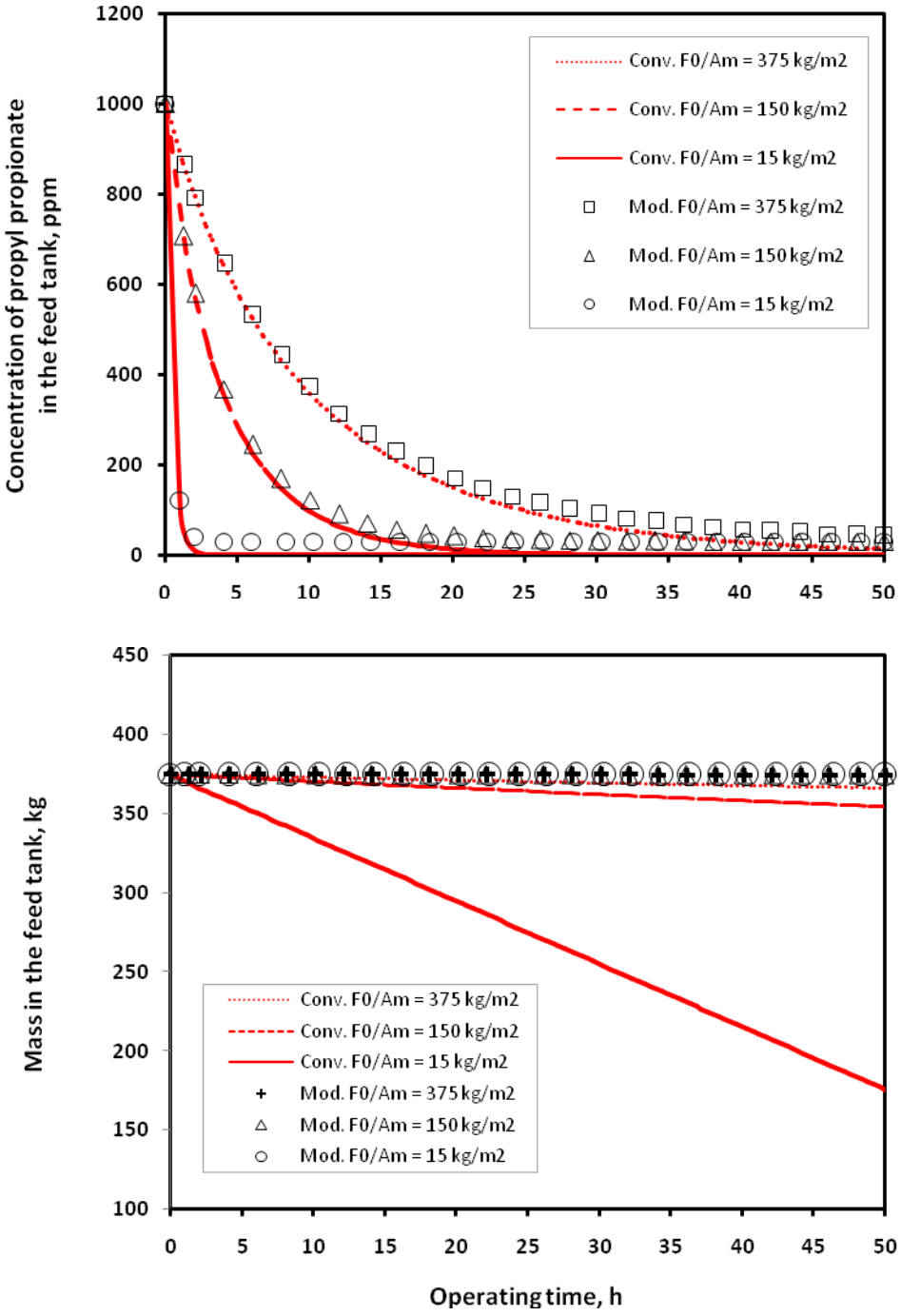

Conv. = convensional pervaporation system
Mod. = modified pervaporation system

Figure 6.2 Profiles of mass in the feed tank and its composition as a function of time.

The dominant phase in the permeate stream can be seen from the overall permeate concentration, which will be shown later. In the conventional operation, however, there is a clear decrease in the mass in the feed tank during the operation, and the extent of decrease depends on the ratio of (F_0/A_m) used. A lower (F_0/A_m), which means a larger membrane area for a given amount of feed, can augment the decrease in the mass of the feed solution. It is reasonable since a larger membrane area gives a higher permeation rate and no permeate is recycled to the system in the conventional mode of operation. In 50 h the mass in the feed tank for the modified pervaporation system decreased by only 0.1 %, whereas in the conventional pervaporation system its decrease reaches 2.4 % for (F_0/A_m = 375 kg/m^2) up to 53.2 % for (F_0/A_m = 15 kg/m^2).

Regarding the feed composition, the two modes of operation show similar trends. In general, the concentration of propyl propionate decreases sharply in the early period and the decrease becomes gradually slower as pervaporation proceeds. During the operation, the feed concentration in the modified pervaporation system is found slightly higher than that in the conventional operation. This makes sense since the water phase recycled still contains a small amount of propyl propionate. It is clear the decrease in feed propyl propionate concentration for both modes of operation is significant. This further justifies that PEBA membrane can concentrate the aroma compounds from aqueous solutions by pervaporation.

It can be concluded that all propyl propionate in the feed stream can be completely taken out through membrane permeation in the conventional pervaporation system; however, some of this amount will be trapped in the water phase in the permeate collector. In contrast, the feed propyl propionate concentration in the modified pervaporation system will decrease with time more slowly because the water phase recycle supplies propyl propionate into the feed stream. The utilization of a larger membrane area (or lower (F_0/A_m)) essentially shortens the operating time required. To achieve zero feed concentration, (F_0/A_m = 375 kg/m^2) operates up to around 50 h, whereas (F_0/A_m = 150 kg/m^2) and (F_0/A_m = 15 kg/m^2) just take around 30 and 4 h, respectively.

The very similar profile between the two systems is also found in permeation flux, but the permeate compositions are a little bit different, as shown in Figure 6.3. For both systems, it can be seen that the permeation flux decreases sharply in the early stages, then becomes slower and finally reaches nearly constant (asymptotic curve). This is reasonable since the permeation flux is affected directly by the feed propyl propionate concentration. The overall concentration of propyl propionate in the permeate stream obtained by pervaporation separation depends on the membrane performance. For a constant enrichment factor, the concentration of propyl propionate in the permeate stream also decreases asymptotically because of the decrease in the feed propyl propionate concentration. From the permeate concentrations, it can be seen that the permeate stream is still dominated by water even at the highest propyl propionate concentration (i.e., 18.5 wt.%). Therefore, by recycling the water phase, the mass in the feed tank changes very slightly as shown in Figure 6.2.

It must be noticed that the applying water phase recycle is only meaningful when the concentration of propyl propionate in the permeate stream exceeds its solubility limit. Once the instantaneous permeate concentration at a certain moment is exactly the same as its solubility limit, the process must stop. Otherwise, there is no phase separation in the newly collected permeate any more, and it is a homogeneous mixture.

Figure 6.4 shows the cumulative mass of product (i.e., organic phase) collected in the permeate decanter and the propyl propionate recovery obtained as a function of time. The two figures are similar but not identical since the organic phase is still filled by a very small amount of water. The recovery is defined as the ratio of the cumulative mass of propyl propionate collected in the organic phase to the initial amount of propyl propionate in the feed tank. The two systems show very similar performance in the early period of permeation. As pervaporation proceeds, pervaporation with two stream recycles shows better performance. As expected, the water phase recycle can improve the recovery of propyl propionate to some extent depending on the operating time set. In the modified pervaporation system, the mass of organic phase and propyl propionate recovered increases continuously and this is not the case for the conventional pervaporation system. In the conventional system, there is an optimum operating time at which a maximum recovery can be obtained.

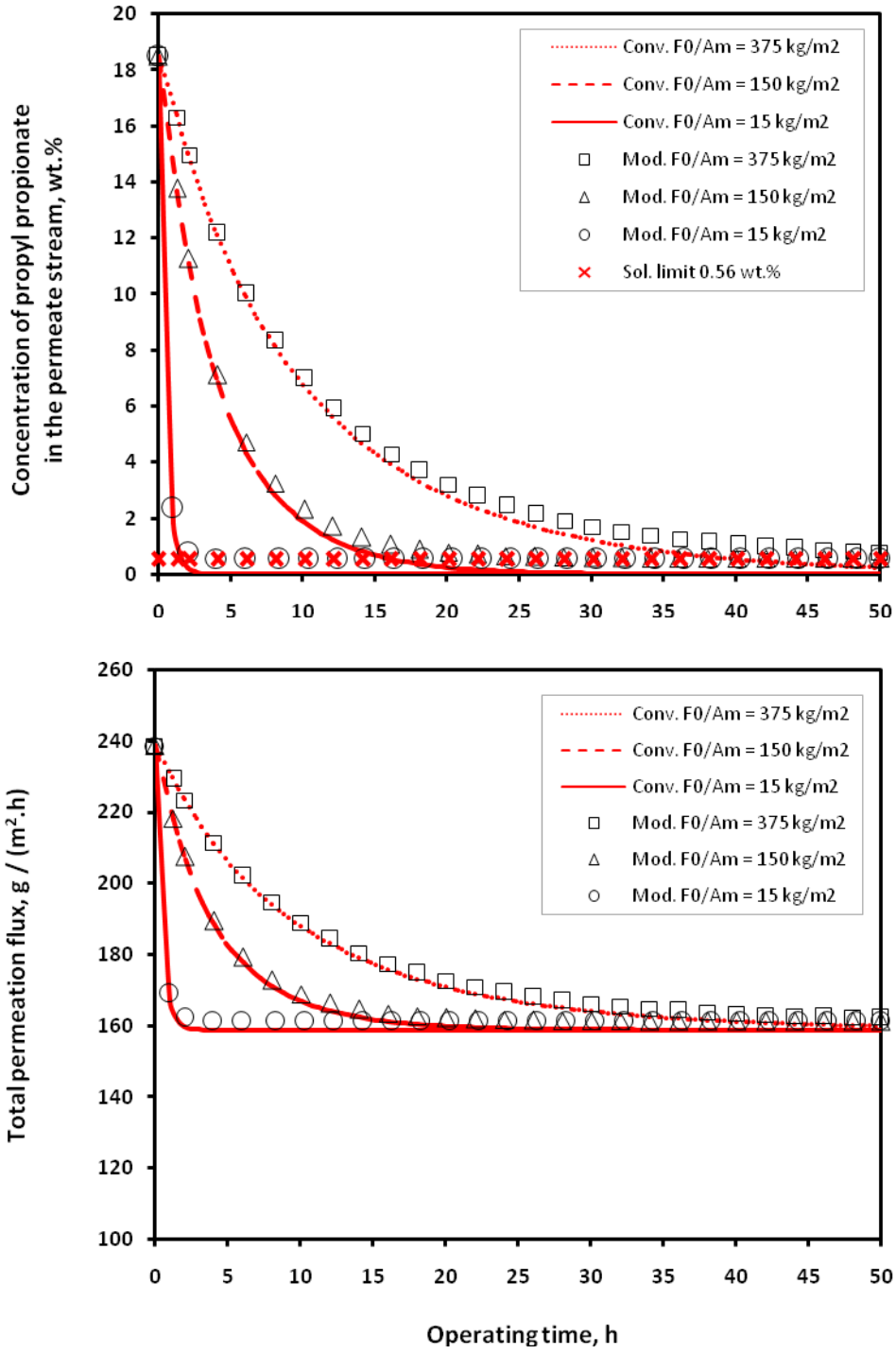

Figure 6.3 Profiles of total permeation flux and the composition in the permeate stream as a function of time.

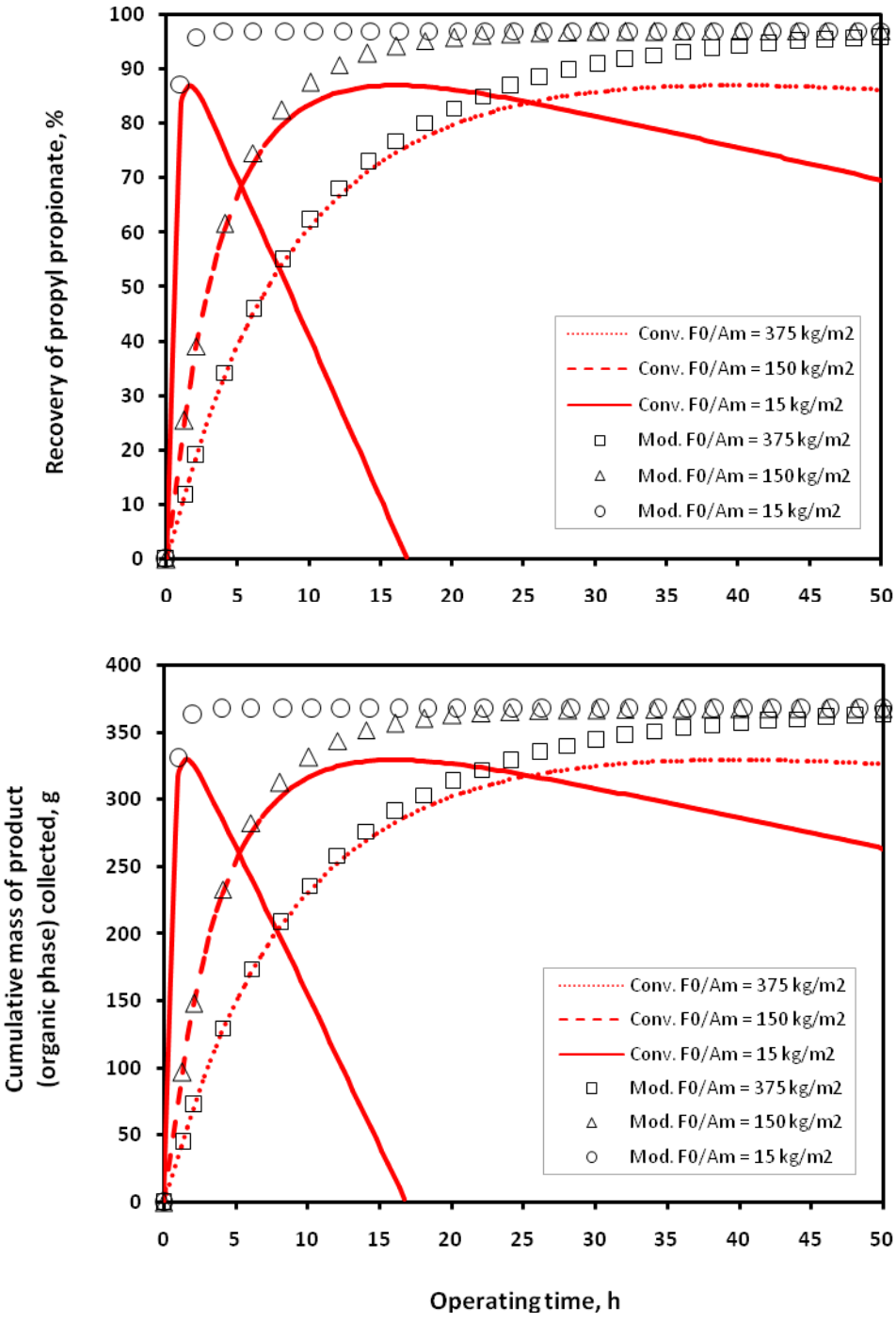

Figure 6.4 Mass of product (organic phase) collected and recovery of propyl propionate as a function of time.

This corresponds to the moment at which the instantaneous permeate concentration reaches the solubility limit. Initially, the mass of propyl propionate recovered increases gradually and then decreases continuously afterward. For this reason, due to the water phase recycle, a longer operating time can be used to improve the propyl propionate recovery.

The existence of optimum operating time in the conventional pervaporation system can be explained from the equilibrium phase concept: in the permeate collector the water phase and organic phase are in contact. Because the concentration of propyl propionate in the permeate stream decreases as the operating time increases (Figure 6.3), the water accumulated in the permeate collector will be more dominant than propyl propionate. There will be mass transfer between the two phases to reach phase equilibrium. The domination of water in the permeate collector attracts propyl propionate from the organic phase to enter the water phase to attain the equilibrium. The migration of propyl propionate causes the mass of propyl propionate in the organic phase decrease with time. At a certain time, the amount of water in the decanter can be large enough that there will be no phase separation, and the decanter only contains the water phase. In addition, the condition when the optimum operating time occurs in the conventional pervaporation system can also be analyzed mathematically. The maximum mass of propyl propionate in organic phase collected is obtained when $\frac{dG}{dt} = 0$. Since during the process the permeation rate (P_V) is not zero, this means $\left(\beta x_F - x_W\right) = 0$. In other words, the optimum operating time is reached when the concentration of propyl propionate in the permeate stream at a given moment (x_P or βx_F) is the same as its solubility limit (x_W). It is clear that the process must be stopped at this point. In the modified pervaporation system, however, the cumulative mass of propyl propionate recovered is found relatively unchanged (with little increase in propyl propionate recovery) when the permeate stream composition approaches to the solubility limit. It is more efficient to operate the modified pervaporation system before the concentration of propyl propionate in the permeate streams reaches its solubility limit, as shown in Figure 6.4.

Interestingly, it can be mentioned that the utilization of larger membrane area does not affect the maximum recovery of propyl propionate that can be achieved; only the time to obtain the

maximum recovery becomes shorter. In the conventional pervaporation system, the maximum recovery is 87.0 %, which is achieved at optimum operating times of 40, 16 and 1.5 h for (F_0/A_m = 375 kg/m^2), (F_0/A_m = 150 kg/m^2) and (F_0/A_m = 15 kg/m^2), respectively, while the modified pervaporation system has a recovery of over 94.0 % recovery.

6.3.2 Effect of Aroma Solubility in Water on Aroma Recovery

The simulation was also performed by varying the aroma solubility in the water phase. Not all the process parameters given in the above simulation are discussed; only the comparison in the recovery will be presented. Figure 6.5 shows the effects of aroma solubility in water (in the range of 0.56-5 wt.%) on the aroma compound recovery.

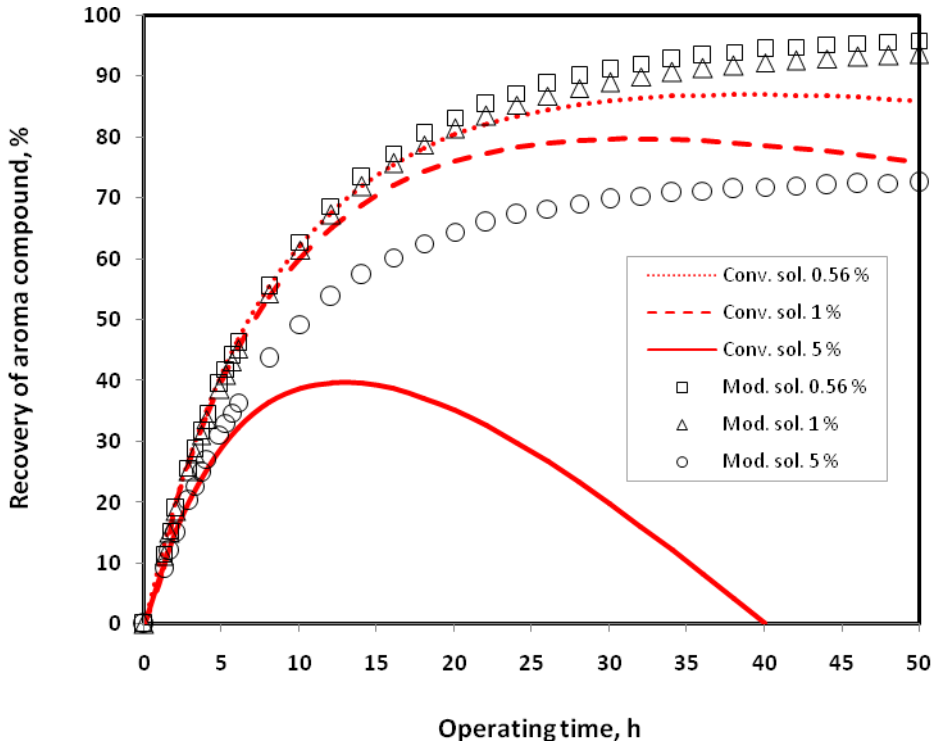

sol. = aroma solubility in water (in wt.%)

Figure 6.5 Recovery of aroma compound as a function of time at various aroma solubility in water (F_0/A_m = 375 kg/m^2).

It can be seen that the two systems show very distinctive performance when the addition of water phase recycle is applied when the aroma compound solubility in water becomes larger. This makes sense that the higher solubility of aroma compound in water means more aroma compound exists in the water phase and thus water phase recycling becomes more indispensable. For the solubility of aroma compound of 0.56, 1 and 5 wt.%, at the optimum operating time in the conventional pervaporation system (which are 40, 32 and 13 h, respectively) as a benchmark, the use of water phase recycle can improve the recovery of aroma compound from 87.0 to 94.0 %, from 80.0 to 90.0 % and from to 40.0 to 56.0 %, respectively. The recovery can be higher if the modified pervaporation system is run for a little longer period of time.

Note that a higher solubility of aroma compound in water can reduce the recovery of aroma compound that can be achieved for both systems. This is especially important when dealing with the selection of operating temperature. Generally speaking, a higher operating temperature increases the permeation flux and thus more aroma compound can be collected; however, the solubility of aroma compound in the water phase will increase as well and thus reduce the recovery of aroma compound. In this sense, it is expected that there will also be an optimum operating temperature in obtaining the maximum recovery of aroma compounds from aqueous solutions.

6.4 Summaries

The following conclusions can be drawn from the simulation of aroma recovery from aqueous solutions by batch pervaporation with two recycle streams:

- The use of water phase recycle could enhance the recovery of aroma compounds, and the degree of improvement depends on the operating time and aroma solubility in water phase.
- The utilization of a larger membrane area did not affect the extent of aroma recovery, but only shortened the operating time.
- In order to attain maximum recovery, the conventional operation must be stopped when the permeate concentration reaches solubility limit.

CHAPTER 7
Conclusions and Contributions to Research

Pervaporation of aroma compound recovery from dilute aqueous solutions using PEBA membranes was studied. Three representative aroma compounds were investigated in this study, i.e., propyl propionate, C_6-aldehyde and benzaldehyde; they represent ester, aldehyde and aromatic aroma compounds, respectively. It is expected that some aspects that are concluded in this study also apply for general pervaporation systems.

It was shown that both process conditions (i.e., feed concentration and operating temperature) affected the permeation flux and selectivity. The temperature dependence of permeation flux followed an Arrhenius type of relation.

Solubility and diffusivity of aroma compounds in the PEBA membrane were also studied. For all systems studied here, the sorption uptake of aroma compounds followed the Henry's law where the sorption uptake was linearly affected by the solution concentration. The solubility of pure propyl propionate and pure water was also measured; the solubility of pure propyl propionate in the PEBA membrane was around 130 times higher than that of pure water. This confirmed that PEBA was an excellent organophilic membrane. Applying the solution-diffusion model and using the data obtained from pervaporation and sorption-desorption experiments, the diffusivity of the aroma compounds was found to be linearly dependent on the feed aroma concentration. However, from the time-dependent sorption kinetics data, the diffusivity of propyl propionate through PEBA membrane was shown to be exponentially dependent on the feed propyl propionate concentration. This may be attributed to the different states of the membrane during the course of pervaporation (a steady state process) and sorption experiment (which was a transient process). Another implication was that the simplest solution-diffusion model used to determine the diffusivity might not be really applicable for the pervaporation systems evaluated in this study.

Among the three aroma compounds studied, propyl propionate had the highest permeability, followed by C_6-aldehyde and benzaldehyde. Interestingly, their solubilities in the membrane were in the order of benzaldehyde > C_6-aldehyde > propyl propionate. The permselectivity for aroma/water separation was in the order of C_6-aldehyde > propyl propionate > benzaldehyde. This confirmed that the molecular interactions between permeant-membrane and permeant-permeant had significant role in affecting the mass transport behavior across the membrane.

Evapermeation did not offer any advantages over pervaporation for recovering aroma compounds from aqueous solutions in terms of permeation flux and selectivity.

Batch pervaporation with permeate decantation and water phase recycle was studied parametrically. It was shown that water phase recycle could enhance the recovery of aroma compound to some extent, depending on the operating time and the solubility of aroma compound in water. Unlike the conventional batch operation where there existed an optimum operating time beyond which the product concentration decreased, the modified batch mode of operation allowed longer period of operation without compromising the product purity.

CHAPTER 8
Recommendations

In addition to conclusions, this study also found some points needs further study. The following are recommended in the future study:

- The molecular interactions between permeant-permeant and permeant-membrane significantly affect the mass transport of permeant inside the membrane; this factor must be considered in the transport studies of pervaporation.
- The application of two-recycle streams in pervaporation of aroma compound recovery is recommended especially for high solubility aroma compounds in water.
- Since the natural sources contain mixed aroma compounds, studies on pervaporation separation of multi-aroma compounds from aqueous solutions are needed to evaluate the change in aroma compounds profiles that could result from permeation since not all aroma compounds have the same permeability.

References

Alvarez, S., F.A. Riera, R. Alvarez, J. Coca, F.P. Cuperus, S. Th Bouwer, G. Boswinkel, R.W. van Gemert, J.W. Veldsink, L. Giorno, L. Donato, S. Todisco, E. Drioli, J. Olsson, G. Tragardh, S.N. Gaeta and L. Panyor, A new integrated membrane process for producing clarified apple juice and aple juice aroma concentrate, J. Food Eng., 46 (2000), 109.

Aptel, P., J. Cuny, J. Josefowich, G. Morel and J. Neel, Liquid transport through membranes prepared by grafting of polar monomers onto poly(tetrafluoroethylene) films. I. Some fractionations of liquid mixtures by pervaporation, J. Appl. Polym. Sci., 16 (1972), 1061.

Aptel, P., J. Cuny, J. Jozefonvicz, G. Morel and J. Neel, Liquid transport through membranes prepared by grafting of polar monomers onto poly(tetrafluoroethylene) films. II. Some factors determining pervaporation rate and selectivity, J. Appl. Polym. Sci., 18 (1974), 351.

Aptel, P., J. Cuny, J. Jozefonvicz, G. Morel and J. Neel, Liquid transport through membranes prepared by grafting of polar monomers onto poly(tetrafluoroethylene) films. III. Steady-state distribution in membrane during pervaporation, J. Appl. Polym. Sci., 18 (1974), 365.

Asada, T., Pervaporation membrane plant, industrial experience and plant design in Japan, In: Pervaporation membrane separation processes, Huang, R.Y.M. (ed.), Elsevier, Amsterdam, 1991.

Baker, R.W., Membrane technology and applications, McGraw-Hill, New York, 2004.

Baltus, R.E., M.M. Alger and T.J. Stanley, Solubility and diffusivity of cyclic oligomers in poly(dimethylsiloxane) using capillary column inverse gas chromatography, Macrom., 26 (1993), 5651.

Baranowski, B., Non-equilibrium thermodynamics as applied to membrane transport, J. Membr. Sci., 57 (1991), 119.

Baudot, A and M. Marin, Dairy aroma compounds recovery by pervaporation, J. Membr. Sci., 120 (1996), 207.

Baudot, A. and M. Marin, Pervaporation of aroma compounds: comparison of membrane performances with vapor-liquid equilibria and engineering aspects of process improvement, Food Bioprod. Process. 75 (1997), 117.

Baudot, A., I. Souchon and M. Marin, Total permeate pressure infuence on the selectivity of the pervaporation of aroma compounds, J. Membr. Sci., 158 (1999), 167.

Beaumelle, D., M. Marin and H. Gilbert, Pervaporation of aroma compounds in water-ethanol mixtures: experimental analysis of mass transfer, J. Food Eng., 16 (1992), 293.

Beaumelle, D., M. Marin and H. Gilbert, Plate and frame modification: improvement of pervaporation efficiency regarding aroma compound transfer, in Proc 6th Int Conf Pervaporation Processes in the Chemical Industry, Bakish, R. (ed.), Bakish Material Corp. Englewood, NJ, USA (1992), 223.

Bell, C.M., F.J. Gerner and H. Strathmann, Selection of Polymers for Pervaporation Membranes, J. Membr. Sci., 36 (1988), 315.

Bengtson, G. and K.W. Boddeker, Extraction of bio-products with homogeneous membranes, in Proc Bioflavour '95, Etievant, P. and P. Schrier (eds.), INRA Editions, Versailles, France (1995), 393.

Bengtsson, E., G. Tragardh and B. Hallstrom, Recovery and concentration of apple juice aroma compounds by pervaporation, J. Food Sci., 10 (1989), 65.

Binning, R.C., R.J. Lee, J.F. Jenning and E.C. Martin, Separation of liquid mixtures by permeation, Ind. Eng. Chem., 53 (1961), 45.

Boddeker, K.W., I.L. Gatfield, J. Jahnig and C. Schorm, Pervaporation at the vapor limit: vanillin, J. Membr. Sci., 137 (1997), 155.

Bonifaci, L., L. Carnelli and L. Cori, Determination of infinite dilution diffusion and activity coefficients of solvents in polystyrene by inverse gas chromatography on a capillary column, J. Appl. Polym. Sci., 51 (1994), 1923.

Borjesson, J., H.O.E. Karlsson and G. Tragardh, Pervaporation of a model apple juice aroma solution: comparison of membrane performance, J. Membr. Sci., 119 (1996), 229.

Brookes, P.R. and A.G. Livingston, Aqueous-aqueous extraction of organic pollutants through tubular silicone rubber membranes, J. Membr. Sci., 104 (1995), 119.

Brun, J.P., C. Larchet, G. Bulvestre and B. Auclair, Sorption and pervaporation of dilute aqueous solutions of organic compounds through polymer membranes, J. Membr. Sci., 25 (1985), 55.

Cabasso, I., J.G. Joseph and D Vofsi, A study of permeation of organic solvents trough polymeric membranes based on alloys of polyphosphonates and acetyl cellulose. II. Separation of benzene, cyclohexene, and cyclohexane, J. Appl. Polym. Sci., 18 (1974), 2137.

Cen, Y., C. Staudt-Bickel and R.N. Lichtenthaler, Sorption properties of organic solvents in PEBA membranes, J. Membr. Sci., 206 (2002), 341.

Chen, F.R. and H.F. Chen, A diffusion model of the pervaporation separation of ethylene glycol-water mixtures through crosslinked poly(vinyl alcohol) membrane, J. Membr. Sci., 139 (1998), 201.

Comyn, J. (Ed.), Polymer permeability, Elsevier Applied Science Publishers, New York, 1985.

Crank, J., The Mathematics of Diffusion, Clarendon Press, Oxford, 1975.

Crank, J. and G.S. Park (Eds.), Diffusion in Polymers, Academic Press, New York, 1968.

Djebbar, M.K., Q.T. Nguyen, R. Clement and Y. Germain, Pervaporation of aqueous ester solutions through hydrophobic poly(ether-block-amide) copolymer membranes, J. Membr. Sci. 146 (1998), 125.

Doong, S.J., W.S. Ho and R.P. Mastondrea, Prediction of flux and selectivity in pervaporation through a membrane, J. Membr. Sci., 107 (1995), 126.

Fadeev, A.G., Ya.A. Selinskaya, S.S. Kelley, M.M. Meagher, E.G. Litvinova, V.S. Khotimsky and V.V. Volkov, Extraction of butanol from aqueous solutions by pervaporation through poly(1-trimethylsilyl-1-propyne), J. Membr. Sci. 186 (2001), 205.

Feng, X., Studies on pervaporation membranes and pervaporation processes, PhD dissertation, University of Waterloo, Ontario, Canada, 1994.

Feng, X. and R.Y.M. Huang, Concentration polarization in pervaporation separation processes, J. Membr. Sci., 92 (1994), 201.

Feng, X. and R.Y.M. Huang, Preparation and performance of asymmetric polyetherimide membranes for isopropanol dehydration by pervaporation, J. Membr. Sci., 109 (1996), 165.

Feng, X. and R.Y.M. Huang, Pervaporation with chitosan membranes. I. Separation of water from ethylene glycol by a chitosan/polysulfone composite membrane, J. Membr. Sci., 116 (1996), 67.

Feng, X. and R.Y.M. Huang, Estimation of activation energy for permeation in pervaporation process, J. Membr. Sci., 118 (1996), 127.

Flory, J., Principles of Polymer Chemistry, Cornell University Press, Ithaca, New York, 1953.

Fries, R. and J. Neel, Transferts selectifs a travers des membranes actives, J. Chim. Phys., 62 (1965), 494.

Friesen, D.T., D.D. Newbold, S.B. McCray and R.J. Ray, Pervaporation by Counter-current Condensable Sweep, US Patent 5,464,540 (1995).

Fujita, H., Diffusion in polymer-diluent systems, Adv. Polym. Sci., 3 (1961), 1.

Gray, D.G. and J.E. Guillet, The application of the molecular probe technique to a study of polymer crystallization rates, Macrom., 4 (1971), 129.

Greenlaw, F.W., W.D. Prince, R.A. Shelden and E.V. Thompson, Dependence of diffusive permeation rates on upstream and downstream pressures: I. Single component permeant, J. Membr. Sci., 2 (1977), 141.

Greenlaw, F.W., W.D. Prince, R.A. Shelden and E.V. Thompson, Dependence of diffusive permeation rates on upstream and downstream pressures. II. Two component permeant, J. Membr. Sci., 2 (1977), 333.

Hannsen, C.M. and A. Beerbower, Encyclopedia of Chemical Technology, Supplement Volume, 1971.

Heintz, A., H. Funke and R.N. Lichtenthaler, Sorption and diffusion in pervaporation membranes, In: Pervaporation membrane separation processes, Huang, R.Y.M. (ed.), Elsevier, Amsterdam, 1991.

Heintz, A. and W. Stephan, A generalized solution-diffusion model of the pervaporation process through composite membranes. Part I. Prediction of mixture solubilities in dense active layer using the UNIQUAC model, J. Membr. Sci., 89 (1994), 143.

Hertel, M.O., H. Scheuren and K. Sommer, Solubilities of hexanal, benzaldehyde, 2-furfural, 2-phenylethanol, phenylethanal, and γ-nonalactone in water at temperatures between (50 and 100 ^{0}C), J. Chem. Eng. Data, 52 (2007), 2143.

Hofmann, D., L. Fritz and D. Paul, Molecular modeling of pervaporation separation of binary mixtures with polymeric membranes, J. Membr. Sci. 144 (1998), 145.

Hong, Y.K. and W.H. Hong, Influence of ceramic support on pervaporation characteristics of IPA/water mixtures using PDMS/ceramic composite membrane, J. Membr. Sci. 159 (1999), 29.

Hopfenberg, H., N.S. Schneider and F. Votta, Monohydric alcohol transport in a rubbery poly(urethane), J. Macromol. Sci. Phys. B, 3 (1969), 751.

Huang, R.Y.M. (Ed.), Pervaporation membrane separation processes, Elsevier, Amsterdam, 1991.

Huang, R.Y.M. and V.J.C. Lin, Separation of liquid mixtures by using polymer membranes. I. Permeation of binary organic liquid mixtures through polyethylene, J. Appl. Polym. Sci., 12 (1968), 2615.

Huang, R.Y.M. and N.R. Jarvis, Separation of liquid mixtures by using polymer membranes. II. Permeation of aqueous alcohol solutions through cellophane and poly(vinylalcohol), J. Appl. Polym. Sci., 14 (1970), 2341.

Huang R.Y.M. and J.W. Rhim, Separation characteristics of pervaporation membrane separation processes, In: Pervaporation membrane separation processes, Huang, R.Y.M. (ed.), Elsevier, Amsterdam, 1991.

Ji, W., S.K. Sikdar, S.T. Hwang, Sorption, diffusiom and permeation of 1,1,1-trichloroethane through adsorbent-filled polymeric membranes, J. Membr. Sci. 103 (1995), 243.

Jian, K. and P.N. Pintauro, Asymmetric PVDF hollow-fiber membranes for organic/water pervaporation separations, J. Membr. Sci., 135 (1997), 41.

Jiraratananon, R., A. Chanachai, R.Y.M. Huang and D. Uttapap, Pervaporation dehydration of ethanol–water mixtures with chitosan/hydroxyethylcellulose (CS/HEC) composite membranes I. Effect of operating conditions, J. Membr. Sci. 195 (2002), 143.

Jiraratananon, R., A. Chanachai, R.Y.M. Huang, Pervaporation dehydration of ethanol–water mixtures with chitosan/hydroxyethylcellulose (CS/HEC) composite membranes: analysis of mass transport, J. Membr. Sci. 199 (2002), 211.

Jiraratananon, R, P. Sampranpiboon, D. Uttapap and R.Y.M. Huang, Pervaporation separation and mass transport of ethylbutanoate solution by poly ether block amide membranes (PEBA), J. Membr. Sci., 210 (2002), 389.

Jonquieres, A., D. Roizard, J. Cuny and P. Lochon, Solubility and polarity parameters for assessing pervaporation and sorption properties. A critical comparison for ternary systems alcohol/ether/polyurethaneimide, J. Membr. Sci., 121 (1996), 117.

Kahlenberg, L., On the nature of the process of osmosis and osmotic pressure with observations concerning dialysis, J. Phys. Chem., 10 (1906), 141.

Kamaruddin, H. and W.J. Koros, Some observations about the application of Fick's first law for membrane separation of multicomponent mixtures, J. Membr. Sci. 135 (1997), 147.

Karlsson, H.O.E. and G. Tragardh, Aroma compound recovery with pervaporation – Feed flow effects, J. Membr. Sci., 81 (1993), 163.

Karlsson, H.O.E. and G. Tragardh, Aroma compound recovery with pervaporation – The effect of high ethanol concentration, J. Membr. Sci., 91 (1994), 189.

Karlsson, H.O.E., S. Loureiro and G. Tragardh, Aroma compound recovery with pervaporation – Temperature effects during pervaporation of a muscat wine, J. food Eng., 26 (1995), 177.

Karlsson, H.O.E. and G. Tragardh, Aroma recovery during beverage processing, J. Food Eng. 34 (1997), 159.

Kirk, R.D. and D.F. Othmer, Encyclopedia of chemical technology, 2nd Ed., Vol. 2, Interscience Publishers, New York, 1963.

Kober, P.A., Pervaporation, perstillation and percrystallization, J. of Am. Chem. Soc., 39 (1917), 955.

Kontominas, M.G., R. Gavara and J.R. Giacin, The adsorption of hydrocarbons on polystyrene by inverse gas chromatography: Infinite dilution concentration region, Eur. Polym. J., 30 (1994), 265.

Lamer, T. and A. Voilley, Influence of different parameters on the pervaporation of aroma compounds, in Proc 5th Int Conf Pervaporation Processes in the Chemical Industry, Bakish, R. (ed.), Bakish Material Corp. Englewood, NJ, USA (1991), 110.

Lamer, T., Extraction de composes d'aromes par pervaporation/relation entre les proprietes physico-chimiques des substances d'arome et leurs transferts a travers des membranes a base de polydimethylsiloxane, These de Doctorate universite de Bourgogne, Dijon, France, 1993.

Lamer, T., M.S. Rohart, A. Voillery and H. Baussart, Influence of sorption and diffusion of aroma compounds in silicone rubber on their extraction by pervaporation, J. Membr. Sci., 90 (1994), 251.

Lamer, T., H.E. Spinnler, I. Souchon and A. Voilley, Pervaporation: an efficient process for benzaldehyde recovery from fermentation broth, Process Biochem., 31 (1996), 533.

LaPack, M.A., J.C. Tou, V.L. McGuffin and C.G. Enke, The correlation of membrane permselectivity with Hildebrand solubility parameters, J. Membr. Sci., 86 (1994), 263.

Lee, C.H., Theory of reverse osmosis and some other membrane permeation operations, J. Appl. Polym. Sci., 19 (1975), 83.

Lee, Y.M., D. Bourgeois and G. Belfort, Selection of polymer membrane materials for pervaporation, Proc. 2nd Int. Conf. on Pervaporation Processes in the Chemical Industry, March 8-11, San Antonio, Texas, 1987.

Lipnizki, F., J. Olsson and G. Tragardh, Scale-up of pervaporation for the recovery of natural aroma compounds in the food industry. Part 1: simulation and performance, J. Food Eng., 54 (2002), 183.

Lipnizki, F., J. Olsson and G. Tragardh, Scale-up of pervaporation for the recovery of natural aroma compounds in the food industry Part 2: optimisation and integration, J. Food Eng., 54 (2002), 197.

Liu, F., L. Liu and X. Feng, Separation of acetone-butanol-ethanol (ABE) from dilute aqueous solutions by pervaporation, Sep. Pur. Technol., 42 (2005), 273.

Liu, K., Z. Tong, L. Liu and X. Feng, Separation of organic compounds from water by pervaporation in the production of n-butyl acetate via esterification by reactive distillation, J. Membr. Sci., 256 (2005), 193.

Lloyd, D.R. and T.B. Meluch, Selection and evaluation of membrane materials for liquid separations, ACS Symp. Ser., 269 (1985), Chap. 2.

Loeb, S. and S. Sourirajan, Sea water demineralization by means of an osmotic membrane, in saline water conversion-II, Adv. Chem. Ser., Am. Chem. Soc., 28 (1963), 117.

Long, R.B., Liquid permeation through plastic films, Ind. Eng. Chem. Fundam., 4 (1965), 445.

Matsuura, T. and S. Sourirajan, Properties of polymer-solution interfacial fluid from liquid chromatographic data, J. Colloid Interface Sci., 66 (1978), 589.

Mohammadi, T., Aroujalian, A and Bakhshi, A., Pervaporation of dilute alcoholic mixtures using PDMS membrane, Chem. Eng. Sci., 60 (2005), 1875.

Mulder, M.H.V., Thermodynamic principles of pervaporation, In: Pervaporation membrane separation processes, Huang, R.Y.M. (ed.), Elsevier, Amsterdam, 1991.

Mulder, M.H.V. and C.A. Smolders, On the mechanism of separation of ethanol/water mixtures by pervaporation I. Calculation of concentration profiles, J. Membr. Sci., 17 (1984), 289.

Nabe, A., E. Staube and G. Belfor, Surface modification of polysulfone ultrafiltration membranes and fouling by BSA solutions, J. Membr.. Sci., 133 (1997), 57.

Neel, J., Introduction to pervaporation, In: Pervaporation membrane separation processes, Huang, R.Y.M. (ed.), Elsevier, Amsterdam, 1991.

Neel, J., Q.T. Nguyen, R. Clement and D.J. Lin, Influence of downstream pressure on the pervaporation of water-tetrahydrofuran mixtures through a regenerated cellulose membrane (cuprophan), J. Membr. Sci., 27 (1986), 217.

Neumann, A.W., R.J. Good, C.J. Hope and M. Sejpal, An equation-of-state approach to determine surface tension of low-energy solids from contact angels. J. Colloid Interface Sci., 49 (1974), 291.

Oh, H.K., K.H. Song, K.R. Lee and J.M. Rim, Prediction of sorption and flux of solvents through PDMS membrane, Polym. 42 (2001), 6305.

Olsson, J. and G. Tragardh, Infuence of feed flow velocity on pervaporative aroma recovery from a model solution of apple juice aroma compounds, J. Food Eng., 39 (1999), 107.

Okada, T. and T. Matsuura, A new transport model for pervaporation, J. Membr. Sci., 59 (1991), 133.

Paul, D.R., The solution-diffusion model for swollen membranes, Sep. Purif. Meth., 5 (1976), 35.

Pawlisch, C.A., A. Macris and R.L. Laurence, Solute diffusion in polymers. 1. The use of capillary column inverse gas chromatography, Macrom., 20 (1987), 1564.

Pawlisch, C.A., J.R. Bric and R.L. Laurence, Solute diffusion in polymers. 2. Fourier estimation of capillary column inverse gas chromatography data, Macrom., 21 (1988), 1685.

Pereira, C.C., J.R.M. Rufino, A.C. Habert, R. Nobrega, L.M.C. Cabral and C.P. Borges, Aroma compounds recovery of tropical fruit juice by pervaporation: membrane material selection and process evaluation, J. Food Eng., 66 (2005), 77.

Pereira, C.C., C.P. Ribeiro Jr., R. Nobrega and C.P. Borges, Pervaporative recovery of volatile aroma compounds from fruit juices, J. Membr. Sci., 274 (2006), 1.

Perry, R.H. and D.W. Green, Perry's Chemical Engineers' Handbook, Seventh Edition, McGraw-Hill Book Companies, Inc., New York, 1999.

Pougalan, M.F. and G. Holzner, Perfumed polymeric resin essentially consisting of a polyether-esteramide, US Patent No. 4,734,278 (1988).

Psaume, R., P. Aptel, Y. Aurelle, J.C. Mora and J.L. Bersillon, Pervaporation: importance of concentration polarization in the extraction of trace organics from water, J. Membr. Sci., 36 (1988), 373.

Qin, R., H.P. Schreiber and A. Rudin, Assessment of degree of fusion of rigid PVC from IGC measurements, J. Appl. Polym. Sci., 56 (1995), 51.

Rajagopalan, N. and M. Cheryan, Pervaporation of grape juice aroma, J. Membr. Sci., 104 (1995), 243.

Rautenbach, R. and R. Albrecht, Separation of organic binary mixtures by pervaporation, J. Membr. Sci., 7 (1980), 203.

Rautenbach, R. and R. Albrecht, The separation potential of pervaporation. Part I. Discussion of transport equations and comparison with reverse osmosis, J. Membr. Sci., 25 (1985), 1.

Ravindra, R., S. Sridhar and A.A. Khan, Separation studies of hydrazine from aqueous solution by pervaporation, J. Polym. Sci. Polym. Phys. Ed., 37 (1999), 1969.

Robertson, A.E., Separation of Hydrocarbons, US Patent 2,475,990 (1949).

Sampranpiboon, P., R. Jiraratananon, D. Uttapap, X. Feng and R.Y.M. Huang, Pervaporation separation of ethyl butyrate and isopropanol with polyether block amide (PEBA) membranes, J. Membr. Sci. 173 (2000), 53.

Sampranpiboon, P., R. Jiraratananon, D. Uttapap, X. Feng and R.Y.M. Huang, pervaporation using polyoctylmethyl siloxane (POMS) and polydimethyl siloxane (PDMS) membranes, J. Membr. Sci., 174 (2000), 55.

Schaetzel, P., Z. Bendjama, C. Vauclair and Q.T. Nguyen, Ideal and non-ideal diffusion through polymersapplication to pervaporation, J. Membr. Sci. 191 (2001), 95.

Schafer, T., G. Bengtson, H. Pingel, K. W. Boddeker and J. P. S. G. Crespo, Recovery of aroma compounds from a wine-must fermentation by organophilic pervaporation, Biotech. and Bioeng., 62 (1999), 412.

She, M. and S.T. Hwang, Recovery of key components from real flavor concentrates by pervaporation, J. Membr. Sci., 279 (2006), 86.

Shelden, R.A. and E.V. Thompson, Dependence of diffusive permeation rates and selectivities on upstream and downstream pressures. IV. Computer simulation on nonideal systems, J. Membr. Sci., 19 (1984), 39.

Shieh, J.J., Novel pervaporation membranes for the separation of ethanol-water systems and development of a phase-change solution-diffusion pervaporation model, PhD dissertation, University of Waterloo, Ontario, Canada, 1994.

Shimidzu, T. and M. Yoshikawa, Synthesis of novel copolymer membranes for pervaporation, In: Pervaporation membrane separation processes, Ed. by R.Y.M. Huang, Elsevier, Amsterdam, 1991.

Simpson, R.F., Some important aroma components in white wine, Food Technol. Australia, 31 (1979), 516.

Sluys, J.T.M., F.G.C.T. Sommerdijk and J.H. Hanemaaijer, Recovery of flavor compounds by pervaporation, progress en Genie des Procedes, Aimar, P. and P. Aptel (eds.), Tech & Doc Lavoisier, Paris, France, 21 (1992), 401.

Smitha, B., D. Suhanya, S. Sridhar and M. Ramakrishna, Separation of organic-organic mixtures by pervaporation – a review, J. Membr. Sci., 241 (2004), 1.

Souchon, I., F.X. Pirre, Athes-Dutour and M. Marin, Pervaporation as deodorization process applied to food industry effluents: recovery and valorization of aroma compounds from cauliflower blanching water, Desalination, 148 (2002), 79.

Souchon, I., C. Fontanini A. and Voilley, Extraction of aroma compounds by pervaporation, in Flavour Science – Recent Developments, Mottram, D.S. and A.J. Taylor (eds.), The Royal Society of Chemistry, Cambridge, UK (1997), 305.

Sourirajan, S., S. Bao and T. Matsuura, An approach to membrane separation by pervaporation in Proc. Sec. Int. Conf. On pervaporation processes in the Chem.. Ind., Bakish Materials Corp., Englewood, NJ (1987), 9.

Spitzen, J.W.F., Pervaporation: Membranes and models for the dehydration of ethanol, Twente University, Netherlands, 1988.

Stephenson, R. and J. Stuart, Mutual binary solubilities: water-alcohols and water-esters, J. Chem. Eng. Data, 31 (1986), 56.

Tan, Z., R. Jaeger and J. Vancso, Crosslinking studies of poly(dimethylsiloxane) networks: a comparison of inverse gas chromatography, swelling experiments and mechanical analysis, Polym., 35 (1994), 3230.

Tian, X., B. Zhu and Y. Xu, P(VDF-*co*-HFP) membrane for recovery of aroma compounds from aqueous solutions by pervaporation I. Ethyl acetate/water system, J. Membr. Sci., 248 (2005), 109.

Tusel, G.F. and A. Ballweg, Method and apparatus for dehydrating mixtures of organic liquids and water, U.S. Pat. 4,405,409 (1983).

Uchytil, P. and R. Petrickovic, Vapor permeation and pervaporation of propan-1-ol and propan-2-ol in polyethylene membrane, J. Membr. Sci., 209 (2002), 67.

Van Krevelen, D.W. and P.J. Hoftyzer, Properties of Polymers Correlation with Chemical Structure, Elsevier, Amsterdam, 1972.

Van Oss, C.J., J. Visser, D.R. Absoom, S.N. Omenyi and A.W. Neumann, The concept of negative hamaker coefficients. II. Thermodynamics, experimental evidence and applications, Adv. Colloid Interface Sci., 18 (1983), 133.

Vrentas, J.S. and J.L. Duda, Diffusion in polymer-solvent systems. I. Reexamination of the free-volume theory, J. Polym. Sci. Polym. Phys. Ed., 15 (1977), 403.

Vrentas, J.S. and J.L. Duda, Diffusion in polymer-solvent systems. II. A predictive theory for the dependence of diffusion coefficients on temperature, concentration, and molecular-weight, J. polym. Sci. Polym Phys. Ed., 15 (1977), 417.

Walas, S.M., Chemical Process Equipment: Selection and Design, Butterworths, Boston, 1988.

Watson, J.M. and P.A. Payne, A study of organic compound pervaporation through silicone rubber, J. Membr. Sci., 49 (1990), 171.

Watson, J.M., G.S. Zhang and P.A. Payne, The diffusion mechanism in silicone rubber, J. Membr. Sci., 73 (1992), 55.

Yuan, S. and H.G. Schwartzberg, Mass transfer resistance in cross membrane evaporation into air, Rrecent Advances in Separation Sciences, AIChE Symposium Series Number 68, AIChE, New York, 120 (1972), 41.

Zhang, S.Q. and T. Matsuura, Recovery and concentration flavour compounds in apple essence by pervaporation, J. Food Process Eng., 14 (1991), 291.

Zellers, E.T., Three-dimensional solubility parameters and chemical protective clothing permeation. I Modelling the solubility of organic solvents in Viton ® gloves, J. Appl. Polym. Sci., 50 (1993), 513.

Appendix

A. Sample Calculations

A.1 Determination of Permeation Flux

Using Eqn. (2.1): $J = \frac{Q}{A_m t}$

Example:

Given data from pervaporation of propyl propionate/water separation through PEBA membrane,

- Effective membrane area = A_m = 20.43 cm^2 = 20.43 x 10^{-4} m^2
- Operating time = t = 1 h
- Mass of permeate collected = Q = (45.393 – 45.104) g = 0.289 g

Total permeation flux = J = 0.289 g / (20.43 x 10^{-4} m^2 . 1 h) = 141.5 g/(m^2.h)

The partial permeation flux of aroma compound is determined from,

$$J_i = c' J$$

where *c'* is the mass fraction of aroma component in the permeate.

A.2 Determination of Experimental Error

Using Eqn. (3.1): $$E_{rr} = \left| \frac{Y - \bar{Y}}{\bar{Y}} \right| x100\%$$

Example:

Given data from pervaporation of propyl propionate/water separation through PEBA membrane,

[Propyl propionate], ppm	Total flux (2-3 measurements), g / (m^2.h)	Average total flux, g / (m^2.h)	Experimental error, %
389.5	132.66; 135.11; 137.56	133.89	0.92; 0.92; 2.75
460	141.47; 139.51; 147.84	142.94	1.03; 2.40; 3.43
596.5	154.20; 155.67; 151.75	154.94	0.47; 0.47; 2.06
622	153.71; 155.67	154.69	0.63; 0.63
721.5	159.1; 157.14; 163.99	160.08	0.61; 1.84; 2.44
974.5	171.82; 173.29; 177.70	172.56	0.43; 0.43; 2.98
1228	187.00; 185.04; 193.36	186.02	0.53; 0.53; 3.95
1474	208.05; 202.17; 203.61	204.61	1.68; 1.19; 0.49
1734	227.14; 230.60; 216.37	228.87	0.76; 0.76; 5.46
2270.5	256.51; 262.87	259.69	1.23; 1.23
2549	296.55; 311.83	304.19	2.51; 2.51
3207	396.03; 407.77	401.90	1.46; 1.46

The experimental errors are found within (in the range below) 5 %.

A.3 Determination of Separation Factor and Enrichment Factor

Using Eqns. (2.2) and (2.3):

$$\alpha = \frac{c'(1-c)}{c(1-c')} \quad ; \quad \beta = \frac{c'}{c}$$

Example:

Given data from pervaporation of propyl propionate/water separation through PEBA membrane,

- Feed propyl propionate concentration = c = 460 ppm
- Mass of permeate sample = 0.279 g
- Total mass of permeate sample diluted with de-ionized water = 205 g
- Concentration of diluted permeate from TOC analysis = 133 ppm

Concentration of permeate = c' = (133 ppm x 205 g) / 0.279 g = 97,700 ppm

Separation factor = $\alpha = \frac{97{,}700(1{,}000{,}000 - 460)}{460(1{,}000{,}000 - 97{,}700)} = \mathbf{235}$

Enrichment factor = $\beta = \frac{97{,}700}{460} = \mathbf{212}$

A.4 Determination of Activation Energy of Permeation

Permeation flux versus temperature according Arrhenius type of relation,

$$J = J_0 \exp\left(\frac{-E_P}{RT}\right)$$

or $$\ln J = \ln J_0 - \frac{E_P}{R}\frac{1}{T}$$

The graph of ln$J$ versus $1/T$ will be a straight line with an intercept of lnJ_0 and a slope of ($-E_P/R$); thus the activation energy of permeation (E_P) is:

$$E_P = - R \text{ x slope}$$

Example:

The graphs of ln(J) versus $1/T$ are given below:

For aroma compounds:

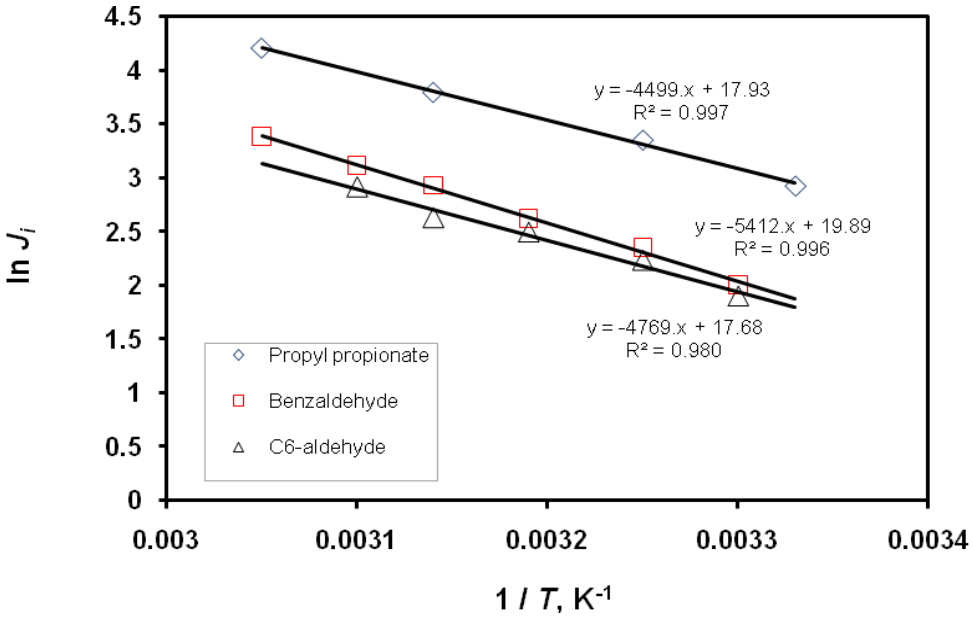

For water:

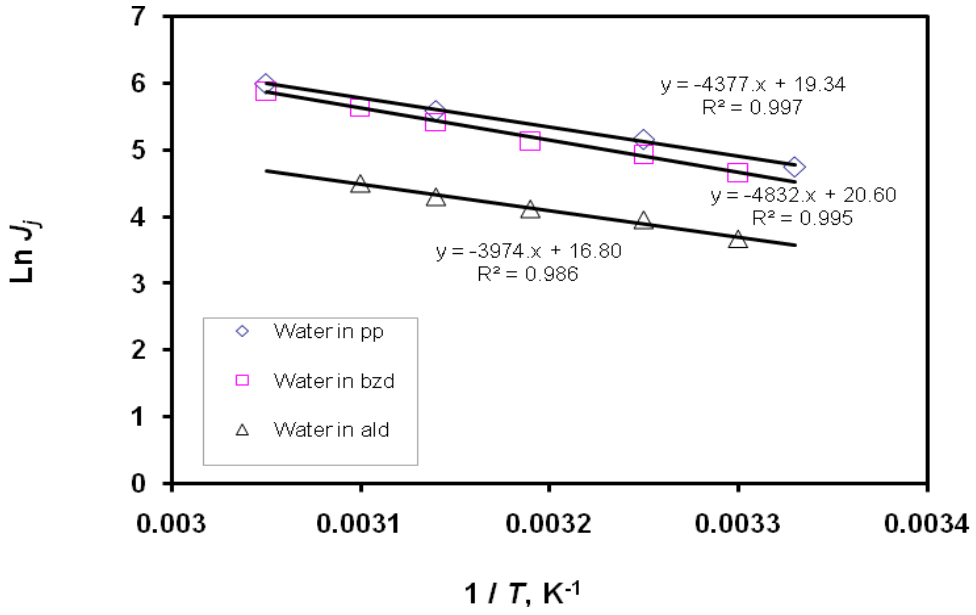

pp = propyl propionate; bzd = benzaldehyde; ald = C_6-aldehyde

For example from the benzaldehyde and water permeation data:

$$E_{P,bzd} = 5{,}412\ R = 5{,}412\ \text{K} \times 8.314 \times 10^{-3}\ \text{kJ/(mol.K)} = 45.0\ \text{kJ/mol}$$

$$E_{P,water} = 4{,}832\ R = 4{,}832\ \text{K} \times 8.314 \times 10^{-3}\ \text{kJ/(mol.K)} = 40.2\ \text{kJ/mol}$$

A.5 Solubility Selectivity

Eqn. (4.1): $$\alpha_S = \frac{c''(1-c)}{c(1-c'')}$$

Example:

Given data from sorption-desorption of propyl propionate-water mixtures on PEBA membrane,

- Concentration of propyl propionate in the feed solution = 603 ppm
- Concentration of propyl propionate in the membrane = 0.00294 g / g membrane
- Concentration of water in the membrane = 0.00981 g water / g membrane

Solubility selectivity = $\alpha_S = \frac{0.00294(1-603x10^{-6})}{603(0.00981)} =$ **496**

B. Determination of Permeant Concentration Dependency of Diffusivity Based on Steady State Pervaporation and Equilibrium Sorption Data

B.1 For Constant Diffusivity

Using Eqn. (4.5): $$J_i = \frac{D_0 S_i x_{F,i} \rho_m}{l_m}$$

Given data for **propyl propionate**,

- Solubility coefficient of propyl propionate in the PEBA membrane:

  S_i = 4.601 x 10^{-6} g / (g membrane.ppm)

- Density of PEBA membrane = ρ_m = 1.01 g/cm^3

- Membrane thickness = l_m = 25 μm = 25 x 10^{-4} cm

- Permeation flux versus feed propyl propionate concentration:

[Propyl propionate], ppm	Permeation flux, g / (cm^2.s)
389.5	2.908 x 10^{-7}
460	3.842 x 10^{-7}
596.5	5.536 x 10^{-7}
622	5.994 x 10^{-7}
721.5	7.106 x 10^{-7}
974.5	9.686 x 10^{-7}
1228	12.819 x 10^{-7}
1474	17.511 x 10^{-7}
1734	21.853 x 10^{-7}
2270.5	29.500 x 10^{-7}
2549	36.089 x 10^{-7}
3207	60.533 x 10^{-7}

The regression results given by Polymath including the comparison between permeation flux from experiment and calculations are provided below:

POLYMATH Results
No Title 12-05-2007

Nonlinear regression (L-M)

Model: J = Do/25*10000*4.601*10^(-6)*x*1.01

Variable	Ini guess	Value	95% confidence
Do	1.0E-05	**7.881E-07**	1.152E-07

Nonlinear regression settings
Max # iterations = 300

Precision

R^2	**=**	**0.8993488**
R^2adj	=	0.8993488
Rmsd	=	1.501E-07
Variance	=	2.951E-13

General

Sample size	= 12
# Model vars	= 1
# Indep vars	= 1
# Iterations	= 4

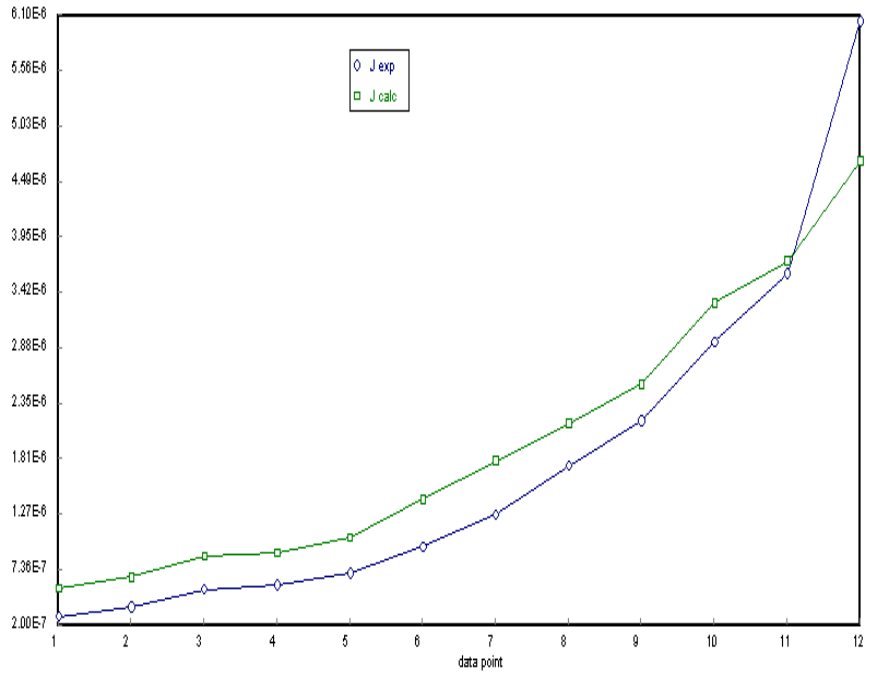

For C_6-aldehyde:

POLYMATH Results

No Title 12-05-2007

Nonlinear regression (L-M)

Model: J = Do/25*10000*8.351*10^(-6)*x*1.01

Variable	Ini guess	Value	95% confidence
Do	1.0E-05	**2.051E-07**	2.76E-08

Nonlinear regression settings
Max # iterations = 300

Precision

R^2	**=**	**0.8864705**
R^2adj	=	0.8864705
Rmsd	=	2.817E-08
Variance	=	7.254E-15

General

Sample size	= 8
# Model vars	= 1
# Indep vars	= 1
# Iterations	= 4

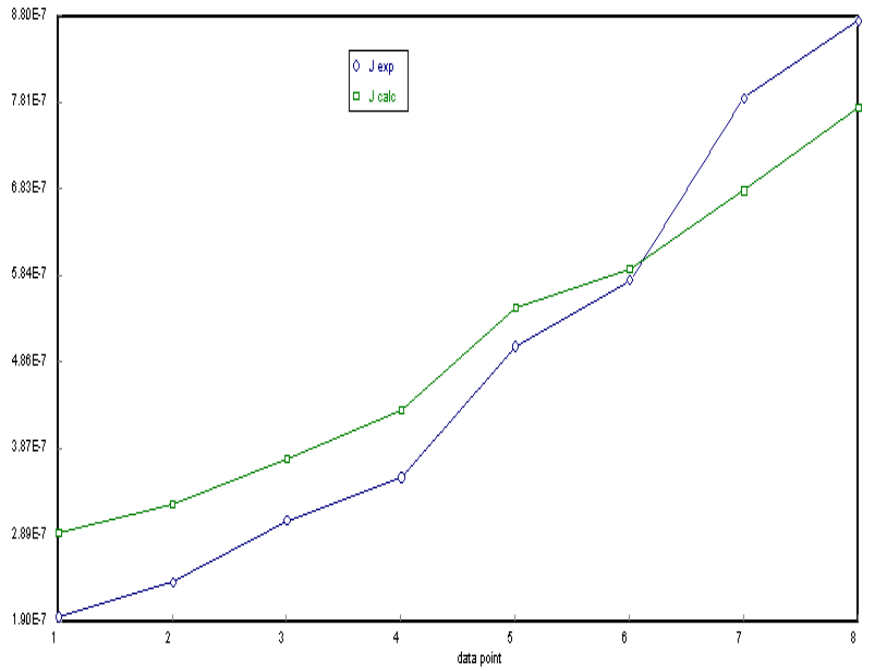

For benzaldehyde:

POLYMATH Results

No Title 12-05-2007

Nonlinear regression (L-M)

Model: J = Do/25*10000*1.361*10^(-5)*x*1.01

Variable	Ini guess	Value	95% confidence
Do	1.0E-05	**7.024E-08**	3.802E-09

Nonlinear regression settings
Max # iterations = 300

Precision

R^2	**=**	**0.9420789**
R^2adj	=	0.9420789
Rmsd	=	1.433E-08
Variance	=	4.326E-15

General

Sample size	= 20
# Model vars	= 1
# Indep vars	= 1
# Iterations	= 4

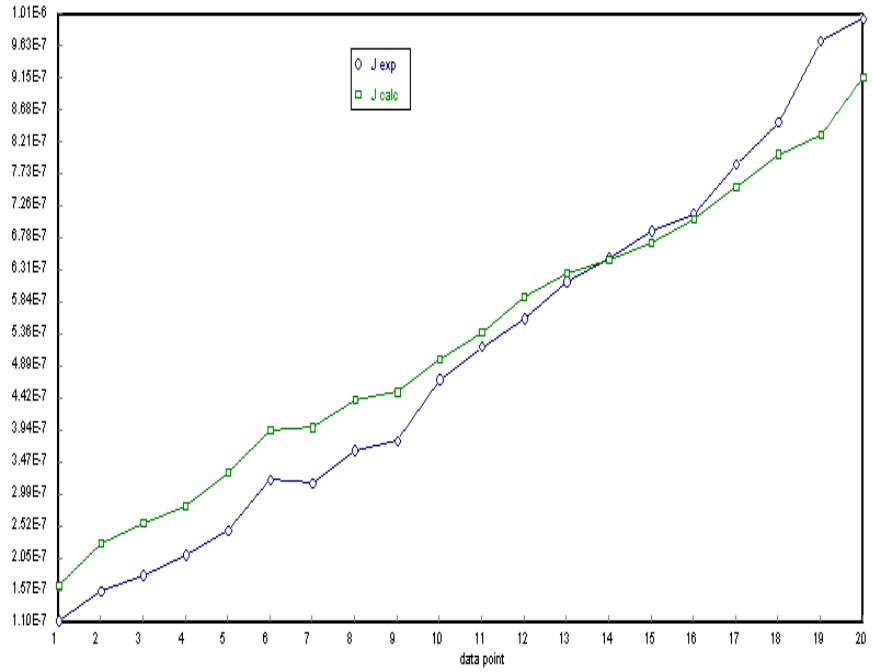

B.2 For Linear Concentration Dependency of Diffusivity

Using Eqn. (4.6): $$J_i = \frac{\left(D_0 + \frac{\kappa S_i x_{F,i} \rho_m}{2}\right) S_i x_{F,i} \rho_m}{l_m}$$

For propyl propionate:

POLYMATH Results
No Title 12-05-2007
Nonlinear regression (L-M)

Model: J = 1/25*10000*((Do+K*4.601*10^(-6)*x*1.01/2)*4.601*10^(-6)*x*1.01)

Variable	Ini guess	Value	95% confidence
Do	1.0E-05	**2.961E-07**	1.229E-07
K	0.1	**8.997E-05**	2.132E-05

Nonlinear regression settings
Max # iterations = 300
Precision

R^2	=	**0.9897704**
R^2adj	=	0.9887474
Rmsd	=	4.787E-08
Variance	=	3.299E-14

General

Sample size	= 12
# Model vars	= 2
# Indep vars	= 1
# Iterations	= 5

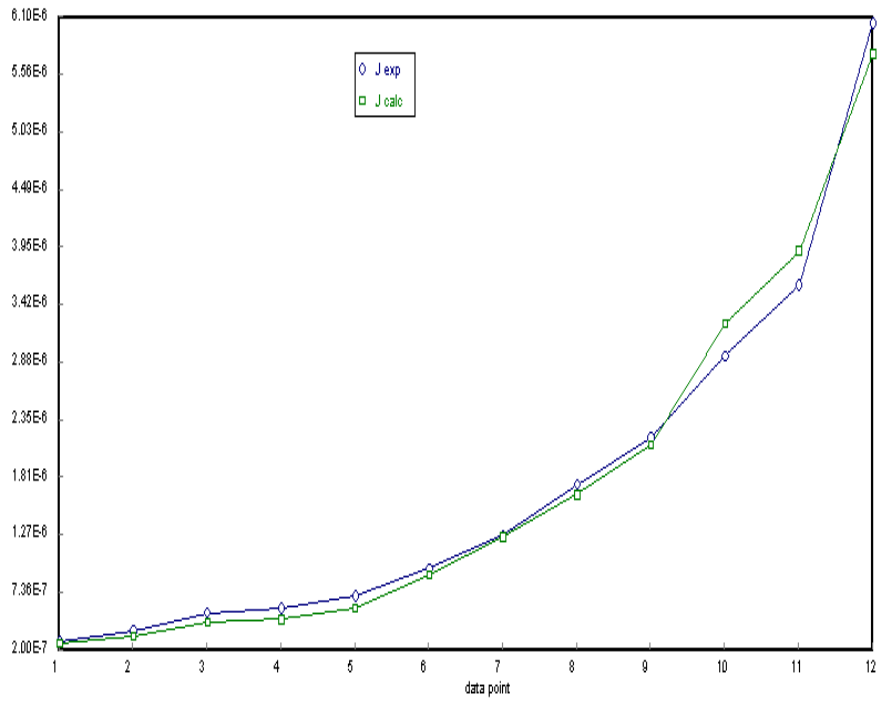

For C_6-aldehyde:

POLYMATH Results

No Title 12-05-2007

Nonlinear regression (L-M)

Model: J = 1/25*10000*((Do+K*8.351*10^(-6)*x*1.01/2)*8.351*10^(-6)*x*1.01)

Variable	Ini guess	Value	95% confidence
Do	1.0E-05	**8.726E-08**	3.729E-08
K	0.1	**3.201E-05**	9.827E-06

Nonlinear regression settings
Max # iterations = 300

Precision

R^2	**=**	**0.990205**
R^2adj	=	0.9885725
Rmsd	=	8.274E-09
Variance	=	7.302E-16

General

Sample size	= 8
# Model vars	= 2
# Indep vars	= 1
# Iterations	= 6

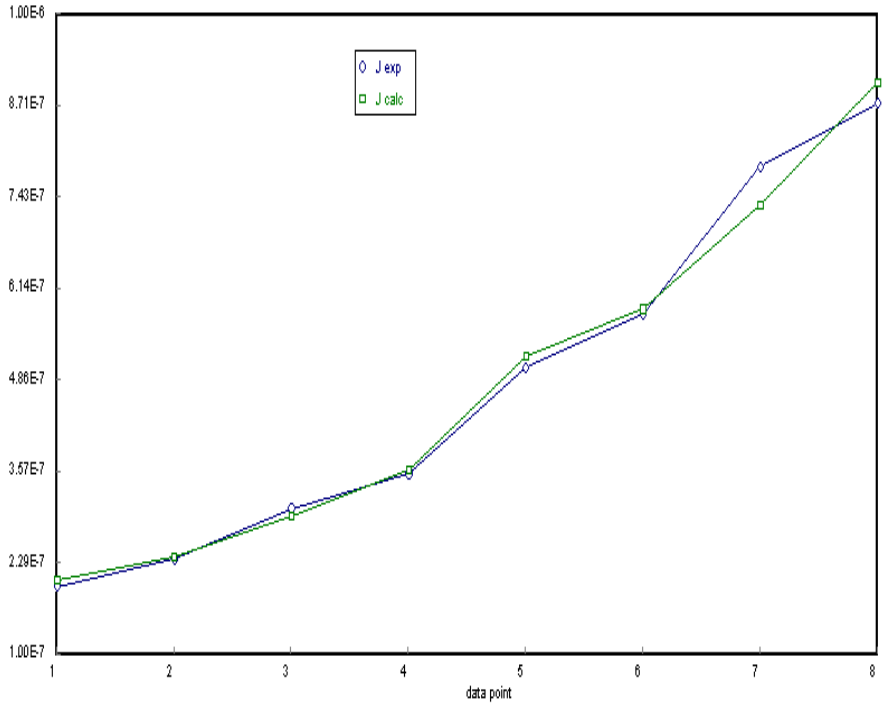

For benzaldehyde:

POLYMATH Results

No Title 12-05-2007

Nonlinear regression (L-M)

Model: J = 1/25*10000*((Do+K*13.61*10^(-6)*x*1.01/2)*13.61*10^(-6)*x*1.01)

Variable	Ini guess	Value	95% confidence
Do	1.0E-05	**4.135E-08**	5.139E-09
K	0.1	**2.402E-06**	4.138E-07

Nonlinear regression settings
Max # iterations = 300

Precision

R^2	**=**	**0.9937482**
R^2adj	=	0.9934008
Rmsd	=	4.71E-09
Variance	=	4.929E-16

General

Sample size	= 20
# Model vars	= 2
# Indep vars	= 1
# Iterations	= 6

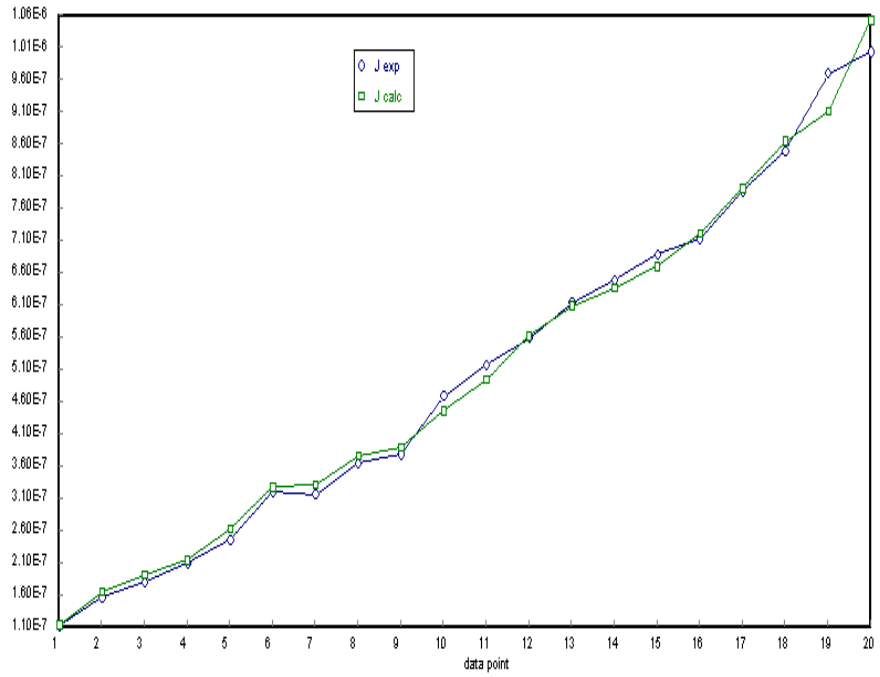

B.3 For Exponential Concentration Dependency of Diffusivity

Using Eqn. (4.7): $$J_i = \frac{D_0}{l_m \gamma}\left[\exp\left(\gamma S_i x_{F,i} \rho_m + \kappa\right) - 1\right]$$

For propyl propionate:

POLYMATH Results
No Title 12-05-2007
Nonlinear regression (L-M)

Model: J = Do/lamda/25*10000*(exp(lamda*4.601*10^(-6)*x*1.01+k)-1)

Variable	Ini guess	Value	95% confidence
Do	1.0E-05	**9.569E-07**	5.915E-11
lamda	0.001	**1.1009861**	0.0117299
k	1.0E-04	**6.131E-05**	5.127E-07

Nonlinear regression settings
Max # iterations = 300
Precision

R^2	=	**0.7892007**
R^2adj	=	0.7423564
Rmsd	=	2.173E-07
Variance	=	7.555E-13

General

Sample size	= 12
# Model vars	= 3
# Indep vars	= 1
# Iterations	= 29

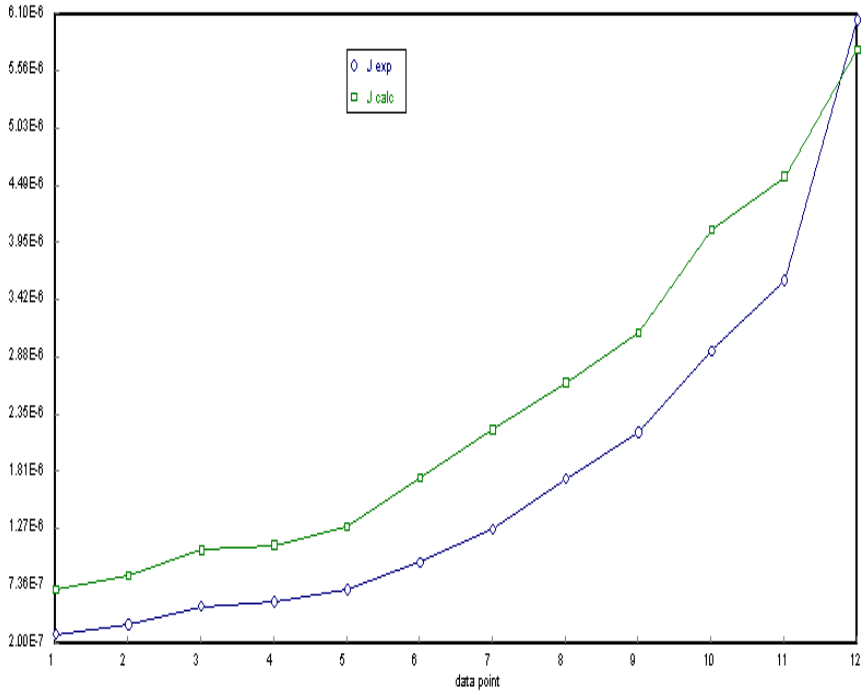

For C_6-aldehyde:

POLYMATH Results

No Title 12-05-2007

Nonlinear regression (L-M)

Model: J = Do/lamda/25*10000*(exp(lamda*8.351*10^(-6)*x*1.01+k)-1)

Variable	Ini guess	Value	95% confidence
Do	1.0E-05	**2.847E-07**	3.168E-11
lamda	0.001	**1.1009562**	0.0405458
k	0.001	**4.023E-05**	7.924E-07

Nonlinear regression settings
Max # iterations = 300

Precision

R^2	**=**	**0.0788472**
R^2adj	=	-0.289614
Rmsd	=	8.024E-08
Variance	=	8.241E-14

General

Sample size	=	8
# Model vars	=	3
# Indep vars	=	1
# Iterations	=	31

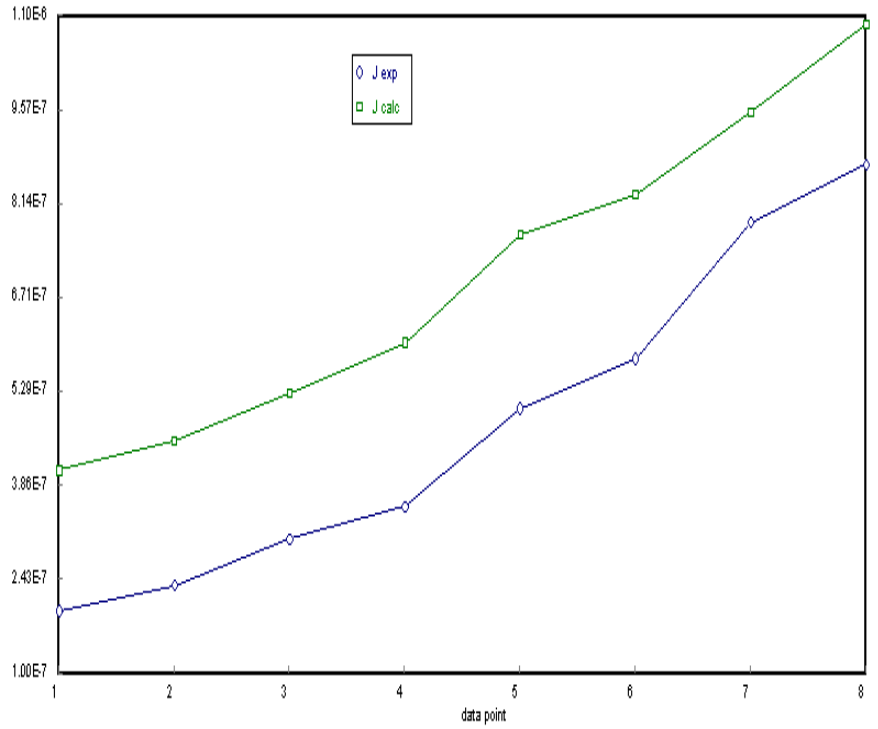

For benzaldehyde:

POLYMATH Results

No Title 12-05-2007

Nonlinear regression (L-M)

Model: J = Do/lamda/25*10000*(exp(lamda*1.361*10^(-5)*x*1.01+k)-1)

Variable	Ini guess	Value	95% confidence
Do	1.0E-05	8.575E-08	3.38E-11
lamda	0.001	1.1009775	0.0140683
k	1.0E-04	9.541E-04	9.061E-06

Nonlinear regression settings

Max # iterations = 300

Precision

R^2 = 0.5520908
R^2adj = 0.4993957
Rmsd = 3.986E-08
Variance = 3.739E-14

General

Sample size = 20
Model vars = 3
Indep vars = 1
Iterations = 18

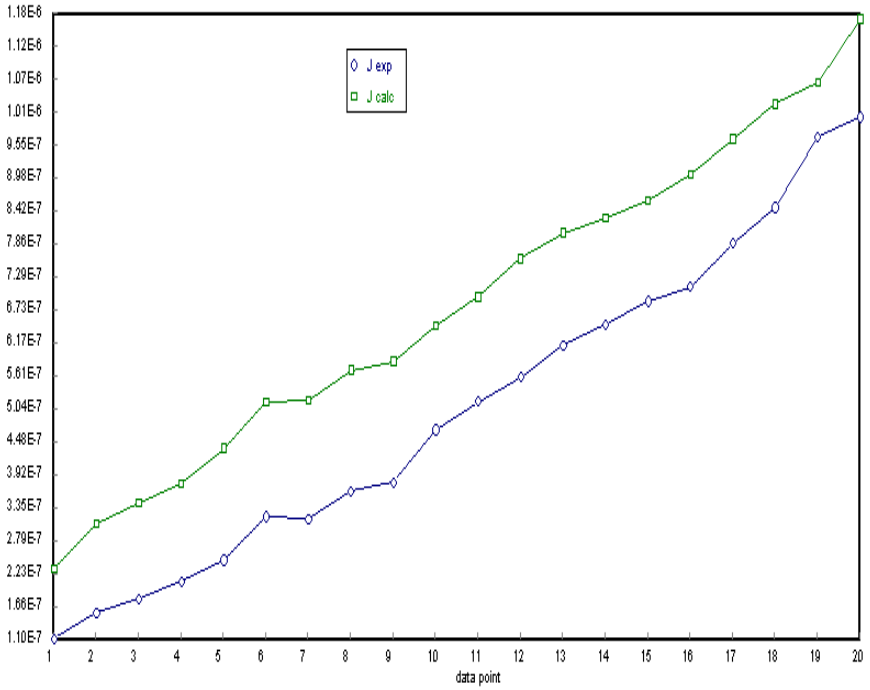

C. Determination of Diffusivity Using Time-Dependent Sorption Method

Using Eqn. (2.13): $$\frac{M_t}{M_\infty} = 1 - \sum_{n=0}^{\infty} \frac{8}{(2n+1)^2 \pi^2} \exp\left(- \frac{(2n+1)^2 \pi^2 D t}{l_m{}^2} \right)$$

Simplification of terms,

$$\frac{M_t}{M_\infty} = M \qquad ; \qquad \frac{\pi^2 D}{l_m{}^2} = A$$

The data required for regression: M versus t

For [Propyl propionate] = 603 ppm

(membrane thickness, l_m = 50 μm = 0.0050 cm)

***t*, h**	***M*, g pp / g membrane**
0	0
1	0.00108
2	0.001
3	0.00125
4	0.00142
5	0.0018
6	0.00204
7.5	0.00256
9.417	0.00264
11.5	0.00289
26.25	0.00282
33	0.00294

pp = propyl propionate

The regression results given by Polymath are provided below:

POLYMATH Results
No Title 11-30-2007

Nonlinear regression (L-M)

Model: M = 1-0.81057*exp(-A*t)-1/9*0.81057*exp(-9*A*t) -1/25*0.81057*exp(-25*A*t) -1/49*0.81057*exp(-49*A*t) -1/81*0.81057*exp(-81*A*t)-1/121*0.81057*exp(-121*A*t)-1/169*0.81057*exp(-169*A*t)-1/225*0.81057*exp(-225*A*t)-1/289*0.81057*exp(-289*A*t)-1/361*0.81057*exp(-361*A*t)

Variable	Ini guess	Value	95% confidence
A	0.1	**0.1676052**	0.0242725

Nonlinear regression settings
Max # iterations = 64

Precision
R^2 = 0.94979
R^2adj = 0.94979
Rmsd = 0.0197357
Variance = 0.0050989

General
Sample size = 12
Model vars = 1
Indep vars = 1
Iterations = 6

From the regression, $A = 0.1676052\ \text{h}^{-1}$

So, diffusivity: $$D = \frac{l_m^{\,2} A}{\pi^2} = \frac{(0.0050cm)^2\, 0.1676052 h^{-1}}{\pi^2}\left(\frac{h}{3600s}\right) = \mathbf{0.118 \times 10^{-9}\ cm^2/s}$$

D. Determination of Vapor Phase Composition in Evapermeation

Steps to take out the vapor feed samples up to analysis:

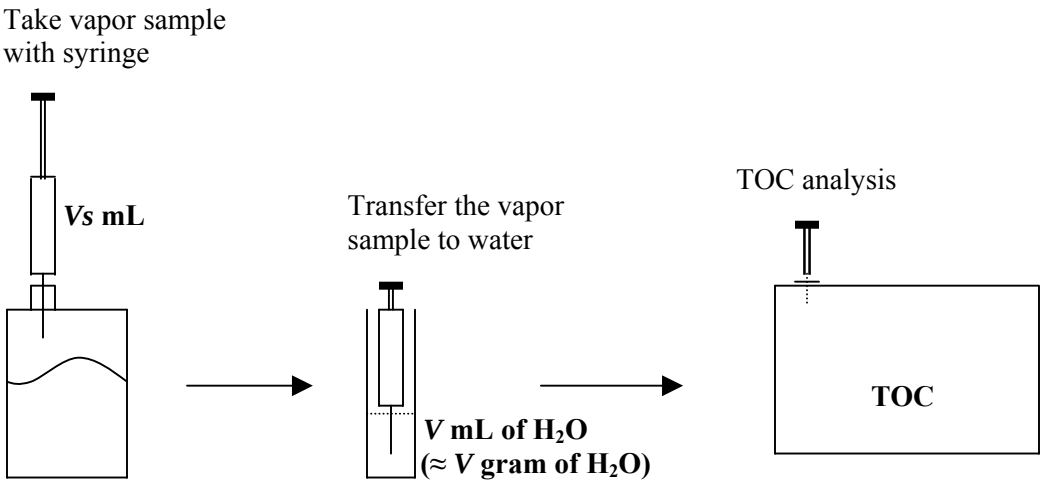

Concentration of propyl propionate (pp) sample injected in TOC = x ppm (mass)

Mass of pp in the dilution of V gram of H_2O = $\frac{x}{(1000000 - x)}.V$ gram

Considering the temperature and pressure in the syringe are same as those in the vapor feed, the concentration of pp in the syringe = the concentration of pp in vapor phase

= mass of pp in V gram of H_20 / volume of syringe

= $\frac{x}{(1000000 - x)}\frac{V}{Vs}$ gram pp / mL vapor

Example:

Given data from evapermeation experiments for propyl propionate-water mixtures,

- Concentration of pp in liquid phase = 534.8 mg/L
- Volume of syringe = 15 mL
- Volume of de-ionized water to dilute the vapor sample = 22.5 mL ≈ 22.5 g
- The concentration of diluted pp from TOC analysis = 26 ppm

The concentration of vapor pp = $\frac{26}{(1000000 - 26)}\frac{22.5}{15}$ = **39.0 x 10^{-6} g/mL = 39.0 mg/L**

E. Simulation of Batch Pervaporation Using Polymath

E.1 Conventional Pervaporation Process (1 stream recycle)

For $F_0/A_m = 375$ kg/m^2

POLYMATH Results
No Title 12-05-2007, Rev5.1.225

Calculated values of the DEQ variables

Variable	initial value	minimal value	maximal value	final value
t	0	0	50	50
F	3.75E+05	3.662E+05	3.75E+05	3.662E+05
xf	0.001	1.296E-05	0.001	1.296E-05
W	0	0	8426.7489	8426.7489
rho	1.01E+06	1.01E+06	1.01E+06	1.01E+06
lm	2.5E-05	2.5E-05	2.5E-05	2.5E-05
Dw	5.04E-07	5.04E-07	5.04E-07	5.04E-07
beta	185	185	185	185
Fv	9.864E+04	9.864E+04	9.864E+04	9.864E+04
xw	0.0056	0.0056	0.0056	0.0056
xg	0.99	0.99	0.99	0.99
Spp	4.601	4.601	4.601	4.601
Dpp	2.34E-07	2.34E-07	2.34E-07	2.34E-07
Am	1	1	1	1
xp	0.185	0.0023979	0.185	0.0023979
F0	3.75E+05	3.75E+05	3.75E+05	3.75E+05
Ppp	43.496014	0.5637801	43.496014	0.5637801
Pw	195.14557	159.29131	195.14557	159.29131
Pv	238.64159	159.85509	238.64159	159.85509
Rt	9.84E+04	9.84E+04	9.848E+04	9.848E+04
xr	5.538E-04	9.09E-06	5.538E-04	9.09E-06
J	238.64159	159.85509	238.64159	159.85509
G	0	0	329.45995	326.3263
Mrec	0	0	326.16535	323.06304

ODE Report (RKF45)

Differential equations as entered by the user

[1] d(F)/d(t) = Rt-Fv
[2] d(xf)/d(t) = Rt*(xr-xf)/F
[3] d(W)/d(t) = Pv*(beta*xf-xg)/(xw-xg)

Explicit equations as entered by the user

[1] rho = 1010000
[2] lm = 0.000025
[3] Dw = 0.000000504
[4] beta = 185
[5] Fv = 98640
[6] xw = 0.0056
[7] xg = 0.99
[8] Spp = 4.601
[9] Dpp = 0.000000234
[10] Am = 1
[11] xp = beta*xf
[12] F0 = 375000
[13] Ppp = Spp*Dpp*Am*xf*rho/lm
[14] Pw = Dw*Am*(1.784*xf+0.0078)*rho/lm
[15] Pv = Ppp+Pw
[16] Rt = Fv-Pv
[17] xr = xf*(Fv-beta*Pv)/Rt
[18] J = Pv/Am
[19] G = F0-F-W
[20] Mrec = xg*G

Independent variable

variable name : t
initial value : 0
final value : 50

Precision

Step size guess. h = 0.000001
Truncation error tolerance. eps = 0.000001

General

number of differential equations: 3
number of explicit equations: 20
Data file: N:\My Documents\Batch pervaporation with one recycle (retentate F0Am 375).pol

E.2 Pervaporation Coupled with Permeate Decantation and Water Phase Recycle

For F_0/A_m = 375 kg/m^2

POLYMATH Results
No Title 12-05-2007, Rev5.1.225

Calculated values of the DEQ variables

Variable	initial value	minimal value	maximal value	final value
t	0	0	50	50
F	3.75E+05	3.746E+05	3.75E+05	3.746E+05
xf	0.001	4.232E-05	0.001	4.232E-05
Am	1	1	1	1
rho	1.01E+06	1.01E+06	1.01E+06	1.01E+06
lm	2.5E-05	2.5E-05	2.5E-05	2.5E-05
Dw	5.04E-07	5.04E-07	5.04E-07	5.04E-07
F0	3.75E+05	3.75E+05	3.75E+05	3.75E+05
beta	185	185	185	185
Fv	9.864E+04	9.864E+04	9.864E+04	9.864E+04
xw	0.0056	0.0056	0.0056	0.0056
xg	0.99	0.99	0.99	0.99
Spp	4.601	4.601	4.601	4.601
Dpp	2.34E-07	2.34E-07	2.34E-07	2.34E-07
Ppp	43.496014	1.8406533	43.496014	1.8406533
xp	0.185	0.0078288	0.185	0.0078288
G	0	0	362.77394	362.77394
Pw	195.14557	160.35768	195.14557	160.35768
Pv	238.64159	162.19833	238.64159	162.19833
Rt	9.84E+04	9.84E+04	9.848E+04	9.848E+04
xr	5.538E-04	2.949E-05	5.538E-04	2.949E-05
W	195.15083	161.8311	195.15083	161.8311
J	238.64159	162.19833	238.64159	162.19833
Mrec	0	0	359.1462	359.1462

ODE Report (RKF45)

Differential equations as entered by the user

[1] d(F)/d(t) = Rt+W-Fv
[2] d(xf)/d(t) = (Rt*(xr-xf)+W*(xw-xf))/F

Explicit equations as entered by the user

[1] Am = 1
[2] rho = 1010000
[3] lm = 0.000025
[4] Dw = 0.000000504
[5] F0 = 375000
[6] beta = 185
[7] Fv = 98640
[8] xw = 0.0056
[9] xg = 0.99
[10] Spp = 4.601
[11] Dpp = 0.000000234
[12] Ppp = Spp*Dpp*Am*xf*rho/lm
[13] xp = beta*xf
[14] G = F0-F
[15] Pw = Dw*Am*(1.784*xf+0.0078)*rho/lm
[16] Pv = Ppp+Pw
[17] Rt = Fv-Pv
[18] xr = xf*(Fv-beta*Pv)/Rt
[19] W = (beta*xf-xg)*Pv/(xw-xg)
[20] J = Pv/Am
[21] Mrec = xg*G

Independent variable

variable name : t
initial value : 0
final value : 50

Precision

Step size guess. h = 0.000001
Truncation error tolerance. eps = 0.000001

General

number of differential equations: 2
number of explicit equations: 21
Data file: N:\My Documents\Batch pervaporation with two recycles (F0Am 375).pol

F. Publications

Some parts of this thesis research have been published in journal, conference and symposium:

- Permselectivity, solubility and diffusivity of propyl propionate/water mixtures in poly(ether block amide) membranes, ***Journal of Membrane Science***, 300 (2007), 95-103.

- Poly(ether block polyamide) membranes for recovery of propyl propionate from aqueous solution by pervaporation, ***Twenty-Ninth Annual Symposium on Polymer Science/Engineering***, Institute for Polymer Research, Waterloo, Ontario, Canada, May 15, 2007.

- Pervaporation of propyl propionate-water mixtures through PEBA membranes, ***56th Canadian Chemical Engineering Conference***, Sherbrooke, Quebec, Canada, October 15-18, 2006.